UCRL-18216

cy. 2

CHEMICAL BIODYNAMICS
Annual Report 1967

Lawrence Radiation Laboratory
University of California Berkeley

4

DISCLAIMER

UCRL-18216
UC-4 Chemistry
TID-4500 (52nd Ed.)

UNIVERSITY OF CALIFORNIA

Lawrence Radiation Laboratory
Berkeley, California

AEC Contract No. W-7405-eng-48

CHEMICAL BIODYNAMICS ANNUAL REPORT, 1967

M. Calvin, Director, Laboratory of Chemical Biodynamics

June 1, 1968

Work done under auspices of the
U. S. Atomic Energy Commission

Printed in the United States of America
Available from
Clearinghouse for Federal Scientific and Technical Information
National Bureau of Standards, U. S. Department of Commerce
Springfield, Virginia 22151
Price: Printed Copy $3.00; Microfiche $0.65

CHEMICAL BIODYNAMICS ANNUAL REPORT, 1967

Contents

*Preceding Reports: UCRL-17520, UCRL-16806.

FOREWORD

The Chemical Biodynamics Laboratory continues to adjust its activities in accordance with the growth of science in general and with biological science in particular. We consider the next major stage in the development of biology and medicine to be an understanding of the dynamics of a living organism in molecular terms; hence our name--Chemical Biodynamics.

Our general objective is the determination of the responses of a living organism to any variation in external environment, such as light, radiation, temperature, and other chemical and/or physical variables. For this study we use predominantly the tools of radioisotopes in determining the dynamic response of the organism to external changes and in understanding the molecular events that lead to the response. This general problem, understanding the dynamics of a living organism, is the principal guiding directive of all our activities.

In line with this objective, we work toward the development of physical equipment, entirely new, for the recognition of the molecular changes involved in the regulation of growth, differentiation, development, and other behavioral responses to environment. This effort is now taking the form of initial steps toward the establishment of a more general component of the Chemical Biodynamics Laboratory, which we have called a Laboratory of Biomolecular Structure. The envisaged laboratory will depend on the particular talents available at the Lawrence Radiation Laboratory, and the AEC in general, for the design and construction of physical equipment particularly suited to the definition of the changes in molecular shape and form, changes that constitute the regulatory mechanism of the living organism. It is our hope that as this field of science develops we will continue to lead in the evolution of the information, concepts, and instruments which are required for its growth.

As is customary, we have selected for this annual report a number of specific activities which we have broken down into four subgroups labeled biochemistry (animal, plant and bacterial), biophysical chemistry and biophysics, organic chemistry and geochemistry, and, finally, photochemistry and radiation chemistry. In each of these four general categories we have activities under way which constitute a step toward the fulfillment of our general objective as defined above.

These activities have taken us further into photobiology and radiation chemistry. One example of recent advances is our identification of metabolic regulation by light in plants. During this past year we have reported on the discovery of a regulatory mechanism in the carbon reduction cycle of photosynthesis which is controlled by the light; detailed mechanisms of that control are not yet known and are under investigation. Another aspect of our radiation chemistry research has evolved in the studies of chemical evolution and organic geochemistry. Here we have found that both heat pulses and radiation pulses, under suitable, controlled conditions, will produce many of the biomolecules which heretofore have been thought to be uniquely the product of the enzyme systems of modern organisms. Our studies on the molecular mechanisms of brain function, in particular the chemistry and chemical changes involved in the transmitter substances and in the macromolecules of nerve cells, are now beginning to take a

shape that will allow the expanded use of tracers in determining the changes which the process of learning might introduce in the various parts of the brain.

These particular examples are only specific cases, a wider variety of which may be found in the body of this report.

Melvin Calvin, Director
Chemical Biodynamics Group
Lawrence Radiation Laboratory

ANIMAL, PLANT, AND BACTERIAL BIOCHEMISTRY

TIME COURSES OF EFFECTS OF DIFFERENTIAL EXPERIENCE ON BRAIN MEASURES AND BEHAVIOR OF RATS†

Edward L. Bennett, Mark R. Rosenzweig, ‡ Marian C. Diamond §
Hiromi Morimoto, and Marie Hebert

For a number of years we have been investigating the cerebral and behavioral changes induced by differential experience in hopes of shedding light on brain mechanisms of learning and memory storage. In previous publications we have shown that significant cerebral effects occur when littermate rats are exposed to enriched or impoverished environments for a period of 80 days following weaning.[1-3] We have also demonstrated effects of differential experience on problem-solving behavior when animals were kept in the enriched or impoverished environments for 30 days following weaning.[4] After reviewing these studies briefly, we will turn to results of recent experiments in which we have varied both the duration and the starting age of exposure to differential experience. This survey is based in part on work in progress; it is possible to give only some of the highlights of the current research of our group.

ENRICHED AND IMPOVERISHED BEHAVIORAL CONDITIONS

In most of the experiments to be reported here, littermate male rats were assigned to the enriched condition (EC) or the impoverished condition (IC). In the enriched condition, rats are housed in groups of 10 to 12 in a large cage that is provided with "toys" such as ladders, wheels, boxes, platforms, etc. The cage arrangement is changed daily, with some toys being exchanged for objects from a large set. To enrich their experience further, the rats are taken out each day in a group for a half-hour exploratory session in a 3-ft-square field with a pattern of barriers that is also changed daily. Each EC rat has a littermate assigned to the impoverished condition in which animals live in individual cages with solid walls so that the animals cannot see or touch one another. These isolation cages are placed, in most experiments, in a separate, quiet, dimly-lit room. In other experiments, the lighting and sound have been the same for enriched and deprived groups, with no apparent change in the EC-IC cerebral effects. Littermates are assigned to groups randomly, with the restrictions that littermates differing widely in body weight are excluded and that total body weight of groups be substantially equal. All of the experiments reported in this paper have employed only male rats. Unless otherwise noted, the subjects were of the Berkeley S_1 strain; but other strains have also been used to cross-check many of these results. After rats have been maintained in the differential conditions for the experimental period, they are sacrificed and various anatomical and biochemical measures are made of their brains.

CEREBRAL EFFECTS OF DIFFERENTIAL EXPERIENCE

When animals have been kept for the 80 days after weaning in the differential conditions,

we have found a number of differences in the cerebral cortex between enriched and impoverished rats; these differences include changes in tissue weight, in enzymatic activity, and in a number of anatomical measures. In 13 replications of this experiment the most consistent result has been that the enriched-environment rat has a heavier cerebral cortex than the littermate kept in the isolated condition. Weight refers to wet weight of tissue samples, taken by our standardized dissection methods.[5] The consistency of the EC-IC weight differences is shown in Fig. 1, which presents results of experiments run from 1960 through 1965. Each experiment included from 10 to 12 EC-IC littermates. In the top graph, the bar for each experiment indicates the percentage by which the EC group exceeded the IC group in weight of total cortex. The effects ranged from 1 to 6 percent, with each experiment showing a positive effect and with an overall mean EC-IC difference of slightly greater than 4 percent.

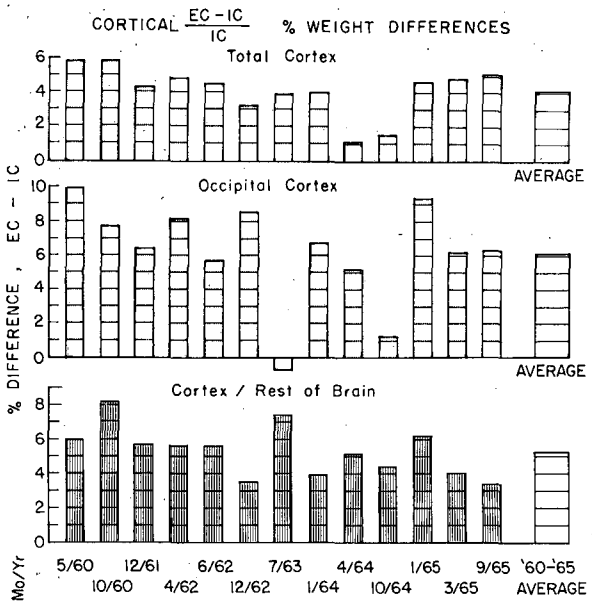

Fig. 1. Percentage differences between brain weight measures of littermate S_1 rats from enriched condition (EC) and impoverished condition (IC). Stability of effects is seen in 13 experiments performed over a six-year period.

The effects of differential experience are larger, although somewhat more variable, in the occipital or visual region of the cortex, as is shown in the middle panel of the figure. Here it will be seen that the average effect was about a 6 percent difference. These weight differences in the occipital cortex have been found to be significantly larger than similar effects in the nearby somesthetic region of the cortex. Many of our histological measures have been restricted to the occipital area. Although the EC-IC effects are especially prominent in the occipital region, we do not believe that visual experience plays a major or even necessary role in producing the effects. We have found significant EC-IC differences in the occipital cortex even when we used rats that were blinded by enucleation at weaning,[6] or when we conducted such experiments in absolute darkness. Why the occipital region is especially susceptible to differential experience remains at present an unsolved question.

A rather stable measure of EC-IC effects has been the ratio of weight of the cortex to that of the rest of the brain. Some investigators have indicated that various cortical/subcortical

ratios increase with phylogenetic development of the brain. We will show in a later section of this paper that the cortical/subcortical weight ratio is correlated with a measure of problem-solving ability. The stability of EC-IC differences in the ratio is shown at the bottom of Fig. 1.

Results for the occipital region--in tissue weight, enzymatic activity, and histological measures--are summarized in Table I. Let us now consider each of these measures and its implications briefly.

Changes in Cortical Bulk

Tissue weight, as is the case for all measures that we will discuss, is taken without knowledge of the experimental condition to which the particular animal had been exposed. A change in weight alone is not very revealing; this might be due to change in either bulk or density of the tissue; it might be due to increase of fluid or increase of formed material. The further measures serve to give more information about the ways in which the brain is changing as a consequence of differential experience. Measures of depth or thickness of the cerebral cortex indicate that it is, at least in large part, the bulk rather than the density of the tissue that is changing. It will be noted here that the increase in depth of the cortex is very similar to the increase in its weight. The increase in total protein, which closely parallels the weight difference, serves to show that our effect is not due simply to "water on the brain."

Changes in Brain Enzymes

While the foregoing changes are all closely similar in magnitude, enzymatic changes show rather different patterns. Acetylcholinesterase was chosen for study since it is an enzyme intimately concerned with transmission at many central synapses; it is found especially in neural cells. Cholinesterase, an enzyme that also splits the synaptic transmitter acetycholine, but less specifically, is of interest because it is found primarily in the glial cells.[7-9] Hexokinase is an enzyme important in energy transformation, but it does not have a specifically neural role. Total acetylcholinesterase increases with enriched experience but less than does tissue weight, whereas total cholinesterase increases even more than does tissue weight (Table I). Total hexokinase increases to about the same extent as does tissue weight. The different EC-IC pattern of changes in acetylcholinesterase and cholinesterase led us to investigate whether there might be a change in relative numbers of neurons (which are rich in acetylcholinesterase) and glial cells (which are relatively rich in cholinesterase).

Histological Measures

To obtain reliable counts of neurons and glia we devised a method using composite photographs representing a large standard area of occipital cortex.[10] The results of two experiments shown in Table I indicate that while differential experience does not lead to any significant change in the number of neurons, it does lead to a significant difference in the number of glia. Altman and Dass[11] independently found an increase in number of new glial cells in animals exposed to an enriched environment as compared with isolates. Finally, although the number of neurons does not increase with enriched experience, we have recently found the cross-sectional area of neuronal cell bodies to be greater by about 13 percent in EC over IC for two experiments.[3] If the cell body is considered to be roughly spherical in shape, then a difference of 13 percent in cross-sectional area indicates a difference of about 20 percent in volume.

Table I. Effects of differential experience on occipital cortex (differences between littermates of S_1 strain in EC or IC from 25 to 105 days of age).

Measure	Difference	P	EC > IC/Total pairs
Weight	6.1	<.001	106/141
Depth	6.3	<.001	36/41
Total protein	7.8[a]	<.001	25/32
Total AChE	2.3	<.01	83/140
Total ChE	10.2	<.001	77.5/98[c]
Total hexokinase	6.9[b]	<.001	17/21
No. neurons	-3.1	NS	7/17
No. glia	14.0	<.01	12/17
Perikaryon cross-section	13.4	<.001	11.5/13[c]

a. Weight diff. 7.0% in these experiments.

b. Weight diff. 5.5% in these experiments.

c. Fractional value indicates tied score.

Subcortical Changes with Differential Experience

Measures of weight and enzymatic activity have also been taken in the "subcortex" or "rest of brain"; we are defining these terms to mean all of the portions of brain remaining after total cortex has been stripped away. In general the effects at the subcortex are rather small, and in some cases they are even opposite in direction from the effects found at the cortex. For example, after 80 days in the EC or IC conditions, we usually find that the enriched-experience animals have slightly lesser weight of subcortex, although they have greater weight of cortex. It might also be noted that the enriched-experience animals are about 9 percent less in total body weight at the end of the experiment than are their isolated brothers. A ratio of cortical to subcortical measures often gives the most reliable index of EC-IC effects.

In looking back over these cerebral effects of differential experience, we see that the brain is sensitive to experience in a variety of ways. Its weight, and the distribution of bulk between cortex and subcortex, activities of enzymes, and a number of histological measures can all be influenced significantly by the conditions under which the animals live.

Distinguishing Influences of Enrichment from Those of Impoverishment

The results that we have given so far have been expressed entirely in terms of EC-IC differences. Are such differences to be ascribed chiefly to the enrichment of experience of the EC group or to the impoverishment of experience of the IC group, or to the joint effect of both treatments? In the absence of a baseline it is impossible to allocate the causes of these differences. Choice of an appropriate baseline is a difficult matter; but in 1964 we suggested the use of the colony animal as one appropriate baseline, since the colony rat is the subject of most experimental work.[1] (We recognize that in an ethological sense the EC environment probably approaches the "normal" environment of the rat more closely than does the standard colony (SC) condition.) In several experiments we have therefore taken three male animals from each litter and have randomly assigned one of the animals to remain in the SC condition. Fig. 2

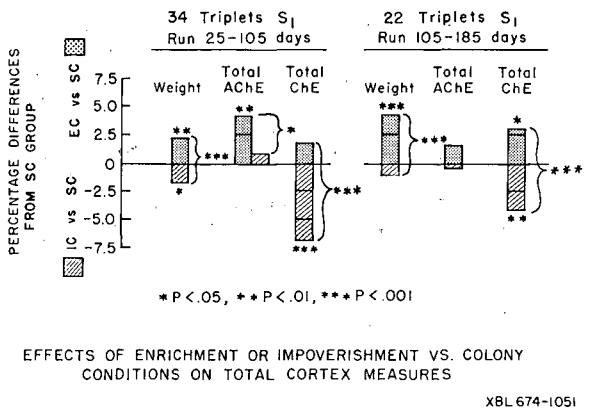

Fig. 2. Effects of enrichment or impoverishment on total cortex measures, taken against standard colony (SC) littermates as a baseline. The left half of the figure is based on three experiments using male triplets from 34 S_1 litters, with exposure to the differential conditions extending from 25 to 105 days of age. The right half is based on two experiments, including male S_1 triplets from 22 litters, the exposure extending from 105 to 185 days of age. The differences in cortical weight and total AChE activity are seen to be larger between EC and SC than between IC and SC; that is, they are due more to enrichment than to impoverishment of experience. On the other hand, impoverishment (IC vs SC) produces larger differences in total ChE activity than does enrichment (EC vs SC).

shows results obtained when we compare EC animals with the SC littermate baseline and similarly compare IC results with the SC baseline. The figure is based on measures made on total cortex and shows results both for animals run from 25 to 105 days of age and for animals run from 105 to 185 days of age. In the case of weight of total cortex, we see that the EC-SC difference is larger than the corresponding IC-SC difference; this is especially the case for the older animals. In total activity of acetylcholinesterase, again a larger difference is found between EC and SC than between IC and SC. For activity of cholinesterase, the pattern is reversed, the larger difference occurring between the IC and SC littermates, rather than between EC and SC. Thus it appears that the EC-IC differences in weight and total acetylcholinesterase (AChE) should be attributed largely to enriched experience, whereas the differences in total cholinesterase (ChE) activity must be attributed chiefly to the restricted experience of the IC animals. This is one of several sets of results indicating that various consequences of differential experience do not necessarily covary as the type, duration, or starting age of experience are modified.

CEREBRAL EFFECTS OF VARIED DURATION OF DIFFERENTIAL EXPERIENCE

A few years ago we had not only found that the brain was quite plastic to effects of experience, but we had also shown that differential experience of 30 days duration after weaning led to significant differences in problem-solving behavior.[4] In order to test whether the cerebral and the behavioral effects of experience were critically related, we decided to vary the length of exposure to enriched or impoverished conditions and to study the effects on both brain and behavior. We anticipated that both sorts of effects would increase in magnitude with increasing duration of exposure, at least up to a ceiling. The design of such experiments in which both duration of EC-IC experience and the starting age are varied is shown in Fig. 3. For each age and duration of exposure, there are duplicate pairs of groups, one EC-IC pair being sacrificed immediately at the end of the experimental period, while the other pair is pretrained and tested on a behavioral test and then sacrificed. The groups sacrificed at the outset of behavioral testing indicate the cerebral values found at this point. It appears that pretraining and testing further alter brain measures, but this is a story that we will have to leave for another time. Let

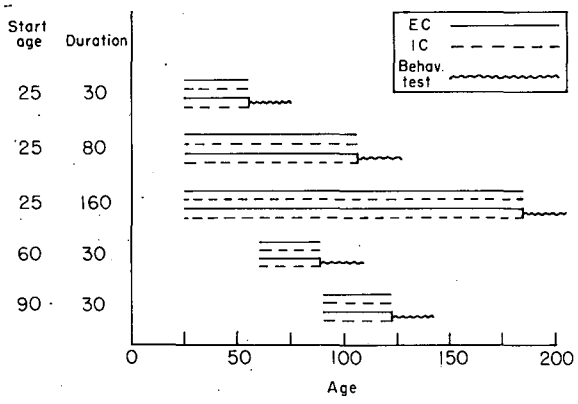

Fig. 3. Design of experiments to test effects of varied durations and varied starting ages of EC or IC experience on brain and on behavior. For each starting age and duration, one pair of EC-IC groups is sacrificed for measurement of brain values at the end of the period of differential experience; the other pair is trained and tested behaviorally, then sacrificed.

us turn first to the cerebral effects of EC-IC experience for various durations and with various starting ages. We will limit ourselves here to observations of brain weights, since data on other cerebral measures are not yet as complete.

Figure 4 shows the increase of weight of total cortex in animals put into the enriched or impoverished situations at 25 days of age. This figure is based on three pairs of EC-IC groups, all taken from the same breeding of S_1 rats. One paired group was taken out of the EC-IC conditions after 30 days (at 55 days of age), a second pair was taken out of the differential conditions after 80 days (at 105 days of age), and the third pair was removed after 160 days of differential experience (at 185 days of age). Both the EC and IC curves show growth after 25 days of age, but the EC (solid) curve spurts up more rapidly at the start. The difference between the curves increases over the first month and then the two curves come closer together. At 55 days of age the EC-IC difference amounted to 8 percent; at 105 days of age, the difference had dropped to 4.1 percent, and at 185 days of age the difference had decreased still further to 3.2 percent. These results can be added to those of other experiments for the same three EC-IC durations but where the various groups were not all taken from the same breeding (see Table II). Table II shows results not only for weight of total cortex but also for the weight of the rest of the brain (subcortex) and for the ratio of weight of cortex to that of the rest of the brain. It will be seen that the EC-IC difference in total cortex weight decreases steadily with duration of EC-IC experience. The EC-IC difference in weight of rest of brain changes from a small posi-

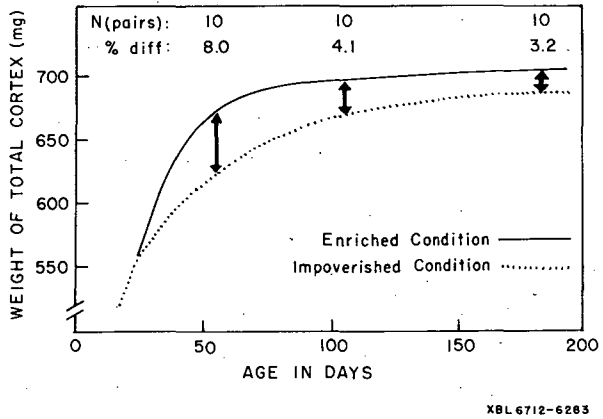

Fig. 4. Growth of weight of total cortex for S_1 rats put into enriched or isolated conditions at 25 days of age. Ten EC-IC littermate pairs were sacrificed at 55 days of age, ten pairs at 105 days, and ten pairs at 185 days. The relative difference between groups was greatest after 30 days of differential experience (at 55 days of age) and declined thereafter.

Table II. Percentage differences in brain weight between S_1 littermates put in enriched or impoverished conditions at weaning.

EC-IC Duration	30 days	80 days	160 days
N (pairs)	32	151	22
Total cortex	7.4[c]	4.1[c]	2.8[a]
Rest of brain	1.5	-1.1	-3.4[b]
Cortex/Rest	5.8[c]	5.2[c]	6.2[c]

a. $P < .05$

b. $P < .01$

c. $P < .001$

tive effect at 30 days to a significantly negative effect at 180 days. The ratio of weight of cortex to the rest of the brain shows an EC-IC difference that is both highly significant and substantially constant for all three EC-IC durations.

We have done two sets of experiments in which animals were placed in the differential conditions at 60 days of age and the subgroups were removed after 15, 30, 45 or 60 days; results of these experiments are shown in Table III. Here we see that EC-IC differences for both cortex and rest of brain increased from 15 to 30 days and then declined. The differences in cortical/subcortical ratio were statistically significant and quite constant for all four durations. If we exclude the 15-day column, in which the effects may not yet have become fully developed, the trends in the rest of Table III resemble rather closely those of Table II, in which animals were put in the EC-IC conditions at 25 days of age and left there for various durations. Although the effects beginning at 60 days were smaller than those for experiments beginning at 25 days of age, in both cases the percentage magnitude of the cortical effect reached a maximum at about 30 days and then declined, as did the magnitude of the effect in the rest of the brain, leaving the EC-IC difference in ratio of cortex to rest of the brain substantially constant.

Varied Starting Ages

Now let us see what happens when the EC-IC duration is held fixed at 30 days but the starting age is varied; this design is shown in Fig. 3 in the top, fourth, and fifth sets of lines. The upper half of Table IV shows results obtained when the 30-day EC-IC period was started at 25, 60, or 90 days of age. It should be noted that these experiments were taken from different breedings. When the start of the experimental period was delayed beyond weaning at 25 days of age, the animals were kept in standard colony conditions (3 to a cage) prior to being assigned to the EC or IC condition. Starting the EC-IC period at different ages appears to have differential effects depending on whether one is examining total cortex, rest of brain, or the ratio of cortex to rest of brain. The EC-IC effects on weight of total cortex were largest when the treatment was initiated at 25 days of age, slightly less when it began at 60 days of age, and apparently smaller at 90 days of age. (The 90-day results should be considered with caution, since they are based on only a single experiment with 10 pairs of animals.) For the subcortex the results go in the opposite direction. The EC-IC differences were small and not statistically significant for experiments started at 25 and 60 days of age, but for the one experiment started

Table III. Percentage differences in brain weight between S_1 littermates in enriched or impoverished conditions for various durations beginning at 60 days of age.

Duration	15 days	30 days	45 days	60 days
N (pairs)	21	20	21	20
Total cortex	3.7[c]	6.2[c]	3.9[c]	3.2[b]
Rest of brain	0.5	2.6[a]	0.3	-0.4
Cortex/Rest	3.2[c]	3.5[c]	3.6[c]	3.7[c]

a. $P < .05$
b. $P < .01$
c. $P < .001$

Table IV. Percentage differences in brain weight between S_1 littermates in enriched or impoverished conditions for 30 or 80 days, starting at different ages.

	30-day EC-IC Duration, Starting at Age:		
	25 days	60 days	90 days
N (pairs)	32	63	10
Total cortex	7.4[c]	6.1[c]	4.6[a]
Rest of brain	1.5	2.1	4.0[a]
Cortex/Rest	5.8[c]	3.9[c]	0.5

	80-day EC-IC Duration, Starting at Age:	
	25 days	105 days
N (pairs)	151	45
Total cortex	4.1[c]	5.4[c]
Rest of brain	-1.1	1.7[a]
Cortex/Rest	5.2[c]	3.7[c]

a. $P < .05$
b. $P < .01$
c. $P < .001$

at 90 days of age they reached 4 percent ($P < .05$). Because the results for cortex and subcortex went in opposite directions, the ratio of cortex to the rest of the brain clearly showed the largest results in experiments started at 25 days of age, smaller results at 60 days, and nonsignificant results in the experiment started at 90 days of age.

The lower part of Table IV shows the effects of 80-day EC-IC, beginning either at 25 or 105 days of age. The effects seen here are rather similar to those in the upper half of the table, for 30-day EC-IC starting at three different ages. The dissimilarity is that in the 80-day experiments there was a slightly larger effect on weight of total cortex for the experiments begun at 105 days of age than for the experiments begun at 25 days of age. For rest of brain and for the ratio of total cortex to rest of brain, the results were similar to those seen in the

30-day experiments; that is, the effect for rest of brain was larger when the start of the experiment is delayed to 105 days, and the effect in cortical/subcortical ratio was larger with animals started at weaning.

Distinguishing Effects of Enrichment from Normal Maturation of Brain

Is it possible that the effects of enrichment which we have been describing represent merely an acceleration of normal maturation of the brain? We believe not, for several reasons: (a) Significant increases in cortical weight are obtained even when the growth of brain in colony animals has practically ceased. (The brain of the rat never completely stops growing, but the rate of growth is slow after about 100 days of age.) Figure 5 shows changes in cortical weight when two animals of a litter were put into the EC or IC conditions at 105 days of age, the third littermate remaining in the colony condition. The EC curve is seen to rise promptly and significantly above the SC plateau. (b) Total AChE activity of brain remains practically constant after about 80 days of age.[12] Enriched experience begun after this age nevertheless leads to a significant increase in total AChE activity. (c) Perhaps the clearest evidence distinguishing the two factors is that maturation and enriched experience lead to opposite effects in depth of cerebral cortex. The cortex of the rat normally decreases progressively in thickness, at least after weaning, whereas enriched experience, as we have seen in Table I, leads to a significant increase in cortical depth in relation to the impoverished condition. The cortex on the dorsal aspect of the occipital area measures 1340 micra in depth in the 25-day-old S_1 rat, but only 1200 micra in the 100-day-old rat kept under standard colony conditions. (These measures were made on formalin-perfused frozen sections.) This decrease in cortical thickness with age apparently occurs as the cortex, which is adding weight more slowly than the rest of the brain, is stretched thinner to cover the subcortex. There is an anterior-posterior cortical gradient in both the age and the experience effects, such that the posterior or occipital region shows both the greatest decrease of depth as a function of age and the greatest increase of depth as a function of environmental enrichment.

SUMMARY OF CEREBRAL EFFECTS OF DIFFERENTIAL EXPERIENCE

Let us emphasize six of the results brought out in the foregoing discussion: (a) The EC-IC

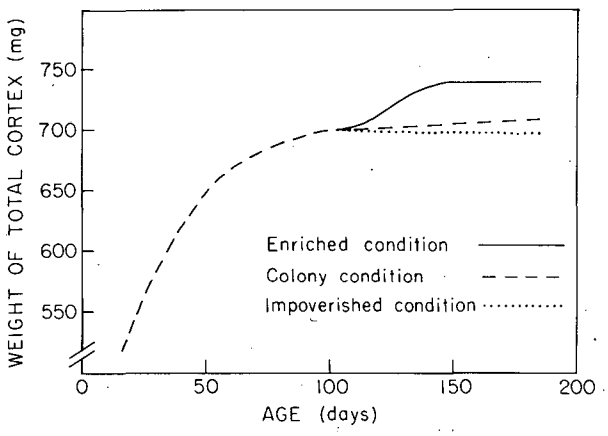

XBL 681-4012

Fig. 5. Growth of weight of total cortex for S_1 rats put into enriched or isolated conditions at 105 days of age. A third animal in each litter remained in the colony condition. All animals were sacrificed at 185 days of age. The 185-day values were based on three experiments including three male rats from each of 34 litters. The initial 105-day point and the intermediate values are estimated from other experiments.

cortical weight differences are to be attributed more to enrichment than to restriction of experience (Fig. 2). (b) Increasing the length of the EC-IC experience, at least beyond 30 days, does not enhance the EC-IC differences found in measures of weight of brain tissue (Fig. 4 and Tables II and II). (c) This sensitivity of the brain to experiential influence is not restricted to weanlings, for significant changes in brain weights are found when animals are put into the experimental conditions at 60, 90, or 105 days of age (Figs. 2 and 5, Table III). (d) For 30-day EC-IC experience, the largest effects in weight of cortex and in the cortical/subcortical ratio are found when the animals are put into the experimental conditions at weaning; for the 80-day duration this appears clearly only for the cortical/subcortical ratio (Table IV). (e) Effects of differential experience can be distinguished from changes in the brain due to maturation. (See preceding paragraph and Fig. 5.) (f) Several weight measures yield different temporal courses as the animals are kept for varying periods in the experimental conditions (Table II). Weight of total cortex shows a transitory component in the EC-IC effect, the difference first increasing to 30 days and then decreasing. On the other hand the cortical/subcortical ratio shows an EC-IC difference that appears to be relatively constant as the duration of the experiment is varied. Having found these differences in time courses, we are now examining time courses of EC-IC effects on brain chemistry and on histological measures; we would expect to find a variety of time courses among these measures as well.

EFFECTS OF DIFFERENTIAL EXPERIENCE ON PROBLEM-SOLVING BEHAVIOR

Now let us turn to experiments performed to determine whether effects of differential experience on problem-solving behavior might be related to the effects produced on the brain. We had earlier reported that when littermate animals were put into EC or IC environments at 25 days of age and left there for one month, the EC animals were significantly better in solving visual reversal discrimination problems in the Krech Hypothesis apparatus.[4] Since then we have also found, but not published, that the same period of EC-IC experience would differentiate animals in performance on the Lashley III and Dashiell Checkerboard mazes; in both cases the EC animals performed significantly better than their IC littermates. In all of this earlier behavioral work, the EC-IC period was restricted to the 30 days following weaning. We therefore decided to vary the duration and starting age of EC-IC experience preceding behavioral tests, as described for brain and behavior in Fig. 3, and in 1967 we ran 10 behavioral experiments of this sort.

At the end of the EC-IC period, the rats were removed from the differential environments and were recaged in individual colony cages. The experimenters who tested the rats did not know from what condition any individual animal had come, so that the behavioral tests were run "blind," just as were the chemical and anatomical determinations.

The Visual Reversal Discrimination Test

In all of the 1967 behavioral work we used the visual reversal discrimination problem in the Krech Hypothesis apparatus. Reversal discrimination tasks, as Warren has pointed out, have certain characteristics, required of a test of animal intelligence, in that performance is correlated with both phyletic status and maturation.[13] The Krech apparatus is a linear maze with four successive Y-shaped choice points. At each choice point the right or the left alley is illuminated, and the experimenter can make either of the alleys correct on a given trial by

changing the position of a swinging door at the end of the unit. In a 10-day pretraining period, the animals were accustomed to the 24-hr food deprivation schedule. They were pretrained in a straight runway to leave the start box, run through doorways, and enter the goal box. Following the pretraining period, the 9-day testing session began; on each day there were 10 trials in the 4-unit apparatus, thus giving 40 choices. On each trial the pattern of lights and doors followed a different pre-set order. The reversal discrimination schedule followed that used by Krechevsky.[14] The animals were first trained to go to all the lighted alleys. To reach criterion the animal could not make more than one error in five successive trials; i.e., 19 correct choices out of 20. When an animal reached criterion, the very next trial (which might occur on the same test day) began the first reversal problem, dark-correct. Training on the dark-correct problem was continued until the criterion was reached, whereupon the problem was switched to light-correct. During the 9 days most animals solved four or more reversal problems.

The use of an automatic recording system made scoring somewhat more reliable than in our previous work. In the earlier work observers had some difficulty in accurately scoring choices, especially on trials when an animal darted back and forth, making "vicarious trials and errors." For the automatic scoring system, segments of the floor of the apparatus were painted with electrically conductive paint. Entry of the rat into either alley at a choice point completed a circuit and lighted a light on a panel. Holding circuits kept the record of each of the four choices until the experimenter copied them down and reset the device at the end of each trial.

Behavioral Results

Results of five experiments, all done with S_1 rats from a single breeding, are shown in Fig. 6. In experiments A, B, and C, the animals were put in EC or IC at 25 days of age and were kept in the differential conditions for 30 or 160 days, respectively. (These EC-IC periods coincided with those of the rats which furnished data for the curves of cortical growth in Fig. 4.) In experiments D and E, 30-day EC-IC periods started at 60 and 90 days, respectively.

In each experiment, animals solved the initial light-correct problem (L-1) with relatively few errors. The next problem, dark-correct (D-1), involved more errors. Re-reversing to light-correct (L-2) was harder still. Thereafter, the animals reversed more readily, and errors were reduced. Each curve is drawn only to the last problem that was solved by at least half the animals in the group. Thus in experiment A, at least half the EC rats solved the third dark-correct problem (D-3), while the last problem solved by at least half the IC's was D-2. In experiments A, B, and C--the groups assigned to the experimental conditions at 25 days of age--the EC curve lies below the IC curve at most points, and the EC curve stretches farther out to the right. In experiment D--where EC-IC lasted from 60 to 90 days of age--the results are reversed; the EC rats made more errors per problem and solved fewer problems than their IC littermates. In experiment E—EC-IC from 90 to 120 days of age—neither group was clearly superior to the other. Where differences exist between groups, they tend to be largest, both absolutely and relatively, on problem L-2. Thereafter the curves tend to converge, so that differences in scores on this test as a function of earlier experience do not persist.

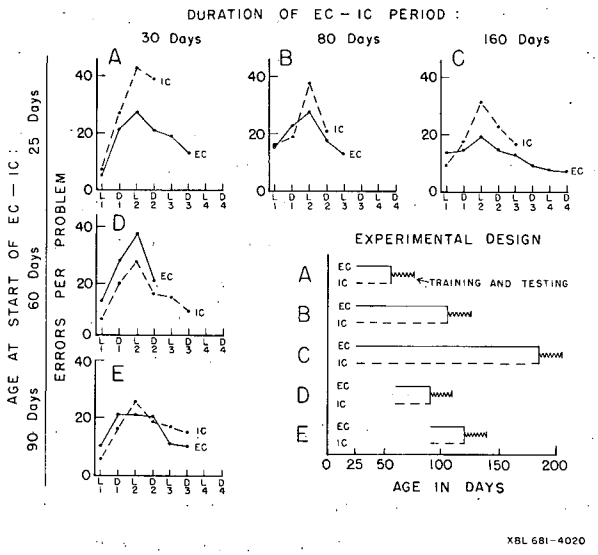

Fig. 6. Errors per problem on successive visual reversal discrimination problems, for groups exposed to enriched or isolated conditions for various durations and from various starting ages. The design of the experiment is shown in the lower right section of the figure. The successive problems are designated as L-1 (first light-correct problem), D-1 (first dark-correct), L-2 (second light-correct), and so on. Each curve extends through the last problem solved by at least half the members of the particular group. Errors increase over the first two reversals (through L-2), and then decrease. Relative errors of the groups, depending upon the particular EC-IC conditions, are discussed in the text.

The five other experiments run in 1967 replicated experiments A, D, and E, and added groups kept in EC-IC from 25 to 85 and from 60 to 120 days of age. Data for all 10 experiments are presented in Table V. The results are expressed in two ways: (a) The EC/IC ratio of mean numbers of problems solved during the 9 days. If the animals that had been in EC solve more problems than their IC littermates, then the EC/IC ratio on this measure will be significantly greater than 1.0. (b) The EC/IC ratio of mean number of errors made per reversal problem. If the EC animals make fewer errors than their IC littermates in solving an average problem, then the EC/IC ratio on this measure will be significantly less than 1.0.

Looking at the upper half of the table, for all experiments in which the animals were put into the differential conditions at about 25 days of age (weaning age), we see that the expectation of superior performance on the part of the EC animal appears to be justified. The EC animals in general solved significantly more problems and made significantly fewer errors per reversal problem than the IC's. Analyses of variance on the scores confirm the following impressions: In number of reversals completed, the actual scores did not differ significantly among the five experiments, and the overall EC-IC difference was highly significant ($P < .001$). There was not a significant interaction between experiment and EC-IC effect, so all experiments contributed similarly to the overall effect. The other measure--errors per reversal completed--was not as stable, since actual scores varied significantly among experiments ($P < .01$). Nevertheless this measure also showed both a highly significant overall EC-IC effect ($P < .001$) and no significant difference among effects in the various experiments. Thus, when S_1 rats were put into EC or IC at 25 days of age, the difference in problem-solving ability in favor of the EC's could not be distinguished according to whether the animals remained in the experimental conditions for 30, 60, 80 or 160 days. In this connection, it might be recalled that one of the brain weight measures--the ratio of weight of cortex to that of the rest of the brain--also showed EC-IC differences that were significant and of about the same magnitude regardless of length of treatment, when this started at 25 days of age.

Now let us look at the lower parts of Table V which show behavioral results when animals were put into the EC or IC conditions at either 60 or 90 days of age. It will be recalled that

Table V. Relative performance on visual reversal discrimination after enriched (EC) or impoverished (IC) experience of various durations and different starting ages (S_1 rats).

Period	Terminal Date	N (litters)	EC/IC Mean No. Probs. Solved	P	EC/IC Mean Errors per Reversal	P
25-55 (A)[a]	7/67	10	1.45	<.01	0.64	<.01
25-55	11/67	7	1.30	<.10	0.66	<.05
25-85	12/67	10	1.10	--	0.93	--
25-105 (B)	9/67	10	1.36	<.10	0.78	--
25-185 (C)	11/67	10	1.27	<.05	0.66	<.01
60-90 (D)	8/67	10	0.63	<.01	1.60	<.05
60-90	12/67	10	0.88	--	1.31	<.10
60-120	4/67	10	1.13	--	0.83	--
90-120	4/67	10	0.86	--	0.93	--
90-120 (E)	9/67	10	0.89	--	1.15	--

a. The letters correspond to the group designations in Fig. 6.

prior to being put into the experimental conditions, all animals were held in standard colony (SC) conditions, three animals to a cage.

The replication 60-90 day experiment reproduced the results of the first, in which EC's solved fewer problems and made more errors per reversal problem than did the IC's. Taken together, the two experiments show the EC's to be significantly worse on both counts ($P < .01$). For the 60-120 day experiment, the EC and IC groups did not differ significantly. The two 90-120 day experiments did not show significant differences either, although the EC solved somewhat fewer problems in both cases.

Considering all of the experiments of 30 days duration, we see a puzzling sequence as the starting age is moved from 25 to 60 days, and from 60 to 90 days. In the 25-55 day experiments, the EC groups performed significantly better than the IC's. Surprisingly, in the 60-90 day experiments, the order was reversed; the EC's made more errors and the IC's made fewer errors than in the 25-55 day experiments. In 90-120 day experiments, neither replication showed a clear difference between the groups. These data give a striking indication of a critical period for beneficial behavioral effects of environmental enrichment. Before we rely upon them, however, we will want to see further replications of these experiments. Such replications are planned for 1968.

Just as in the case of the cerebral differences, one can ask whether the behavioral EC-IC differences found among animals put in the conditions at weaning are due chiefly to enrichment or chiefly to impoverishment of experience. As in the case of the cerebral measures, we have used the standard colony (SC) condition as a baseline against which to measure effects of enrichment or of impoverishment of experience. In the three experiments placed at the top of Table V we actually used not two but three animals from each litter. One of the animals was kept in SC while its brothers were put in EC or IC. Table VI shows the relative performance on the visual reversal discrimination tasks of the SC and IC littermates. It will be seen that

Table VI. Relative performance on visual reversal discrimination after colony (SC) or impoverished (IC) experience (S_1 rats).

Period	Terminal Date	N (litters)	SC/IC Mean No. Probs. Solved	P	SC/IC Mean Errors per Reversal	P
25-55	7/67	10	1.36	<.01	0.62	<.01
25-55	11/67	7	1.42	<.05	0.64	<.05
25-85	12/67	10	1.36	<.10	0.80	--

on both measures for each of the first two experiments the SC animals were significantly better than their IC brothers. In fact, when SC/IC ratios of Table VI are compared with the corresponding EC/IC ratios of Table V, it will be seen that in five of six comparisons the SC animals were somewhat better than their EC brothers. Thus, it appears that performance on the visual reversal discrimination task can be significantly impaired if an animal is placed in isolation immediately after weaning, but that the performance on this task cannot be improved by giving an animal enriched experience over and above the colony experience. This may also help to explain why IC behavior was not inferior when animals were placed in the differential conditions only at 60 or 90 days of age. Apparently, once an animal has been in the colony condition for a month after weaning, it is protected against the deleterious effects of restriction of experience.

The behavioral results on this test thus indicate that the difference between the EC and IC animals should be attributed to early restriction of experience and not to enrichment of experience. In this sense the behavioral results resemble somewhat those found with ChE activity, in distinction to the cerebral results found with AChE activity or with wet weight. It will be recalled that in ChE activity of the cortex the main difference was found between the IC and SC groups, whereas in both AChE activity and weight of the cortex the main differences were found between the EC and SC groups. Having found that the visual reversal discrimination task is not sensitive to enrichment of experience, we are now trying other behavioral tasks to see whether the same will be true of them or whether certain tasks will show effects of enrichment, rather than of impoverishment of experience.

CORRELATIONS BETWEEN BRAIN WEIGHTS AND BEHAVIORAL MEASURES

The behavioral data can fruitfully be considered from another aspect--correlations between brain measures for individual rats and individual behavioral scores. Several years ago we had reported a significant correlation between the cortical/subcortical ratio of brain weights and the mean errors per reversal problem solved.[4] The correlation was negative, meaning that the greater the ratio of cortex to the rest of the brain in an individual rat, the fewer the errors that animal tended to make. This result was obtained for rats kept in the enriched environment from 25 to 55 days and tested over 18 days. For a concurrent IC group, no significant correlation was obtained. We suggested that the brain values of rats from EC would probably be less affected by training and testing than would rats that had been in IC. "... such end-point determinations presumably reflected rather accurately the relatively stable cerebral values of the EC group during the problem-solving phase and less accurately the changing values of the IC group, thus permitting higher correlation of brain measures with behavior for

the EC than for the IC group."[4]

We then tested the generality over strains of the relation between brain weight ratio and behavior, giving all rats EC experience.[15] Two hundred fifty-two rats of 10 strains were tested. The period of testing was reduced in this work to nine days, since scores had tended to convergence in the latter half of the longer period employed previously. These experiments yielded a significant mean correlation of -.27 ($P < .001$) between the brain weight ratio and errors per reversal problem. Each strain was tested in two experiments, and 17 of the 20 individual coefficients were negative; nine of the ten strains gave overall negative correlations, thus indicating that the relationship is indeed general over strains. For the S_1 strain, the correlation was -.32 ($P < .10$, $N = 33$).

The behavioral experiments run in 1967 and described earlier in this paper allow us to test further the reliability of this brain-behavior relation. The results also permit us to determine whether this relation appears most clearly in rats that had been in the enriched condition prior to behavioral testing. For the three experiments that included EC, SC and IC groups, the respective correlations between the cortical/subcortical ratio of brain weight and mean errors per reversal were the following: EC, -.42 ($P < .05$); SC, .06 (NS); and IC, .23 (NS). For all five experiments in which the rats were assigned to conditions at 25 days of age, the correlations were these: EC, -.30 ($P < .05$), and IC, .08 (NS). Four of the five EC groups had negative correlations, the exception being the 25-185 day group which yielded a slightly positive coefficient (.06). Thus the present EC correlations reproduce quite closely the S_1 value of -.32 reported in the 1967 paper (all of those experiments having been done in 1966 or earlier). Furthermore, in the present study only animals from the enriched environment yielded a significant relationship, as was true in the original study reported in 1962.

Now let us look at the results for animals kept in EC from 60 to 90 days of age. Here the within-group brain-behavior relation departs from that of the groups started at 25 days, just as the 60-90 day error-score relation was reversed between the EC and IC groups. The two 60-90 day EC groups yielded positive correlations of .19 and .44, the combined coefficient not being significantly different from zero but certainly departing from the -.30 found for the groups put into EC at 25 days. Curiously, the one 60-120 day EC group yielded a correlation in the "usual" range (-.34). The two 90-120 day EC groups gave negative brain-behavior correlations of -.18 and -.34, the combined coefficient not being significant but resembling closely that of the groups started in EC at 25 days. Thus the relation between the cortical/subcortical weight ratio and ability to solve reversal problems has been abundantly confirmed for groups put into the enriched environment at weaning, but, for reasons as yet unknown, such a relation was not obtained with rats kept in EC from 60 to 90 days of age.

In the experiments reported in the previous section of the present paper, it will be recalled that no consistent relation was found between group means of cerebral-weight measures and mean scores on the reversal discrimination task. In line with results reported in earlier papers, when animals were assigned to EC or IC at weaning, the EC group were superior to the IC littermate group in problem-solving scores, and the EC group had the larger cortical/subcortical weight ratios; this was true regardless of the duration of the EC-IC period. Use of an additional group of SC animals now provided a critical test. The EC animals also had larger cortical/subcortical weight ratios than their SC littermates, yet the EC's were not superior to the SC's in behavioral scores. The groups assigned to differential environments at 60 or 90

days of age also negated the hypothesis that greater cortical/subcortical weight ratios are generally related to superior problem-solving ability. In the 60 to 90 day experiments, the EC rats were actually significantly poorer than the IC's in behavioral scores, although the EC's had the higher cortical/subcortical ratios. In the 90 to 120 day experiments, the EC's did not differ significantly from the IC's in behavior, although again the EC's had the higher brain ratio.

The results obtained with differential experience from 25 to 55 days--both for within-group correlations and for between-group differences--are not upset by the results of the 60 to 90 day experiments, but our ability to generalize on the basis of the earlier results is now considerably restricted. An overall relation between the cerebral and behavioral effects of differential experience has not so far emerged from the range of conditions studied.

DISCUSSION

Discussion of brain plasticity will be brief because one of us has just extensively reviewed this subject elsewhere.[16] It has long been speculated that training and stimulation might lead to changes in the sizes of parts of the brain, in the interconnections of its cells, and in its chemical composition. Until very recently, however, the evidence seemed to show that the brain was very stable in its anatomy and composition. Now we and other investigators are finding that many aspects of the brain can be altered readily by treatments that involve only changing the experience of the subjects.

The variety of cerebral changes with experience is great, ranging from relatively gross measures such as weight or depth of cortex, to refined measures of enzymatic activity and cross-section areas of perikarya and their nuclei. These changes are not large in percentage terms, but they are consistent and reproducible.

Even more delicate measures are being undertaken. For example, Cragg has been studying possible changes in synaptic size and number with experience.[17] He suggested that a reasonable first approach was to look for synaptic changes after first exposure of dark-reared animals to light, since differences in visual experience have been found to give rise to morphological effects in the visual cortex. We had shown that raising rats in the dark reduces the weight of visual cortex.[6] Gyllensten et al. reported that mice raised in the dark have smaller nuclei in cells in the upper half of the visual cortex and less internuclear material per nucleus.[18, 19] Cragg therefore exposed dark-reared rats to light for various periods and compared them with littermates kept in the dark. The results suggested "that exposure to light promotes the formation of new synapses of small diameter in the deeper layers of the visual cortex, while the synapses already formed in the superficial half of the cortex grow slightly larger."

When we began our work, we supposed that it would be difficult to demonstrate cerebral responses to differential experience. It was for this reason that the experience was begun at weaning because we thought that the adult brain might not show any changes due to experience. Furthermore, we chose the relatively long duration of experience of 80 days, and we exposed the animals to the experimental situations for 24 hours a day. The experiments described above have shown that the brain is more readily affected than we had supposed, and we can now add further information along this line. The first requirement that we found could be relaxed was the age at onset of the differential experience. Rats did not have to be placed in the

conditions at weaning; quite similar effects could be obtained when rats were started in experiments as young adults at 105 days of age. Then, also as reported above, it was found that reducing the duration of the EC-IC period to 30 days did not diminish the cerebral effects. Indeed, for weight and total enzymatic activity of total cortex, the results of 30-day experiments were greater than those of 80-day duration. Recently, in experiments being reported elsewhere,[20] we have found that exposing rats to 2 hours of EC per day for either 30 or 60 days brings about cerebral changes as large as those obtained by exposing them for 24 hours a day for the same period. Furthermore, in recent experiments with 2 hours of daily exposure, the IC animals were caged in the same room and same type of cages as their EC littermates. The treatment of the two groups differed only in the 2-hour EC period, yet significant brain differences were produced.

The fact that the brain is plastic in many ways to environmental demands has thus been clearly demonstrated, and detailed evidence is now coming in from a number of laboratories. How to relate this plasticity to learning and storage of memory remains a problem on which less progress has as yet been made. It represents the major challenge before us.

SUMMARY

Differential experience leads to significant changes in both brain and behavior of the rat. The cerebral cortices of rats from enriched conditions exceed those of littermates from impoverished conditions in tissue weight, depth, total protein, total activities of the enzymes acetylcholinesterase, cholinesterase and hexokinase, number of glial cells, and cross-section areas of neural cell bodies and their nuclei. When littermates in colony conditions are used as a baseline, the effects in cortical weight and total acetylcholinesterase are seen to be attributable mainly to enrichment of experience while the difference in total cholinesterase is due chiefly to impoverishment. Anatomical comparisons between environmental manipulations and the baseline colony condition are in progress. The effects of experience can be distinguished from those of normal maturation of the brain, since they occur in adult animals, and since enriched experience increases cortical depth while maturation (at least after weaning) leads to thinning of the rat's cortex. Increasing the duration of differential experience beyond 30 days does not increase the cerebral differences between animals with enriched and impoverished experience. The effect on cortical weight declines with periods of over 30 days, whereas the difference in ratio of cortical weight to that of the rest of the brain remains approximately constant.

Behavioral effects of differential experience were measured by scores on a visual reversal discrimination task. When Berkeley S_1 rats were assigned to the enriched (EC), colony (SC), or isolated (IC) conditions at weaning, IC scores were inferior to EC or SC, but the latter two groups were equivalent. When rats were in EC or IC from 60 to 90 days of age, the effect was reversed--EC scores were inferior to IC. When the EC-IC period extended from 90 to 120 days of age, there was no consistent difference between EC and IC scores. Where differences were found between EC and IC groups in errors per problem, these differences tended to disappear after the first few problems. Significant correlations were obtained between behavioral scores and the ratio of weight of cortex to that of the rest of the brain. Confirming previous studies, these indicated for most EC groups that the greater the cortical/subcortical weight ratio, the fewer the errors the animal tended to make. Here too the 60 to 90

day EC groups differed from the other experiments. Each of these results is based on at least two experiments, and more are being run. No general relation could be found between cerebral and behavioral measures that held over the whole range of conditions studied.

ACKNOWLEDGMENTS

We would like to acknowledge the diligent and skillful aid of co-workers in many phases of this research: In the maintenance of animals in the experimental conditions--Clarence Turtle and Donald Gassie; in the behavioral testing--Clarence Turtle, Su-Yu Chang, Donald Gassie, Yoram Jaffe, and John Frazee; in the histological analyses--Alma Raymond, Bernice Lindner, and Lennis Lyon; in statistical analyses--Ann Muto, Anne Betancourt, and Diane Rein; and in administrative assistance and preparation of the manuscript--Jessie Langford. Finally we would like to thank our students and co-workers for their many comments and suggestions on an earlier draft of this paper.

FOOTNOTES AND REFERENCES

†This research was also supported by National Science Foundation Grant GB-5537.

‡Professor of Psychology, Department of Psychology, University of California, Berkeley.

§Assistant Professor of Neuroanatomy, Department of Physiology-Anatomy, University of California, Berkeley.

1. E. L. Bennett, M. C. Diamond, D. Krech, and M. R. Rosenzweig, Science 146, 610 (1964).
2. M. R. Rosenzweig, Amer. Psychol. 21, 321 (1966).
3. M. C. Diamond, with technical assistance by B. Lindner and A. Raymond, J. Comp. Neurol. 131, 357 (1967).
4. D. Krech, M. R. Rosenzweig, and E. L. Bennett, J. Comp. Physiol. Psychol. 55, 801 (1962).
5. M. R. Rosenzweig, D. Krech, E. L. Bennett, and M. C. Diamond, J. Comp. Physiol. Psychol. 55, 429 (1962).
6. D. Krech, M. R. Rosenzweig, and E. L. Bennett, Arch. Neurol. 8, 403 (1963).
7. G. B. Koelle, J. Pharmacol. Exp. Therap. 106, 401 (1952).
8. G. B. Koelle, J. Comp. Neurol. 100, 211 (1954).
9. E. Giacobini, Acta Physiol. Scand. 45 (Suppl. 156), 1 (1959).
10. M. C. Diamond, F. Law, H. Rhodes, B. Lindner, M. R. Rosenzweig, D. Krech, and E. L. Bennett, J. Comp. Neurol. 128, 117 (1966).
11. J. Altman and G. D. Das, Nature 204, 1161 (1964).
12. E. L. Bennett, M. R. Rosenzweig, D. Krech, H. Karlsson, N. Dye, and A. Ohlander, J. Neurochem. 3, 144 (1958).
13. (a) J. M. Warren, Ann. Rev. Psychol. 16, 95 (1965); (b) J. M. Warren, in Behavior of Nonhuman Primates: Modern Research Trends, A. M. Schrier, H. F. Harlow, and F. Stolnitz, Eds. (Academic Press, New York, 1965), p. 349.
14. I. Krechevsky, J. Comp. Psychol. 14, 263 (1932).
15. M. R. Rosenzweig, E. L. Bennett, and M. C. Diamond, in Psychopathology of Mental Development, J. Zubin and G. Jervis, Eds. (Grune & Stratton, New York, 1967), p. 45.
16. M. R. Rosenzweig and A. L. Leiman, Ann. Rev. Psychol., 1968, in press.

17. B. G. Cragg, Nature 215, 251 (1967).
18. L. Gyllensten, Acta Morphol. Neerl.-Scand. 2, 331 (1959).
19. L. Gyllensten, T. Malmfors, and M. L. Norrlin, J. Comp. Neurol. 124, 149 (1965).
20. M. R. Rosenzweig, W. Love, and E. L. Bennett, Federation Proc., 1968, in press.

A PROCEDURE FOR THE ASSAY OF CHOLINE ACETYLTRANSFERASE

Ann Orme, Stephanie Rosenbaum, and Edward L. Bennett

Acetylcholine is one of the earliest and best recognized neurotransmitters involved in synaptic transmission. For a number of years we have been investigating possible relationships between behavior and experience, and acetylcholine (ACh) and acetylcholinesterase (AChE), two components of the choline acetyltransferase-acetylcholine-acetylcholinesterase system.[1] The synthetic reactions involved in the synthesis of acetylcholine from acetate and choline may be formulated in the following manner:

$$\text{ATP + acetate + CoA} \underset{Mg^{++}}{\overset{\text{acetyl-CoA synthetase}}{\rightleftharpoons}} \text{acetyl-CoA + AMP + PP} \qquad (1)$$

$$\text{acetyl-CoA + choline} \underset{Mg^{++}}{\overset{\text{choline acetyltransferase}}{\rightleftharpoons}} \text{acetylcholine + CoA .} \qquad (2)$$

It is the activity of the enzyme, choline acetyltransferase (ChAt) (System No. 2.3.1.6), involved in the second reaction, that we wish to determine.

We had not previously investigated ChAt activity because its assay, until recently, had involved the bio-assay of acetylcholine, the product of its synthetic activity. These bio-assays are tedious, and it is difficult to obtain better than 5% precision. Recently, four radiometric procedures for the determination of ChAt have been described. The method introduced by McCaman and Hunt[2] utilized preformed ^{14}C-acetyl-CoA. Subsequently, the excess acetyl-CoA was destroyed, and the acetylcholine-^{14}C was precipitated by ammonium reineckate (Reinecke salt) in the presence of carrier choline. The choline reineckate was dissolved in acetone and counted by scintillation techniques. Recently, Schrier and Shuster[3] introduced a variant of this procedure in which the acetylcholine was separated from its precursors, acetyl-CoA and acetate, on Dowex-1 column. Due to the high cost of ^{14}C-acetyl-CoA and acetyl-CoA, these methods are most suitable on a microscale. Also, since acetyl-CoA is not being continuously regenerated, the rate of acetylcholine formation is less than maximal.

Schuberth[4] and Fonnum[5] have introduced procedures circumventing both drawbacks by continuously generating ^{14}C-acetyl-CoA from acetate-^{14}C. The technique is conveniently achieved by the addition of acetyl-CoA synthetase (System No. 6.1.1.1), which can be obtained from several sources, including bakers yeast[4] or acetone powders of pigeon liver.[5] Provided that the rate of formation of acetyl-CoA by this system is much greater than its utilization by the ChAt (Eq. 2 above), maximal rates of choline synthesis may be achieved. In Schuberth's procedure, the excess acetate-^{14}C was evaporated, and the residual acetylcholine-^{14}C activity was determined. In Fonnum's procedure the resulting acetylcholine was precipitated by sodium tetraphenyl boron (Kalingost). Since potassium is also precipitated by this reagent, sodium salts were used almost exclusively in the incubation medium. This results in a high sodium-potassium ratio which is inhibitory for the acetyl-CoA synthetase system. The use of the Reineckate salt as a precipitant was avoided, since the combination of high color and acetone

as a solvent for the resulting acetylcholine reineckate led to low counting efficiency. In addition, the incubation medium described did not include Mg^{++}, an activator of the acetyl kinase system.

The procedure described below has utilized features of the methods described by Fonnum and by McCamen and Hunt. In this report, experiments to develop and test the procedure for our needs are described; and, in another report experiments to determine strain and brain-area differences in 10 lines of rats will be summarized.

MATERIALS AND METHODS

Samples for Enzyme Analysis

These experiments were all done with adult rat brain as a source of tissue for the enzyme, choline acetyltransferase. Rats were sacrificed by decapitation, the brain removed, weighed, frozen on dry ice, and stored in a deep freeze for no more than one week prior to analysis. Rat brain sections were homogenized in cold 0.5% Triton X-100; a Teflon-glass homogenizer was used. The homogenates were stored in an ice-bath for no more than 2 hr before use. The usual concentration of rat brain was 30 to 40 mg/ml and 0.80 ml samples were used for each assay. When small areas of the brain were analyzed--i.e., the visual or somesthetic cortex--the concentration was 10-12 mg/ml. A higher concentration, 60 mg/ml, was used for cerebellum.

Incubation Mixture

The incubation mixture finally adopted consisted of 0.48 M KCl, 0.05 M KF, 0.006 M $MgCl_2$, 0.01 M choline chloride, 1.47×10^{-4} M CoA (Cal Biochem), 1.24×10^{-4} M eserine salicylate,† 0.02 M ATP, disodium salt (pH adjusted to 7.4 with KOH), 0.0125 M glutathione (pH adjusted to 6.5 with KOH), 0.0084 M KOAc and 0.0012 M NaOAc-^{14}C (sp. act. 0.25 $\mu C/\mu mole$), and 0.5 units of aceto-CoA synthetase (units as defined by Berg[6]). The aceto-CoA synthetase was obtained from the supernatant of a 0.4 M tris-chloride buffer (pH 8.0) extract of acetone dried pigeon liver (Sigma). The extract from 10 mg of powder (0.20 ml) was used for each 1.00 ml final volume of incubation mixture. With brain tissue added, the final pH was about 7.8. If a stock solution containing all the inorganic salts was prepared, after several days a precipitate, probably MgF_2, slowly formed. Use of the stock solution then resulted in low values for the ChAt activity.

Incubation and Precipitation Procedure

The incubation mixture was incubated at 37° for approximately 30 min to preform acetyl-CoA before the addition of 0.80 ml to an equal volume of the brain homogenate in 12-ml centrifuge tubes. Immediately after the addition of the incubation mixture to the brain homogenate, the tubes were shaken individually in a Vortex mixer for a few seconds and incubated in a water-bath with shaker at 37° for 60 min. At the end of the 60-min incubation period (120 min for small samples or samples with low activity), the reaction was stopped by the addition of 0.80 ml of a reagent of 40% trichloroacetic acid containing 2 mg/ml acetylcholine perchlorate. The tubes were cooled in an ice bath for 10 min prior to centrifuging in swinging trunnion

buckets. All centrifugations were done at 3000 g for 8 min at 4°C. Two ml of the clear supernatant were pipetted from the total volume of 2.40 ml and added to 0.8 ml of a saturated Reinecke salt in 0.5 M HCl. This reagent should be prepared daily. The mixture of acetylcholine-choline reineckate was then allowed to precipitate completely at 0°; this required 45 to 60 min. The precipitates were then sedimented, resuspended, and washed with 2.5 ml of cold 0.2 N HCl. After centrifugation, the precipitate was again washed with another 2.5 ml portion of 0.2 N HCl. After decanting most of the supernatant, the centrifuge tubes were allowed to stand upside down over a few sheets of absorbent paper to allow the excess liquid to be drained from them as completely as possible.

Appropriate modifications were made in the usual procedure to investigate specific variables. When a large number of samples were to be analyzed in identical fashion, an appropriately large volume of the incubation medium was prepared and incubated at 37° for one-half hour. Aliquots (0.80 ml) of this incubation mixture were then added with a precision automatic pipet (Repipet, Labline Industries, Berkeley) at 10-sec intervals to previously pipetted samples of the tissue. A Repipet was also used to add the TCA-acetylcholine to terminate the enzyme reaction.

Counting Procedure

The precipitate was dissolved in a 1 ml portion of acetonitrile (Baker AR) and transferred quantitatively with 2 additional 1-ml rinses of acetonitrile into 16 ml of scintillation fluid in glass counting vials. The scintillation fluid was composed of 250 ml ethanol and 400 ml dioxane, to which had been added 5.0 g of PPO, 0.2 g DiMePOPOP, 50 g of naphthalene, and sufficient toluene to make 1 liter of final solution. The sample was counted in a Packard 3375 scintillation counter with an external standard. Optimal settings were obtained by using the least quenched of the expected routine samples. For our instrument the settings were: amplification, 40; lower discriminator setting, 100; and the upper discriminator setting, 1000. Under these conditions, the counting efficiency was about 70%. An efficiency curve vs the automatic external standard ratio (AES) was determined by adding 150 μl of toluene-^{14}C (18,000 dpm) to appropriately quenched samples. In our routine experiments, the samples typically contained about 5000 counts/min. Samples were counted for a maximum of either 20 min or 100,000 counts.

Blanks were prepared by adding the TCA-acetylcholine perchlorate mixture to the homogenate prior to adding the incubation mixture.

RESULTS

Formation of Acetyl-CoA

The hydroxamic acid method described by Berg[6] was used to determine the acetyl-CoA synthetase activity of the pigeon liver extract under various conditions. The results summarized in Table I show that magnesium, a high potassium concentration, and a reducing agent are necessary for maximal rates of acetyl-CoA synthesis. High sodium concentration in the presence of low potassium reduced the rate of acetyl-CoA formation by about 1/2. Fonnum did not indicate the buffer used; therefore the potassium and sodium concentrations present in his incubation mixture are not known. Glutathione was chosen as a more convenient reducing agent than potassium borohydride, which had been used by Fonnum and Schuberth. Eserine

Table I. Rate of acetylation of CoA under several incubation conditions.

Incubation Medium	K^+ (M)	Na^+ (M)	μM acetyl-CoA/hr
Complete[a]	0.35	0.02	1.20
Minus Mg^{++}	0.35	0.02	0.27
Minus glutathione	0.35	0.02	0.63
Minus glutathione plus KBH_4	0.35	0.02	1.05
Plus eserine (10^{-4} M)	0.35	0.02	1.20
Complete, modified			
K^+ and Na^+	0.24	0.28	1.20
K^+ and Na^+ modified	0.04	0.35	0.54

a. The complete incubation medium contained 0.1 M potassium phosphate (pH 7.5), 0.005 M $MgCl_2$, 0.01 M Na_2 ATP (pH 7.5), 0.05 M KF, 0.01 M KOAC, 0.01 M glutathione (pH 6.5), 10^{-4} M CoA, 0.2 M hydroxylamine (pH 7.0), and pigeon liver extract.

does not inhibit the reaction. Three commercial sources of acetone dried pigeon liver powders were tested. Only one of these gave satisfactory rates of acetyl-CoA formation. The supernatant from the phosphate buffer extract of the acetone dried pigeon liver was used rather than the pasty suspension itself. The supernatant was much easier to pipet accurately and contained the desired acetyl-CoA synthetase activity. Under our conditions, the rate of acetylation of CoA was 1.2 μmole per hr with the extract from 8 mg of pigeon liver powder. This was at least 5 times the anticipated rate of acetylcholine formation.

The effect on ACh synthesis of the preincubation time of the pigeon liver supernatant prior to the addition of brain homogenate was also investigated. Thirty to 60 min was optimal, and a 30-min period was chosen for our routine experiments. The necessity of preincubation has been described by Hebb and Smallman.[7]

Preparation of Brain Homogenate

Various detergents and organic solvents have been used to obtain maximum activity of ChAt in brain.[7] Fonnum compared several detergents, some of which were not readily available. Treatment with ether, 0.5% Triton X-100, and 0.42% (w/v) saponin on both fresh and frozen brain were compared. The results, summarized in Table II, clearly confirm the necessity of treatment to solubilize and activate ChAt in either fresh or frozen rat brain tissue.[7] The fourfold activation noted by Fonnum was not observed. Although the highest answers were obtained by ether treatment, we chose Triton X-100 as it is easier to use for routine analyses than ether. No correction was made for the slight decrease in volume of the aqueous phase resulting from ether treatment, so that in actual fact the two treatments may give more nearly equivalent results than indicated in Table II.

Effect of pH and Salt Concentration

The effect of varying pH, chloride concentration, and cation for the overall conversion of acetate to acetylcholine was investigated. As shown in Fig. 1, the optimum pH was about 7.5

Table II. Comparison of ether, Triton X-100, and saponin as ChAt solubilizers.

	% of Untreated Brain	% of Ether-Treated Brain
Fresh Brain		
Untreated	100[a]	59
Ether	170	100
Saponin (0.42% w/v)	146	85
Triton-X (0.5%)	154	90
Frozen Brain		
Untreated	100	73
Ether	137	100
Saponin (0.42% w/v)	126	92
Triton-X (0.5%)	131	96

a. The untreated rate for fresh or frozen rat brain (without cerebellum and medulla) was 5.9 μM/g/hr.

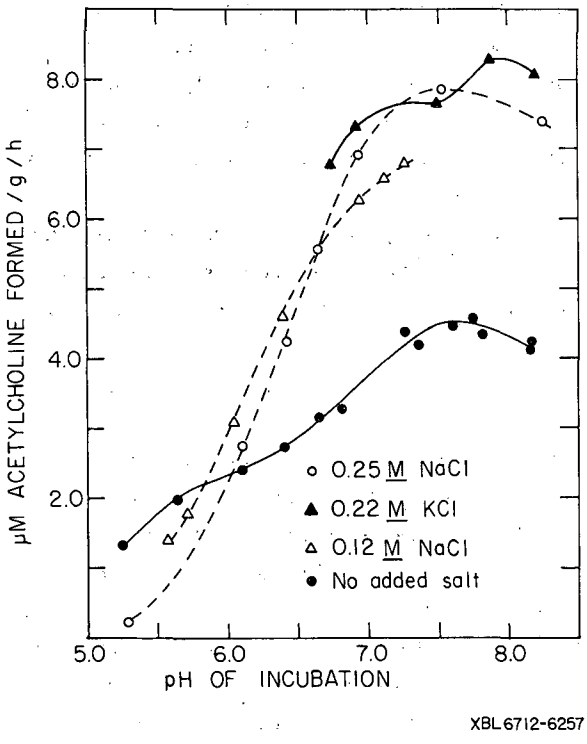

Fig. 1. Effect of pH and added KCl or NaCl on ChAt activity of brain. The chloride concentration was .01 M in the absence of added salt. Both phosphate and tris buffers were used with no apparent difference in the area of overlapping pH.

in the presence of 0.01 M Cl^-. Added Cl^-, either as K^+ or Na^+, markedly increased the overall reaction rate, but did not alter the pH optimum to the extent expected from the studies of Schuberth on ChAt of human placenta.

Effect of Tissue Concentration and Time of Incubation

With the conditions of acetyl-CoA generation used, a linear relationship was found between tissue and ACh formed/hr up to 0.2 μM/ACh/hr. This proportionality decreased when the rate of ACh formation exceeded 0.2 μM/hr (Fig. 2). The limiting amount of tissue used in routine assays was adjusted to give rates of ACh formation in the range of 0.15 to 0.20 μM/hr. The rate of ACh formation as determined at 1/2, 1, 1-1/2, and 2 hr was linear with 4 different amounts of whole brain ranging from 5 to 50 mg.

Precipitation of Acetylcholine

Sodium tetraphenyl boron (Kalingost) was tried as a precipitant of ACh, as described by Fonnum. The resulting precipitate was very amorphous and bulky, in part due to the precipitation of potassium. On the other hand, the mixed acetylcholine-choline reineckate obtained with Reinecke salt as a precipitant was crystalline and sedimented readily. It was insoluble, both initially and during the washing procedures. Experiments utilizing [^{14}C]-acetylcholine showed that 93 to 94% of the acetylcholine was recovered in the washed acetylcholine-choline reineckate. Co-precipitation of acetate-^{14}C by this reineckate was minimal, as demonstrated by the low blanks obtained. At least a fivefold excess of Reinecke salt was used to obtain complete precipitation of the ACh. The saturated Reinecke salt solution used for precipitation decomposed on standing, so new solutions were prepared the previous day and stored in the dark. If this precaution is not taken, incomplete precipitation of the radioactive acetylcholine-^{14}C is

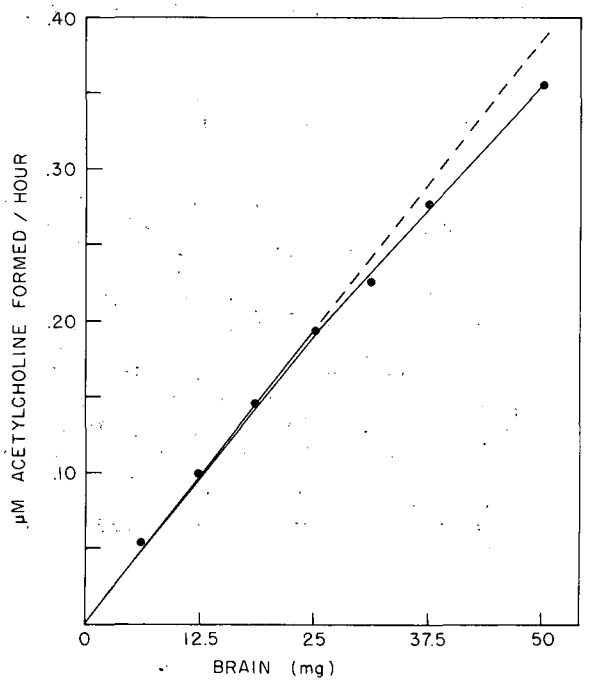

Fig. 2. Relation of ACh formation to amount of whole brain homogenate used. The standard incubation mixture (0.8 ml) was incubated with 0.8 ml of rat brain homogenate. The rate of ACh formation was 8.1 μM/hr/g. Data points are averages of duplicate analyses which agreed within 1%.

obtained with resultant low answers. Washing and solution of mixed acetylcholine-choline reineckate was completed in one day to avoid possible loss of activity.

Solution and Determination of Radioactivity of the Acetylcholine-Choline Reineckate

Numerous solvents were tried to dissolve the acetylcholine-choline reineckate. These included acetone, acetonitrile, methylethylketone, and a mixture of 50% benzyl alcohol, 50% acetonitrile. Acetonitrile was chosen as the most satisfactory, as it had little effect on the counting efficiency, as shown in Fig. 3. Channel 1 had been set up for routine tritium counting, Channel 2 had been set up for ^{14}C determinations, and Channel 3 was set up for optimal counting of the choline reineckate.

The addition of choline reineckate in 3 ml of acetonitrile to 16 ml of scintillation solution resulted in a sharp drop in counting efficiency in Channel 2, the normal channel for ^{14}C counting. In Fig. 4, we have plotted the efficiencies in the three channels against the automatic external standard (AES) ratio and the μM of choline reineckate. The efficiency increased in Channel 1 set for normal tritium determinations, so this channel could be used satisfactorily.

In routine ChAt determinations, the usual AES ratio ranged from 0.35 to 0.40. The settings of Channel 3 resulted in an even flatter slope in the efficiency vs AES ratio curve, and it was this channel that was routinely used. The actual curve used was determined by many points in the AES range of 0.35 to 0.40 and appropriately plotted on a large graph. Thus, although reineckate salts do influence counting efficiencies, quite satisfactory determination of the radioactivity may be made by appropriate choice of counter operating characteristics.

Stability of ChAt in Brain

No difference was observed between the ChAt activity of homogenates of fresh and freshly frozen brain. No systematic studies were made of the stability of ChAt in frozen brain. Less than 10% loss of activity was observed after four weeks of storage of frozen sections at -15°.

Reproducibility of ChAt Procedure

Typically, duplicate samples of each brain section have been analyzed. The reproducibility

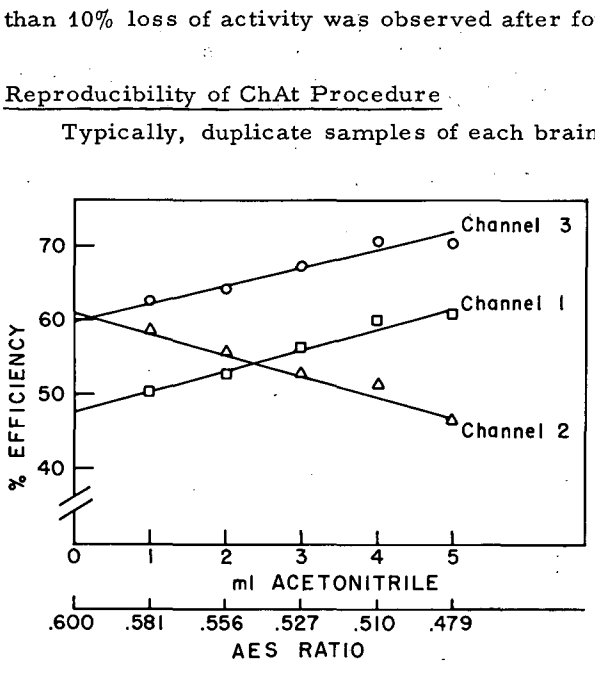

XBL 676-1086

Fig. 3. Effect of acetonitrile on the efficiency of scintillation counting of ^{14}C in three channels. The total volume (including the acetonitrile) was 19 ml. The settings were: Channel 1, amplification 55%, lower discriminator setting 400, and upper discriminator setting 1000; Channel 2, amplification 9.8%, lower discriminator setting 100, and upper discriminator setting 600; and Channel 3, amplification 40%, lower discriminator setting 100, and upper discriminator setting 1000. The efficiencies are also plotted as a function of the automatic external standard (AES) ratio.

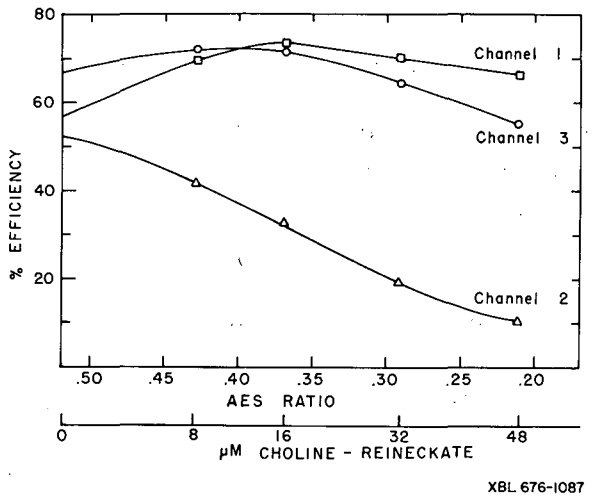

Fig. 4. Effect of choline reineckate on the efficiency of scintillation counting of ^{14}C in three channels. The scintillation mixture consisted of 16 ml of scintillation solution and 3 ml of acetonitrile containing 0, 8, 16, 32, and 48 μM of choline-reineckate. The channel settings were the same as indicated in Fig. 3.

of these duplicate analyses has been high. Data from a series of analyses of 6 sections from 16 rats, summarized in Table III, indicate that the average difference between duplicate samples was 2.5%. In this set of 96 duplicate analyses, only 10 duplicate assays differed by more than 5%, while 17 differed by less than 1%. The average difference of the cerebellum samples was 4.2%. This higher figure was in part due to counting error resulting from low activity.

ChAt of Different Areas of S_1 Rats

As shown in Table III, ChAt activity is lowest in the cerebellum, intermediate in the several cortical areas analyzed, and highest in the medulla and remainder of subcortical brain samples. Variation in activity/mg is observed within the cortex. As is the case with acetylcholinesterase, variability between rats in ChAt activity is small.

Table III. ChAt activity of areas of rat brain.[a]

Area	Weight (mg)	ChAt Activity (μM AcCh/g)	Total ChAt Activity (μM AcCh/hr)
Visual cortex	65 ± 5	4.31 ± 0.20	0.278 ± 0.023
Somesthetic cortex	58 ± 4	4.54 ± 0.39	0.264 ± 0.024
Dorsal cortex	295 ± 17	5.32 ± 0.47	1.57 ± 0.12
Ventral cortex	268 ± 23	7.30 ± 0.48	1.96 ± 0.19
Total cortex	686 ± 37	5.96 ± 0.40	4.12 ± 0.27
Remainder subcortex	477 ± 31	11.56 ± 0.99	5.51 ± 0.58
Cerebellum	220 ± 13	0.78 ± 0.10	0.172 ± 0.024
Medulla	152 ± 12	11.50 ± 0.70	1.75 ± 0.174
Total subcortex	849 ± 54	8.76 ± 0.66	7.43 ± 0.75
Total brain	1535 ± 89	7.53 ± 0.53	11.67 ± 0.95

a. These values were obtained from 12 S_1 60-day-old male rats maintained in an enriched environment for 30 days.[1]

FOOTNOTES AND REFERENCES

†Since this report was written, we have found that 1.2×10^{-3} M eserine salicylate is more suitable.

1. D. Krech, M. R. Rosenzweig, and E. L. Bennett, Physiol. Behav. 1, 99 (1966).
2. R. E. McCaman and J. M. Hunt, J. Neurochem. 12, 253 (1965).
3. B. K. Schrier and L. Shuster, J. Neurochem. 14, 977 (1967).
4. J. Schuberth, Acta Chem. Scand. 17, 233 (1963).
5. F. Fonnum, Biochem. J. 100, 479 (1966).
6. P. Berg, in Methods of Enzymology, Vol. 5, S. Colowick and N. O. Kaplan, Eds. (Academic Press, New York, 1962), p. 461.
7. C. O. Hebb and B. N. Smallman, J. Physiol. 134, 385 (1956).

DYNAMIC METABOLIC REGULATION OF THE PHOTOSYNTHETIC CARBON REDUCTION CYCLE

J. A. Bassham and Martha Kirk

The necessity for metabolic regulation of carbon reduction pathways in photosynthesis became apparent as the result of two discoveries which have altered earlier concepts of photosynthesis. The first of these was the recognition that directs products of photosynthesis include not only carbohydrates, but also amino acids and other compounds. The other discovery was that there is an exchange of molecules of some intermediate compounds of photosynthesis with molecules of the same compounds involved in glycolysis.

Some of the earliest studies of photosynthesis with $^{14}CO_2$ revealed labeling of amino acids and fats at times comparable to those required for the labeling of sugars.[1] Later quantitative tracer studies with $^{14}CO_2$ and photosynthesizing Chlorella pyrenoidosa showed that alanine and other amino acids are formed directly from intermediates of the basic carbon reduction cycle,[2] and that their rate of labeling with ^{14}C can account for as much as 30% of the total $^{14}CO_2$ incorporation during the first minutes of photosynthesis.[3] During that same period, only about one-third as much ^{14}C was found in sucrose, a major carbohydrate product of photosynthesis in Chlorella. Benson and coworkers[4] have shown that galactolipids are rapidly labeled by Chlorella, with 40% of the ^{14}C label of the lipids appearing in the fatty acid moieties after 5 min photosynthesis in Chlorella with $^{14}CO_2$.

This direct formation of amino acids and fatty acids from intermediates of the photosynthetic carbon reduction cycle makes these compounds equivalent in some respects to free sugars as immediate products of carbon reduction in photosynthesis. It seems likely that some regulation of the flow of carbon from the basic cycle to the production of these compounds must be required in order to maintain a balance between their syntheses and their utilization in the further syntheses of macromolecules.

Green plant cells pass through various stages of development requiring synthesis of changing proportions of fats, proteins, carbohydrates, and other macromolecules such as nucleic acids. Cells in the mature leaves of such plants as sugar beet may produce almost exclusively carbohydrate for translocation to other parts of the plant. Yet in young, rapidly growing leaves of these same plants, a considerable portion of the photosynthetically reduced carbon must be allocated to the production of proteins and lipids and other materials required for the building of the chloroplasts themselves and of the new cells.

To a large extent, of course, the regulation of these syntheses of macromolecules will be accomplished through the control of enzyme synthesis, according to mechanisms that are rapidly being discovered. Nevertheless, there would seem to be a need for a dynamic metabolic regulation of the pool sizes of these compounds. This regulation should be capable of rapid response to changing environmental conditions and should not be dependent upon synthesis of new enzymes. In short, the type of regulation needed to maintain reasonable pool sizes for small molecules produced directly from the photosynthetic carbon reduction cycle probably is dynamic regulation of key enzymes at or near the branch points in the cycle itself.

The second development which focused attention on the need for metabolic regulation was the finding that the intermediate compounds of photosynthesis and glycolysis in green cells are not completely isolated from one another. Earlier studies with Chlorella and $^{14}CO_2$, as well as ^{14}C-labeled glucose, had suggested that there is some separation between certain pools of intermediates of the photosynthetic carbon reduction cycle and of glycolysis and respiration.[5] However, it is now clear that there is an important exchange between some pools of photosynthesis and of glycolysis. Heber and Willenbrinck[6] reported that some labeled intermediates of the photosynthetic carbon cycle are transported from the chloroplast to the cytoplasm in Elodea. Based on his experiments with Elodea and Spinacia, Heber[7] concluded that the phosphoglyceric acid (PGA),† dihydroxyacetone phosphate (DHAP), and fructose-1,6-diphosphate (FDP) "function as transport metabolites in photosynthesis." While those results were obtained by a post-mortem "non-aqueous" isolation of chloroplasts after photosynthesis with tracers by the intact leaf, the findings have in general been confirmed by other techniques described below.

In the meantime, studies of ^{14}C- and ^{32}P-labeling of metabolites by Chlorella, photosynthesizing in light and respiring in the dark, had demonstrated a clear interaction between the intermediate compounds of photosynthesis and glycolysis.[8] The results of a similar study are shown in Fig. 1. After some 14 min of photosynthesis with $^{14}CO_2$ and 34 min with ^{32}P-labeled phosphate, PGA was saturated with respect to labeling by each of these isotopes. When the light was turned off and the flow of electrons and ATP from the photochemical apparatus stopped, the reduction of PGA abruptly ceased, leading to a rapid rise in both ^{32}P and ^{14}C label. After about 30 sec the level of PGA declined, since the photosynthetic carboxylation reaction had by then stopped and PGA was no longer being formed. The decline in the level of labeled PGA is due to its conversion to other products, such as alanine, and its consumption by respiration via the tricarboxylic cycle (see Fig. 2).

After about 2 min the level of ^{32}P-labeled PGA rises to a steady-state level in the dark which is higher than the steady-state level in the light, while the ^{14}C-labeling of PGA continues to decline. This shows that the doubly-labeled PGA is being replaced by newly formed, singly-labeled PGA made from the glycolysis of unlabeled carbohydrate stores. Glycolysis of course introduces the same ^{32}P label as photosynthesis, since in each case the phosphate group is derived from a rapidly-turning-over pool of ATP, whether the latter is formed by photosynthetic phosphorylation or oxidative phosphorylation.

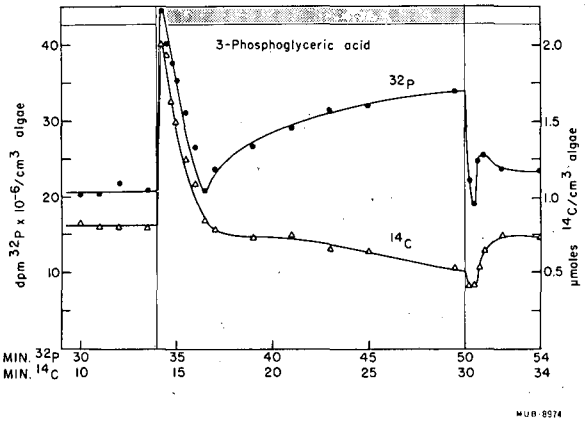

Fig. 1. Levels of ^{14}C- and ^{32}P-labeled PGA in Chlorella pyrenoidosa during photosynthesis and respiration.

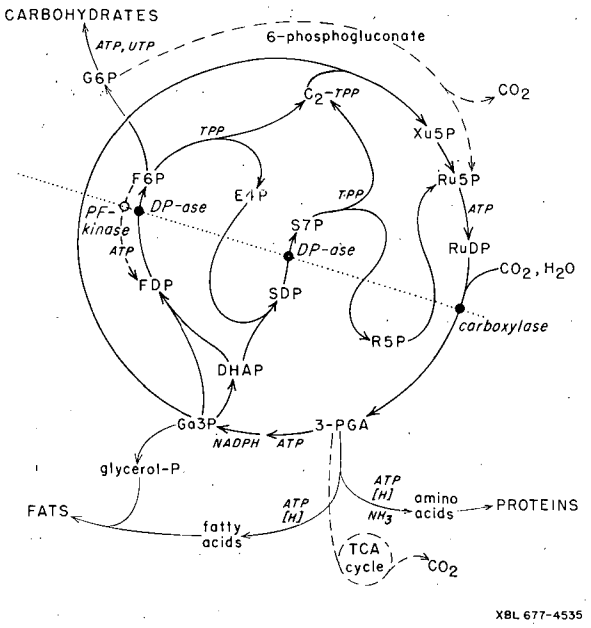

Fig. 2. Relations between photosynthesis, glycolysis, and synthesis of macromolecules, and regulatory control points. Compounds of the photosynthetic carbon reduction cycle above the dotted line are those which tend to be retained in the chloroplasts, those below the dotted line have been found to be readily transported from chloroplasts. Intermediate compounds in paths other than the photosynthetic carbon reduction cycle are not shown.

Abbreviations used in this figure and in the text are: PGA, 3-phosphoglyceric acid; DHAP, dihydroxyacetone phosphate; Ga3P, glyceraldehyde-3-phosphate; FDP, fructose-1, 6-diphosphate; F6P, fructose-6-phosphate; SDP, sedoheptulose-1, 7-diphosphate; S7P, sedoheptulose-7-phosphate; E4P, erythrose-4-phosphate; Xu5P, xylulose-5-phosphate; R5P, ribose-5-phosphate; Ru5P, ribulose-5-phosphate; RuDP, ribulose-1, 5-diphosphate; G6P, glucose-6-phosphate.

Up to this point the results could be interpreted as indicating isolated pools of PGA for photosynthesis and glycolysis. However, if this were the case, when the light is again turned on the glycolytic pool of PGA should be unaffected and the ^{32}P-labeling should not drop significantly more than the ^{14}C label. The ^{32}P label of the PGA drops very much more than the ^{14}C label. This drop indicates that all of the ^{32}P-labeled PGA is immediately affected by the light. Thus, photosynthesis acts on the entire labeled pool of PGA. This data clearly established the fact that PGA, formed in the dark by glycolysis, can be immediately used in the photosynthetic carbon reduction cycle when the light is turned on.

With the interchangeability of PGA between photosynthesis and glycolysis complicating the kinetic studies, it became increasingly urgent that we perform parallel studies of photosynthesis in isolated chloroplasts. Chloroplasts capable of photosynthetic reduction of carbon dioxide at only 20% (usually much less)[9] of the rates to be expected in vivo did not appear to be suitable for quantitative studies, particularly of regulatory mechanisms. By modifying a number of conditions in isolation and incubation, it was possible to obtain rates of carbon dioxide assimilation by isolated spinach chloroplasts approaching in vivo rates for healthy leaves, at least for 10 or 15 min.[10] However, when the labeling of various products of this photosynthesis by isolated spinach chloroplasts was measured,[11] it was apparent that the levels of certain intermediates of the photosynthetic carbon reduction cycle, particularly DHAP, were abnormally high, as compared with levels seen with intact plants. The reason for this difference became clear when we studied the distribution of intermediate products between the chloroplasts themselves and the supernatant solution in which the chloroplasts had been suspended.[11, 12] Over 80% of the carbon fixed appeared in the suspending medium. Of this, by far the greater portion was in PGA and DHAP, with substantial amounts appearing also in FDP, sedoheptulose-1, 7-diphosphate (SDP), and glycolic acid. Ribulose-1, 5-diphosphate (RuDP), fructose-6-phosphate (F6P), glucose-6-phosphate (G6P), and sedoheptulose-7-phosphate (S7P) were well retained in the chloroplasts.

Thus, there is a striking differential behavior in the migration of photosynthetic intermediates from chloroplast to suspending medium. In general, those compounds of the photosynthetic carbon reduction cycle following the carboxylation reaction and preceding the diphosphatase reaction (see Fig. 2) tend to diffuse from the chloroplast to the medium, while those compounds coming after the diphosphatase reaction and preceding the carboxylation reaction (except for pentose monophosphates) are well retained inside the chloroplasts.

Given the interaction between the intermediates of photosynthesis and glycolysis and the demonstrated movement of intermediates between chloroplasts and cytoplasm, it seemed clear that some form of light-dark dynamic metabolic regulation of key enzymes of photosynthesis and glycolysis is required.

Direct kinetic evidence for light-dark changes in the activities of enzymes of the carbon reduction cycle came from the same light-dark studies with Chlorella in the presence of ^{32}P and ^{14}C that were reported above.[8] The level of FDP plus SDP in light and dark is shown in Fig. 3. When the light is first turned off, these sugar diphosphates drop in concentration to nearly zero, as would be expected from the fact that light is no longer supplying cofactors for the reduction of PGA to triose phosphate, from which these sugar diphosphates are formed. However, the level of FDP plus SDP then rises, passing through a maximum to a new steady-state dark level. This result clearly suggests that the diphosphatase has become inactive and that a phosphofructokinase has been activated in the dark, and is utilizing ATP formed by oxidative phosphorylation. Note also that the sugar diphosphates formed in the light are made partly from endogenous sugars that are not fully labeled with ^{14}C.

The levels of ATP, as well as UTP and ADP, in light and dark are shown in Fig. 4. It can be seen that while the ATP initially drops rapidly when the light is turned off, it soon rises to a high dark steady-state level due to oxidative photophosphorylation. Thus, there is ample ATP for the PFkinase reaction.

The time required for activation of the diphosphatase reaction in light was revealed by a detailed kinetic experiment with Chlorella in which, following a period of steady-state photosynthesis with $^{14}CO_2$ and a period of darkness, the light was turned on again and samples were taken at 10-sec intervals for the next 2 min. In Fig. 5 it can be seen that the level of FDP rises very sharply for 30 sec. We attribute this rapid rise to the onset of reduction of PGA due to cofactors from the light reactions, together with the inactivity of the diphosphatase following a period of darkness. After 30 sec the diphosphatase has been activated and the level of fruc-

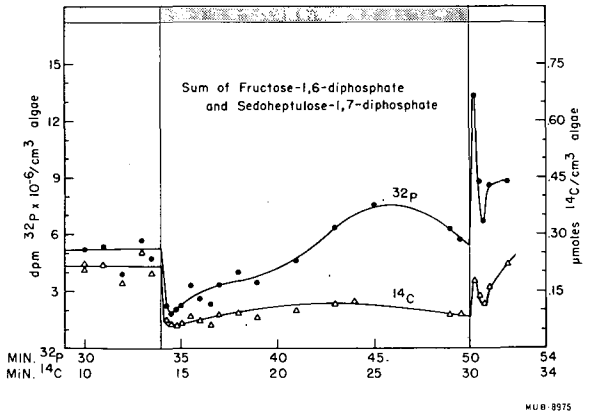

Fig. 3. Levels of ^{14}C-labeled FDP plus SDP in Chlorella pyrenoidosa during photosynthesis and respiration.

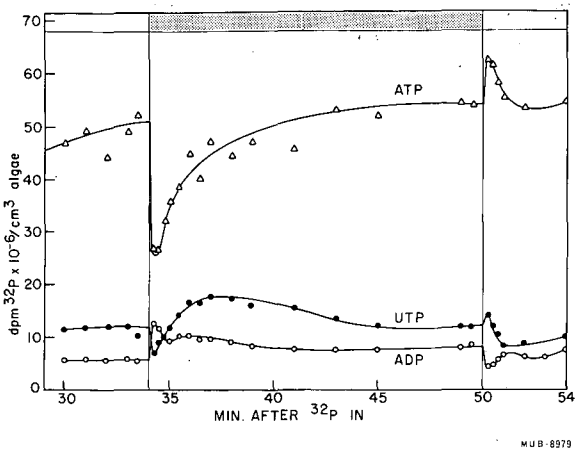

Fig. 4. Levels of ^{32}P-labeled ATP, UTP, and ADP, in Chlorella pyrenoidosa during photosynthesis and respiration.

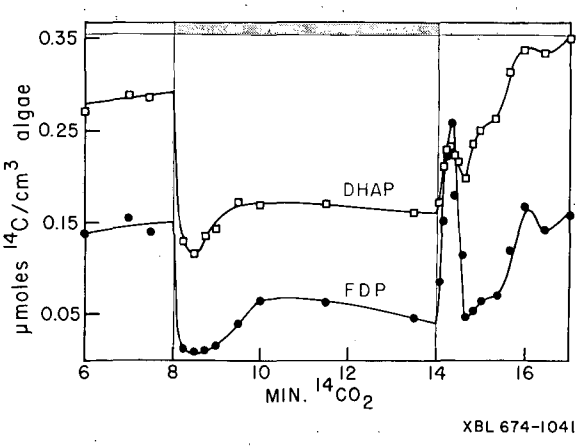

Fig. 5. Levels of ^{14}C-labeled FDP and DHAP, in Chlorella pyrenoidosa, during photosynthesis and respiration.

tose diphosphate then drops rapidly, as the photosynthetic carbon reduction cycle is not yet fully operative and the rate of reduction of PGA to triose phosphate has not reached the steady-state level. Later, the labeled fructose diphosphate level rises more slowly towards the steady-state level.

Fig. 5 also shows that the transient increase in DHAP is much smaller than that of FDP. This means that the transient peaks are not due merely to a wave of carbon coming from the sudden reduction of a large pool of PGA. If that were the case, the transient peak in DHAP, which precedes FDP in the cycle, would be higher than the peak in FDP. Instead, the smaller DHAP peak is a reflection of the higher FDP peak, and indicates an active, reversible aldolase reaction in light and dark.

Also, if the transient peaks were merely wave phenomena induced by the sudden reduction of PGA, one would expect the wave to pass on to the next intermediate in the cycle, F6P, but at a diminished magnitude. What actually happens can be seen in Fig. 6, which compares the behavior of labeled F6P with that of FDP. The level of F6P initially drops while the diphosphatase is inactive and only begins to rise at 30 sec, or precisely the time when the diphosphatase has suddenly become activated. Once the diphosphatase is activated there is a transient peak in the levels of F6P before steady state is achieved. This is due to the sudden removal of the diphosphatase bottleneck, allowing carbon from the accumulated FDP to flow into the sugar monophosphate pool. Precisely the same situation is seen with SDP and S7P (Fig. 7).

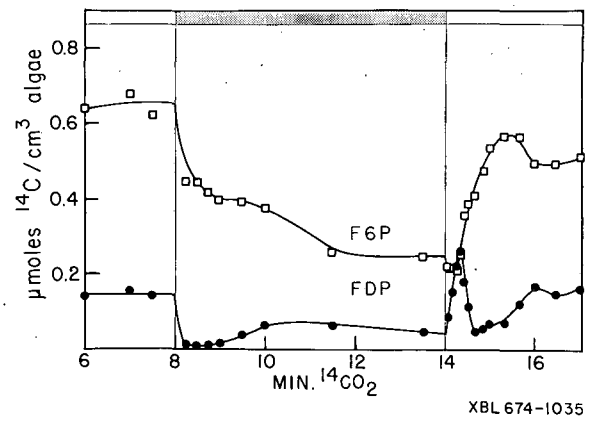

Fig. 6. Levels of ^{14}C-labeled FDP and F6P, in Chlorella pyrenoidosa, during photosynthesis and respiration.

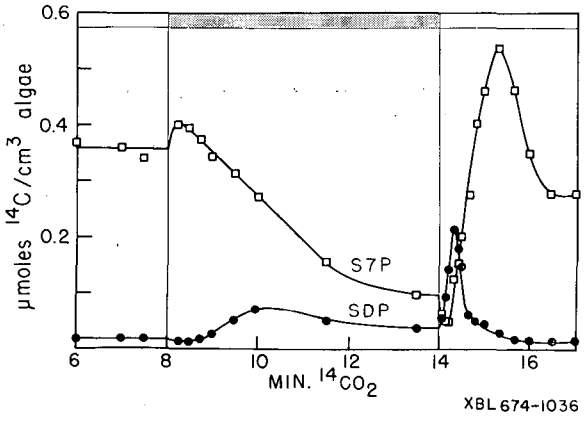

Fig. 7. Levels of ^{14}C-labeled SDP and S7P, in Chlorella pyrenoidosa, during photosynthesis and respiration.

The only difference is in the steady-state pool sizes of the compounds involved. This similarity in the transient peaks of FDP and SDP strongly suggests an identical mechanism of regulation and quite possibly that the same diphosphatase operates for both reactions.

The possibility that the transient peak in FDP and SDP could be caused by residual dark PFkinase activity seems unlikely. PFkinase activity during the first seconds of light should not be greater than the dark activity. The level of ATP does not rise more than 15% when the light is turned on (Fig. 4). The level of F6P, as just mentioned, initially drops.

Evidence for the light-dark regulation of the carboxylation reaction also came first from the light-dark studies of Chlorella pyrenoidosa with $^{14}CO_2$ and $H^{32}PO_4^{-2}$, described earlier.[8] When the light was turned off, the level of the carboxylation substrate, RuDP, fell rapidly at first. After 2 min darkness, the rate of fall in RuDP level was no longer proportional to the RuDP level, indicating that the activity of the enzyme for this reaction had diminished.

Further evidence for the light activation of the carboxylation reaction came from studies of isolated spinach chloroplasts.[11] Fig. 8 shows that when the light was turned off following a period of photosynthesis with spinach chloroplasts, the level of ribulose diphosphate at first dropped rapidly but then leveled off at virtually a constant value in the dark, indicating that the carboxylation reaction was no longer active. When the light was turned on again, the level of RuDP rose very rapidly due to the inactivity of the carboxylation reaction and to the production of ATP from the light, which is required by the ribulose phosphate kinase to convert Ru5P to RuDP. Subsequently, the level of RuDP declined towards a steady-state level.

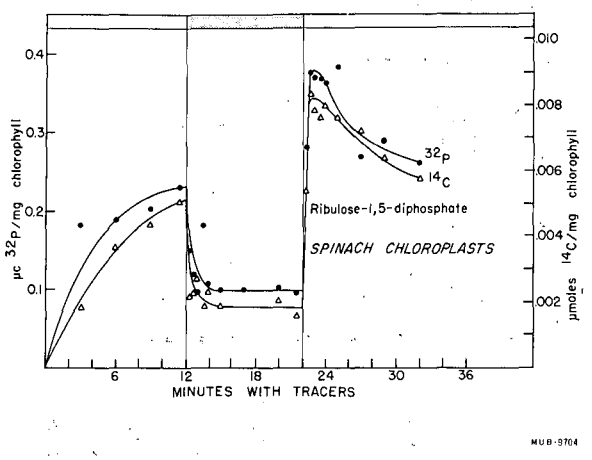

Fig. 8. Levels of RuDP labeled with ^{14}C and ^{32}P in isolated spinach chloroplasts, photosynthesizing, and in the dark.

An even more impressive proof of the inactivity of the carboxylation reaction in the dark is shown in Table I.[13] In this light-dark-light experiment with spinach chloroplasts photosynthesizing with $^{14}CO_2$, additions of ATP and of ATP + R5P were made to separate flasks of chloroplasts just after the light was turned off. As can be seen, the effect of the additions was to maintain the level of RuDP in the dark at its previous light level. In spite of this, there was no fixation in the dark following a period of very active fixation of $^{14}CO_2$ in the light. When the light was again turned on, a smaller but substantial rate of $^{14}CO_2$ fixation was seen in all three flasks. Thus, in this experiment both substrates, RuDP and $^{14}CO_2$, were present in the chloroplasts in the dark, but no carboxylation occurred. Nevertheless, the system was not permanently inactivated, for subsequent light was able to stimulate high fixation rates.

The reason for light-dark diphosphatase regulation seems obvious. Given the diffusion of ATP and of some sugar phosphates between chloroplasts and cytoplasm, phosphofructokinase and fructose diphosphatase should not be active at the same time, lest they together operate as an ATPase.

The reasons for regulation of the carboxylation reaction were not so apparent. Green cells contain a highly active oxidative pentose phosphate cycle. This cycle is immediately activated when the light is turned off, as indicated by the data shown in Fig. 9, obtained during the previously described steady-state experiment with photosynthesizing Chlorella in the presence of $^{14}CO_2$ and ^{32}P-labeled phosphate. As soon as the light is turned off, both the ^{32}P and ^{14}C label of 6-phosphogluconic acid rise rapidly and are maintained at an appreciable level during the entire dark period. When the light is again turned on, the formation of 6-phosphogluconic acid ceases.

The site of the operation of this oxidative pentose phosphate cycle may well be within the chloroplasts. It was found earlier[14] that the addition of vitamin K to photosynthesizing Chlorella causes the immediate appearance of 6-phosphogluconic acid, even while the light is on. Vitamin K is supposed to cause the short circuiting of electrons being transported through the photoelectron transport system, thereby leading to a cyclic photophosphorylation and preventing the reduction of $NADP^+$.

There is evidence[15] that $NADP^+$ and NADPH are not transported between chloroplasts and cytoplasm. Since the effects caused by vitamin K or by interruption of the light seem to be likely results of interruption of photoelectron transport, the sudden appearance of 6-phospho-

Table I. Light-dark-light experiment with spinach chloroplasts photosynthesizing $^{14}CO_2$

	1st Light Period		Dark Period		2nd Light Period	
	Rate[a]	RuDP[a]	Rate	RuDP	Rate	RuDP
Control	143	0.08	-3	0.02	82	0.23
+ ATP	154	0.10	-10	0.07	104	0.37
+ ATP, R5P	145	0.08	-3	0.08	86	0.27

a. Rates are given in μmoles $^{14}CO_2$ (mg Chl hr)$^{-1}$; RuDP concentration is given in μmoles ^{14}C (mg Chl)$^{-1}$.

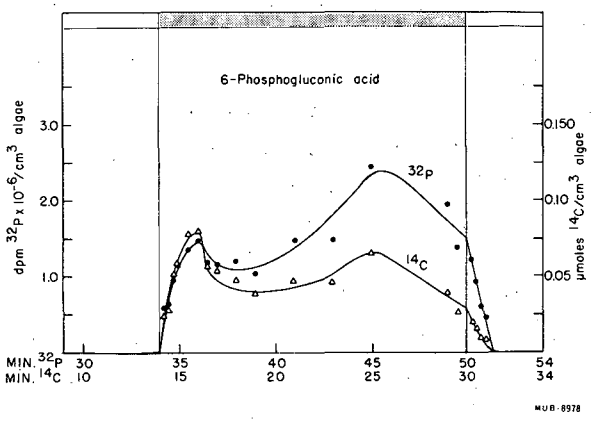

Fig. 9. Levels of 6-phosphogluconic acid labeled with ^{14}C and ^{32}P, in Chlorella pyrenoidosa, during photosynthesis and respiration.

gluconic acid looks like an indication of operation of the oxidative pentose phosphate cycle within the chloroplasts.

While there is probably no oxidative electron transport system within the chloroplasts, NADPH produced by the operation of the oxidative pentose phosphate cycle could be used for biosyntheses within the chloroplasts--for example, the conversion of sugars to fatty acids. Apparently ATP diffuses readily from the cytoplasm into the chloroplasts,[12] and ATP, as already mentioned, is rapidly produced by oxidative phosphorylation in the cytoplasm. Thus, biosynthesis can proceed inside the chloroplasts in the dark with ATP from the cytoplasm and NADPH from the operation of the oxidative pentose phosphate cycle in the chloroplasts.

If this hypothesis is correct, then there should be a regulatory mechanism which in the dark would block the transformation of pentose monophosphates to RuDP to PGA. Only one of these two steps need be inactive in the dark, and it appears that it may be the carboxylation step from ribulose diphosphate to PGA. We have already demonstrated (Table I) that with added ATP, pentose monophosphates can be converted to ribulose diphosphate in the dark.

What is the mechanism of the light-dark regulation of the diphosphatase and ribulose diphosphate reactions? Isolated enzymes which catalyze these reactions are: D-fructose-1,6-diphosphate, 1-phosphohydrolase, 3.1.3.11 (hexose diphosphatase), and 3-phospho-D-glycerate carboxy-lyase (dimerizing), 4.1.1.39 (ribulosediphosphate carboxylase). Both enzymes are characterized by a pH optimum which is higher than normal physiological pH for chloroplasts and by a requirement for a high level of magnesium ion.[16,17] Activation of these enzymes by light could be the result of movements of magnesium and hydrogen ions through membranes.

Dilley and Vernon[18] reported a light-dependent uptake of H^+ and an efflux of K^+ and Mg^{++} ion by isolated spinach chloroplasts. This reported ion flow might appear at first to be contrary to that required for enzyme activation. However, the light-driven flow of ions is across the thylakoid membranes within the chloroplasts, and probably leads to a flow of hydrogen ions from the stroma region into the membrane-enclosed thylakoids, and a flow of magnesium ions into the stroma. Thus, measurements of pH and of metal ions in the suspending medium may well reflect changes occurring within the stroma, particularly if the chloroplasts are broken or "leaky."

Another indication that light-induced ion flow may be responsible for light-dark regulation of the enzymes is to be found in the fact that certain fatty acids and fatty acid esters simultaneously inhibit photophosphorylation, the carboxylation reaction, and the diphosphatase reaction.[19] These inhibitions, which are reversible, are thought to be accomplished by some indirect effect of alteration in the properties of the chloroplast membranes. A likely alteration in membrane properties would be in the light-induced ion pumping capacity. Photophosphorylation is thought to require a pH gradient across the thylakoid membranes,[20] and, like the other inhibited enzymes, photophosphorylation requires magnesium ion.[21]

While light-induced ion pumping provides a plausible mechanism for the light-dark regulation of the diphosphatase and carboxylation reactions, we visualize a different, but as yet unknown, mechanism as providing a fine regulation of the diphosphatase reaction when plants are photosynthesizing with the lights on. At all times while photosynthesis is proceeding, there would be sufficient diphosphatase activity to permit the cycle to regenerate pentose phosphates at a steady-state rate sufficient to provide for the operation of the basic photosynthetic carbon reduction cycle. However, additional diphosphatase activity would be so adjusted as to either pile up the excess fixed carbon at the level of PGA, DHAP, and FDP, which would be used for biosynthesis of proteins, fats, and other materials; or, with greater diphosphatase activity, the excess carbon would be accumulated in fructose-6-phosphate which could then be converted to carbohydrates (Fig. 2). This type of regulation would thus satisfy the changing requirements for biosynthesis in response to physiological change, such as growth and development.

We are inclined to make two predictions about this mechanism. First, it should be related to hormonal or genetic control and may well involve the adjustment of a regulatory factor by the activity of an inducible enzyme. Second, this regulatory factor may exert its effect through some quantitative change in the light activation. In this way it could provide the fine, or vernier, control needed to insure the precise diphosphatase activity to keep the basic carbon cycle running while at the same time adjusting the supply of carbon to biosynthetic pathways.

FOOTNOTES AND REFERENCES

†A list of abbreviations used in this paper is given with Fig. 2.

1. A. A. Benson, J. A. Bassham, M. Calvin, T. C. Goodale, V. A. Haas, and W. Stepka, J. Am. Chem. Soc. 72, 1710 (1950).
2. J. A. Bassham, A. A. Benson, L. D. Kay, A. Z. Harris, A. T. Wilson, and M. Calvin, J. Am. Chem. Soc. 76, 1760 (1954).
3. David C. Smith, J. A. Bassham, and Martha Kirk, Biochim. Biophys. Acta 48, 299-313 (1961).

4. A. A. Benson, R. Wiser, R. A. Ferrari, and J. A. Miller, J. Am. Chem. Soc. 80, 4740 (1958).
5. V. Moses, O. Holm-Hansen, J. A. Bassham, and M. Calvin, J. Mol. Biol. 1, 21-29 (1959).
6. U. Heber and J. Willenbrinck, Biochim. Biophys. Acta 82, 313 (1964).
7. U. Heber, in Biochemistry of Chloroplasts, Vol. II, T. W. Goodwin, Ed. (Academic Press, London and New York, 1967), pp. 71-87.
8. T. A. Pedersen, Martha Kirk, and J. A. Bassham, Physiol. Plantarum 19, 219-231 (1966).
9. D. A. Walker, in Biochemistry of Chloroplasts, Vol. II, T. W. Goodwin, Ed. (Academic Press, London and New York, 1967), pp. 53-69.
10. R. G. Jensen and J. A. Bassham, Proc. Natl. Acad. Sci. 56, 1095 (1966).
11. J. A. Bassham and R. G. Jensen, in Harvesting the Sun: Photosynthesis in Plant Life, A. San Pietro, F. A. Greer, and T. J. Army, Eds. (Academic Press, New York, 1967), pp. 79-110.
12. J. A. Bassham, Martha Kirk, and R. G. Jensen, Biochim. Biophys. Acta (in press).
13. R. G. Jensen and J. A. Bassham, Biochim. Biophys. Acta (in press).
14. E. S. Gould and J. A. Bassham, Biochim. Biophys. Acta 102, 9-19 (1965).
15. U. Heber and K. A. Santarius, Biochim. Biophys. Acta 109, 391 (1965).
16. A. Weissbach, B. L. Horecker, and J. Hurwitz, J. Biol. Chem. 218, 795-810 (1956).
17. J. Preiss, M. L. Biggs, and E. Greenberg, J. Biol. Chem. 242, 2292 (1967).
18. R. A. Dilley and L. P. Vernon, Arch. Biochem. Biophys. 111, 365 (1965).
19. T. A. Pedersen, Martha Kirk, and J. A. Bassham, Biochim. Biophys. Acta 112, 189-203 (1966).
20. A. T. Jagendorf and F. Uribe, in Energy Conversion in the Photosynthetic Apparatus, Brookhaven Symposia in Biology, No. 19, 1967, p. 215.
21. D. I. Arnon, F. R. Whatley, and M. B. Allen, J. Am. Chem. Soc. 76, 6324 (1954).

THE BIOSYNTHESIS OF OPIUM ALKALOIDS. RETICULINE AS THE BENZYLTETRAHYDROISOQUINOLINE PRECURSOR OF THEBAINE IN BIOSYNTHESIS WITH CARBON-14 DIOXIDE†

Robert O. Martin, Mitchum E. Warren, Jr., and Henry Rapoport

The natural occurrence of the diphenolic benzyltetrahydroisoquinoline alkaloid, reticuline, was established in fresh budding plants and seedlings of Papaver somniferum L. Exposure of such plants to $^{14}CO_2$ for 1-3 hr was followed by determination of the radioactivity incorporated: (a) into reticuline and thebaine (I) and (b) into the N- and O-methyl groups for both alkaloids. These results confirm those from feeding experiments, and establish beyond question the role of reticuline as the true biosynthetic benzyltetrahydroisoquinoline precursor of the hydrophenanthrene alkaloids. The high rate of incorporation of radioactivity into the total alkaloids as well as into thebaine and reticuline, both in seedlings and in mature plants, should place beyond doubt the intimate involvement of these alkaloids in the economy of the plant. Our findings constitute positive evidence for the operation of the same biosynthetic relationships (i.e., CO_2 → reticuline → thebaine → codeine → morphine) in seedlings as in mature plants. Simple chambers were developed for the exposure of single mature plants and seedlings to $^{14}CO_2$. The potential of gas chromatography with simultaneous mass and activity measurement, used in conjugation with carbon-14 dioxide feeding of plants in order to detect small amounts of active metabolites and to compare specific activities of related compounds, is clearly illustrated.

---

†Abstract of a paper published in Biochemistry 6, 2355 (1967).

CODEINONE AS THE INTERMEDIATE IN THE BIOSYNTHETIC CONVERSION OF THEBAINE TO CODEINE†

G. Blaschke, H. I. Parker, and H. Rapoport

Formation of codeine from thebaine must involve an additional intermediate, since two processes occur, reduction and demethylation. The nature of this intermediate depends upon which process occurs first. Thebaine could be reduced to codeine methyl ether followed by demethylation to codeine; or demethylation could occur first, yielding codeinone followed by reduction to codeine. Neither codeine methyl ether nor codeinone has been isolated from fresh plants; however, codeine methyl ether has been found in opium. We have now found evidence that codeinone is the intermediate in the biosynthetic conversion of thebaine to codeine. Thus, the later steps in the biosynthesis of morphine have been shown to involve seven compounds in the following sequence: reticuline → solutaridine → solutaridinol → thebaine → codeinone → codeine → morphine.

---

†Abstract of paper published in J. Am. Chem. Soc. 89, 1540 (1967).

THE SYNTHESIS OF THEBAINE AND NORTHEBAINE FROM CODEINONE DIMETHYL KETAL†

Henry Rapoport, Calvin H. Lovell, Helen R. Reist, and Mitchum E. Warren, Jr.

A synthesis of thebaine and northebaine has been developed from codeinone dimethyl ketal and norcodeinone dimethyl ketal. Attempts to prepare the ketal by the action of trimethyl orthoformate on codeinone led only to 8-methoxy-Δ^6-dihydrothebaine. However, addition of methyl hypobromite to Δ^6-dihydrothebaine gave 7-bromodihydrocodeinone dimethyl ketal, and dehydrobromination of the latter gave codeinone dimethyl ketal. Acid-catalyzed elimination of methanol resulted in thebaine; but this reaction was erratic, and codeinone was an accompanying by-product. Good yields of thebaine from codeinone dimethyl ketal were achieved by using phosphorus oxychloride. Northebaine was obtained in the same way from norcodeinone dimethyl ketal, the latter being prepared by the action of cyanogen bromide on codeinone dimethyl ketal followed by lithium aluminum hydride hydrogenolysis of the N-cyano derivative to the nor compound. A method for separating ketonic, α,β-unsaturated ketonic, and nonketonic alkaloidal material based on formation of the bisulfite addition compounds is described.

---

†Abstract of paper published in J. Am. Chem. Soc. 89, 1942 (1967).

THE BIOSYNTHESIS OF NICOTINE IN NICOTIANA GLUTINOSA FROM CARBON-14 DIOXIDE. LABELING PATTERN IN THE PYRROLIDINE RINGS†

Arnold A. Liebman, Bradford P. Mundy, and Henry Rapoport

A systematic degradation has been developed which permits isolation of each carbon atom of the pyrrolidine ring of nicotine. The independent synthesis of specifically labeled intermediates obtained during this sequence and their degradation have confirmed the integrity of the entire process. This degradation has been applied to numerous samples of nicotine obtained from short-term $^{14}CO_2$ biosynthesis with N. glutinosa, and in each experiment the pyrrolidine ring showed an unsymmetrical labeling pattern, a condition contrary to the accepted symmetrical intermediate hypothesis of pyrrolidine ring formation. Ornithine feeding experiments, from which the symmetrical theory had evolved, were applied to N. glutinosa, and results were identical with those in other species. These experiments establish a greatly different labeling pattern in the pyrrolidine ring from CO_2 than from preformed precursors such as ornithine.

---

†Abstract of paper published in J. Am. Chem. Soc. 89, 661 (1967).

COMPARTMENTATION OF THE METABOLISM OF LACTOSE, GALACTOSE, AND GLUCOSE IN ESCHERICHIA COLI†

D. C. H. McBrien and V. Moses

Compartmentation phenomena have been studied in the course of the simultaneous metabolism of glucose, galactose, and lactose by cells of Escherichia coli which were induced for either the lac operon, the gal operon, both, or neither. Metabolic patterns were investigated in each phenotype by incubating parallel identical cultures with the three sugars in equal chemical concentration but labeled differently with ^{14}C. The four labeled substrates were glucose, galactose, and lactose labeled either exclusively in the glucose moiety or exclusively in the galactose moiety.

The metabolites from free glucose in the medium equilibrated with those from free galactose in the medium, but did not equilibrate with metabolic products derived from glucose generated endogenously by the hydrolysis of lactose. Similarly, metabolic products derived from galactose formed in the hydrolysis of lactose equilibrated with those from glucose from the same source, but not with metabolic intermediates formed from either free glucose or free galactose in the medium. Other interpretations of these results, not involving metabolic compartmentation, have been considered and found inadequate to account for the observed results. Some of the implications of compartmentation in bacterial cells are discussed.

---

†Abstract of paper published in J. Gen. Microbiol., 1968 (in press).

BIOPHYSICAL CHEMISTRY AND BIOPHYSICS

RIBONUCLEIC ACID STRUCTURES

Ignacio Tinoco, Jr.

INTRODUCTION

The work of each cell in a living organism is now thought to be controlled by transfer of information from DNA (deoxyribonucleic acid) to RNA (ribonucleic acid) to protein.[1] The DNA stores all the information and imparts some of it to the messenger RNA. This message is in turn translated into a polypeptide chain which is folded into a protein necessary for the function of the cell. Many questions are being asked about both of these systems. We are all interested (either scientifically or personally) in the evolution, replication, and development of these systems. I will limit myself in this article to the chemistry of the RNA-to-protein step. In particular, the way in which the structures of the various RNA molecules determine their functions will be discussed.

There are three known roles for RNA in protein synthesis. Messenger RNA contains the coded amino acid sequence of the protein in a linear sequence of base triplets. Each of these codons is translated into its synonymous amino acid by transfer RNA. This process occurs in contact with ribosomes, which are made up of protein and ribosomal RNA.

RNA molecules are polymers of mononucleotide units. Each unit contains an aromatic base, a sugar, and a phosphate group. There are only four bases, which are specified by the DNA and which in turn can specify the amino acids of proteins. These coding bases are shown in Fig. 1: there are two pyrimidines (uracil and cytosine) and two purines (adenine and guanine). The transfer of genetic information finally must be understood in terms of the interactions of these bases with each other, with the amino acids of the proteins, and with the rest of their environment.

The configuration of the ribose sugar attached to the base and the linkage of the units to form the polynucleotide are shown in Fig. 2. The carbons of the ribose are designated by primed numbers beginning with the carbon attached to the base. The convention that the ribose with the 5' hydroxyl group is always on the left of the polymer, and the 2', 3' hydroxyls are on the right, is also illustrated.

Structural questions that need to be answered about the RNA molecules are: (1) What is the sequence of the 4 bases in the RNA? and (2) How are the bases arranged and why? The first question has a definite answer, which seems nearly impossible to obtain at present except for the smallest RNA molecules. The second question has an indefinitely large number of partial answers. The field is therefore a challenging one.

BASE SEQUENCE

The sequence of bases in each messenger RNA determines the sequence of amino acids in a protein. As a typical protein may contain from one hundred to a few hundred amino acids,

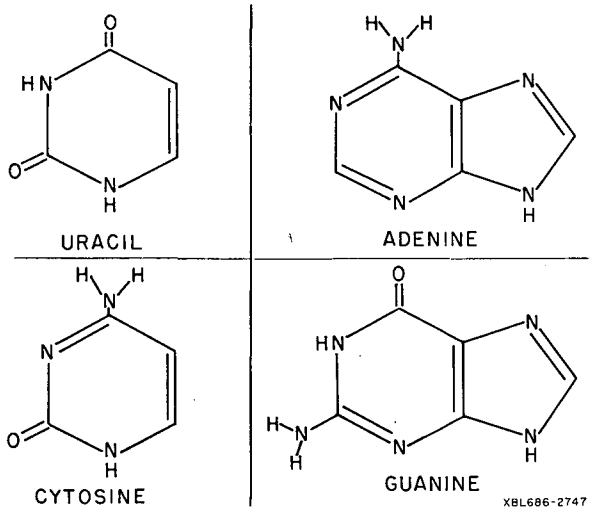

Fig. 1. The four bases in RNA which code for the amino acids polymerized to form proteins.

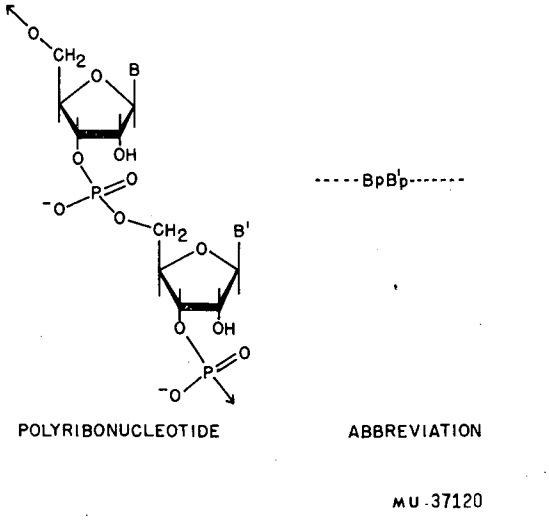

Fig. 2. The units present in RNA. The configuration of the ribose is shown, and the conventional representation and its abbreviation are illustrated.

the typical messenger RNA may contain at least 300 bases. Furthermore, the messenger RNA molecules currently studied have been obtained from viruses. The virus efficiently packages and protects its message in a coat of protein. However, its RNA codes for more than one protein, so that viral RNA molecules usually contain a few thousand bases. If we knew the sequence of these bases, we would know the sequence of the coded amino acids. This in turn would tell us about the coded proteins and the order of synthesis of these proteins. We might also find base sequences inconsistent with present protein coding rules. These sequences might be important for the replication of the RNA or for its binding to ribosomes, for example.

The genetic dictionary has been established by Nierenberg, Ochoa, and many other workers.[2] A recent version[2] is shown in Fig. 3. Each base is represented by the first letter of its name; its structure is shown in Fig. 1. X stands for any of the 4 bases; Pu is a purine, and Py is a pyrimidine. The structures of the side chains of the amino acids are given in the dictionary. Each amino acid is coded by at least one, but usually more, triplet codons. The third base is apparently not very specific in its coding properties. Many correlations are obvious from the figure, but no generally accepted explanations have been published. We would like to have a consistent story to tell about this dictionary. For example, we notice that similar amino acids have similar codons, but differences may occur for any of the three bases. There is UCX and ACX for serine and threonine, UUPy and UAPy for phenylalanine and tyrosine, and finally GAPu and GAPy for glutamate and aspartate. Why? The number of different codons for each amino acid is approximately proportional to the frequency of occurrence of the amino acids in proteins. Methionine (AUG) and tryptophane (UGG) are rare, but serine (UCX, AGPy), arginine (CGX, AGPu), and leucine (CUX, UUPu) are present in large amounts. How this coding scheme evolved so that a particular triplet of bases specifies a certain amino acid is not known.

The message is read from left to right, with definite signals to start a new protein and to

THE GENETIC DICTIONARY

Amino Acid	Triplet	Amino Acid	Triplet
H-	GGX	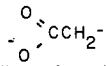	GAPy
	GCX	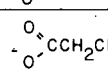	GAPu
	GUX	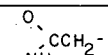	AAPy
	AUPy AUA	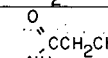	CAPu
	CUX UUPu	$H_2NCH_2CH_2CH_2CH_2$-	AAPu
	UUPy		CAPy
	UAPy	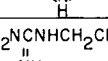	CGX AGPu
	UGG	$HOCH_2$-	AGPy UCX
$HSCH_2$-	UGPy	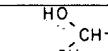	ACX
	CCX	$CH_3SCH_2CH_2$-	AUG
Start	AUG	Stop	UAPu UGA

XBL 683-317

Fig. 3. The genetic dictionary. Each amino acid in a protein is coded by the corresponding triplet of bases in the messenger RNA. The amino acid is represented by the R group in the polypeptide

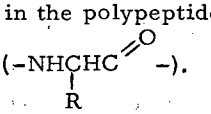

For proline (CCX), the polypeptide chain is also shown. Any of the 4 bases is represented by X, whereas Pu is a purine and Py is a pyrimidine.

end it. The codon AUG begins the message; it signifies that formylmethionine be the first amino acid of the protein. This special amino acid is subsequently removed. The stop signals are apparently either UAA, UAG, or UGA; they do not code for any amino acids.

With this dictionary we could translate a messenger base sequence, if we could only determine the sequence. The problem can be stated very simply. How do you determine the linear arrangement of four different units in a polymer of about 1000 units?

Sequence methods which work for polymers containing about 100 units can not be applied to polymers which are an order of magnitude longer. The overlap method has been used to determine the sequences of transfer RNA molecules containing about 80 nucleotides[2] and a ribosomal RNA containing 120 nucleotides.[3] In this method, two specific enzymes are used to hydrolyse the RNA into two different sets of fragments. All the fragments must be separated and their base sequences determined. The RNA base sequence is then reconstructed, if possible, by looking for sequences consistent with the fragments obtained from both enzymes. Reading the papers[2] describing the application of this method to 100-mers filled me with admiration for the authors and discouraged me from attempting to extend it to 1000-mers.

We have been thinking of sequence methods which could work for any chain length.[4] The one we favor, the chain-length method, does not involve any sequence determinations at all. You simply have to count nucleotides, that is, determine the chain length of various enzymatically produced fragments. There are three steps to the method: (1) Partially hydrolyse with

a specific enzyme. (2) Note fragments which contain an end of the RNA molecule. (3) Determine their chain lengths. The specific enzyme designates the base, and the chain length positions the base with respect to one end of the RNA molecule. This is illustrated in Fig. 4. In this example, T_1 ribonuclease, which catalyzes the hydrolysis of the bond following the 3' phosphate of a guanine nucleotide, is used. To identify fragments containing the left-hand end of the RNA molecule, a label (L^*) must be placed on this end before hydrolysis. The fragments containing the right-hand end of the RNA molecule are already unique. Determination of the chain length of any one of the right-hand-end or left-hand-end fragments specifies the location of a guanine in the RNA. The positions of the guanines deduced from right-hand ends can be checked by those deduced from left-hand ends.

In principle this method will work for any RNA molecule. In practice, the third step—determination of chain length—limits the application. The first step is straightforward. Enzymes specific for guanine[5] and pyrimidines[5] are well-known. A cytosine-specific enzyme has been reported.[6] Chemical modification of uracil has been used to make pancreatic ribonuclease specific for cytosine.[7] The second step involves labelling or separating the 5' free hydroxyl (left-hand) or 2', 3' free hydroxyl (right-hand) ends. Many methods for labelling and separating the right-hand ends are known; they all use the specific oxidation of vicinal hydroxyls by periodate.[8-12] The left-hand ends contain the only primary alcohol in the molecule; a phosphate group can be specifically attached to it.[13] Besides providing a label and a point of further chemical modification,[14] this phosphate protects the left-hand end from attack by spleen exonuclease.[15] Therefore, addition of this exonuclease would hydrolyse all fragments except those containing the left-hand ends.

The third step requires the determination of a chain length to one part in a thousand. Furthermore, an average chain length is useless; the exact distribution of chain lengths must be

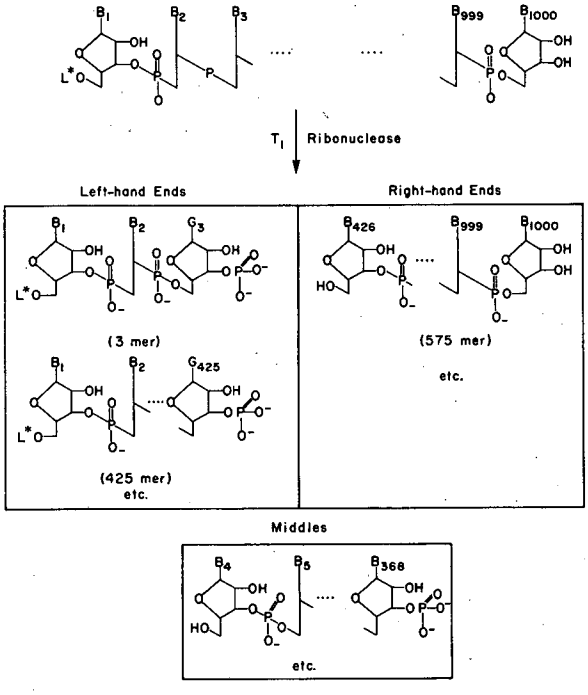

Fig. 4. The chain-length method for determining the sequences of bases in an RNA. The 3-mer and 425-mer found among the left-hand-end fragments place guanine at positions 3 and 425. The 575-mer found among the right-hand-end fragments verifies guanine at position 425. The middle fragments give no sequence information.

known. Possibilities for doing this include improvement of chromatographic methods,[16] electron microscopy,[17] and mass spectroscopy.[18]

The description of this sequence problem and the presentation of a possible solution are included mainly to encourage others to devise better methods which will really work.

THREE DIMENSIONAL STRUCTURES

The field of molecular (or chemical) biology can be considered to have started with the publication of the structure of DNA in 1953.[19] The double-stranded structure in which adenine paired only with thymine (5-methyl uracil), and guanine paired with cytosine immediately implied a mechanism for replication of DNA and specific synthesis of RNA. More recent findings of double-stranded RNA molecules[20] and circular DNA molecules[21] provide more information about the mechanisms of DNA and RNA synthesis. What can be said about the mechanism of protein synthesis, once we know RNA structures? We cannot answer this question until we do know the RNA structures and how they change with environment. But we can learn the differences in transfer RNA molecules which allow each RNA to recognize both its specific amino acid and its specific codon. We can also learn the similarities in transfer RNA structure which allow them all to fit on the ribosomes and to place the amino acids in the proper position for polypeptide formation. We may also learn how the environment can control protein synthesis or how mistakes in synthesis are likely to occur. It is clear that new structural details can lead to new understanding.

For large rigid molecules which can be crystallized, the best method to determine structure is x-ray scattering. However, no polynucleotide has yet been crystallized. Fibers which yield usable x-ray patterns can be pulled from some polynucleotide solutions. These patterns have always led to multistranded structures such as Watson-Crick DNA. As most RNA molecules do not give useful x-ray fiber patterns, we must use less conclusive methods. However, whatever method we use, it will be extremely helpful to know the general rules which characterize polynucleotide structures. These rules are necessary to put constraints on structures which are determined by relatively few experimental measurements. Even if (or when) RNA molecules are crystallized, these rules will be very useful in limiting the number of trial models to be compared with the large amount of x-ray data. Of course, if we knew the complete rules of polynucleotide structure, we need not make any structural measurements at all. From the sequence of bases, the three dimensional structure could be deduced. The types of rules we are looking for include: (1) What parts of RNA structure are definitely fixed by the covalent bonds? (2) What structures are favored by local interactions in the mononucleotides and among nearest neighbors? (3) What structures are most sensitive to solvent? By studying the components of RNA we hope to provide some answers.

Mononucleotides

The most significant aspect of mononucleotide conformation is the position of the base relative to the ribose. What is the average orientation about the glycosidic bond? Analysis of 15 crystal structures of nucleotides and nucleosides by Haschemeyer and Rich[22] showed that the orientation of the base is fairly restricted. Two orientations differing by 180° are possible; these were defined as *syn* and *anti*.[23] For the two pyrimidines, the carbonyl group at the 2 position tends to point away from the sugar; this is the *anti* orientation. The purines showed

more variation. Adenine compounds were anti (the six-membered ring away from the sugar), but the one guanine compound studied was syn. The authors concluded from calculations of steric repulsions that, although syn and anti conformations were possible for both purine and pyrimidine nucleosides, the syn conformation was much less likely for the pyrimidines. Calculations by Davis[24, 25] of repulsive and attractive forces between a base and ribose or deoxyribose lead to similar conclusions. Two minima in the potential energy for rotation about the glycosidic bond were found; they correspond to syn and anti. For adenosine and guanosine, the difference between the syn and anti minima is 1 to 2 kcal/mole; and the barriers to rotation are low. For cytidine and uridine, the anti minimum is favored by 5 to 7 kcal/mole; and the barrier between the syn and anti conformation is very high.

The conclusion is that polynucleotide structures should have the pyrimidine bases anti unless there is a distinct improvement in interaction with the pyrimidines syn. Purines may be either syn or anti. X-ray data for DNA and polyadenylic acid show the anti conformation for the bases, but the polyinosinic and polycytidylic acid complex may contain syn conformations.[22]

Dinucleotides

To find out about the orientation of one base relative to its neighbors in a polynucleotide chain we can study dinucleotides. Warshaw[26] has studied the optical rotatory dispersion and ultraviolet absorption of the sixteen dinucleoside phosphates in aqueous solution at three pH's. Brahms, Michelson, and coworkers have done similar work.[27, 28] Chan and coworkers have measured the nuclear magnetic resonance of some of these compounds.[29, 30] The aim of all these investigations was to determine the conformations of the dinucleoside phosphates. Properties of the compounds were compared with those of their constituents. The extreme examples of the sixteen dinucleoside phosphates are adenylyl (3'-5') adenosine, ApA, and uridylyl (3'-5') uridine, UpU.[26] These compounds differ most in properties and presumably in conformation.

The optical rotation per residue of UpU at pH 7 and 25°C is compared with that of uridylic acid in Fig. 5. There are only small differences. However, the same comparison (Fig. 6) for ApA shows a marked difference in magnitude and shape of the optical rotatory dispersion between mononucleotide and dinucleoside phosphate. As the temperature is raised (Fig. 7), the rotation decreases and approaches—but does not reach—the rotation of adenylic acid (or adnosine). This behavior is completely reversible; when the temperature is reduced, the rotation increases. At constant temperature, a non-aqueous solvent such as 95% ethanol (Fig. 8) will cause the rotation to become essentially the same as the mononucleotide.[31] These data imply a strong interaction between the adenine bases at room temperature in neutral aqueous solution. The experimental shape and magnitude of the rotation for ApA can be calculated[32] from a conformation in which the bases are stacked and begin to form a right-handed helix. The exact geometry cannot be determined from the optical rotation, but the sign of the rotation almost surely requires a right-handed helix. From this type of data on 16 dinucleoside phosphates, plus absorption measurements,[26] NMR data,[29, 30] and studies of aggregation of bases,[33, 34] we can conclude that the nucleic acid bases tend to stack in water at neutral pH. However, uracil stacks the least of the bases; and we simplify the results by saying that adenine, guanine, and cytosine stack, but uracil does not.

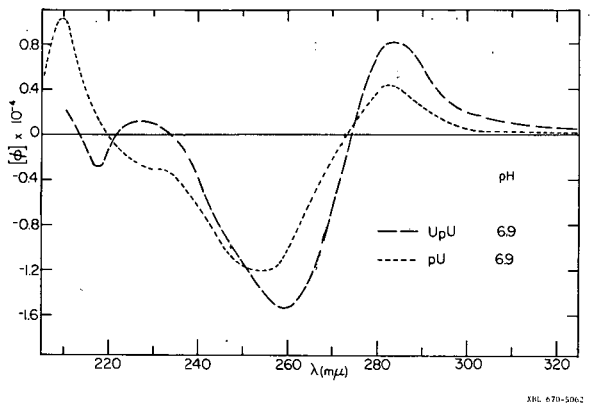

Fig. 5. Comparison of optical rotatory dispersion curves of uridylic acid (5') and uridylyl (3'-5') uridine. The good agreement implies that the bases in this dinucleoside phosphate do not interact strongly.

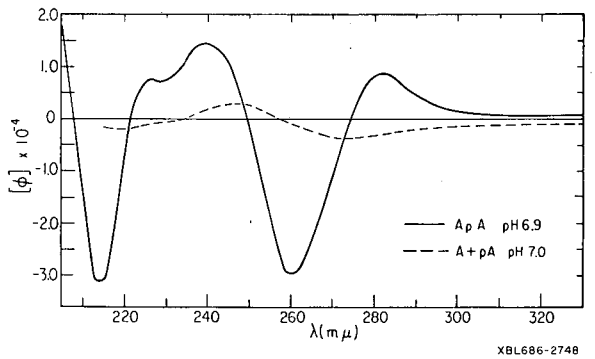

Fig. 6. Comparison of optical rotatory dispersion curves of a mixture of adenosine plus adenylic acid (5') and adenylyl (3'-5') adenosine. The large difference in shape and magnitude implies that the bases in this dinucleoside phosphate interact strongly; presumably they stack.

We would like to know in detail the average conformation of each dinucleoside phosphate and the fluctuations in conformation about the mean. Furthermore, it is important to know how these characteristics change with temperature, pH, salt concentration, and solvent. Finally, we need to know the amount of energy necessary to distort the normal conformation. A theory of the factors involved in the conformations would obviously be very helpful in minimizing the experiments necessary to obtain this information. Such a theory does not at present exist; we only know some unorganized facts. Some bases stack strongly; others do not. By ionizing the bases[26] or by adding ethanol, trimethyl phosphate, or many other solvents,[31] we can cause unstacking of any of the bases. Raising the temperature seems to increase the relative motion of the two bases, but does not seem to lead to complete unstacking.[35] To correlate these and other results, various authors have emphasized particular types of interaction.

In Table I we list the interactions involved in the conformation of a dinucleoside phosphate and give references for their enthusiasts. It would be convenient if one type of interaction dominated, but this does not seem to be so. Studies of aggregation of bases,[33] and mononucleosides,[33,36] give a range of values of +0.5 kcal/mole to -2 kcal/mole for the standard free energy of association in water at room temperature. The purine-purine interaction is the strongest, and the pyrimidine-pyrimidine interaction is the weakest. To get values useful for dinucleoside phosphate conformation we must add approximately -2.5 kcal/mole to these numbers.[36] This accounts for the loss of entropy in the aggregation of the monomers which is not pertinent to their interaction in the dinucleoside phosphate. Therefore, stacking might be favored by -2.0 kcal/mole for pyrimidines to -4.5 kcal/mole for purines. However, interpre-

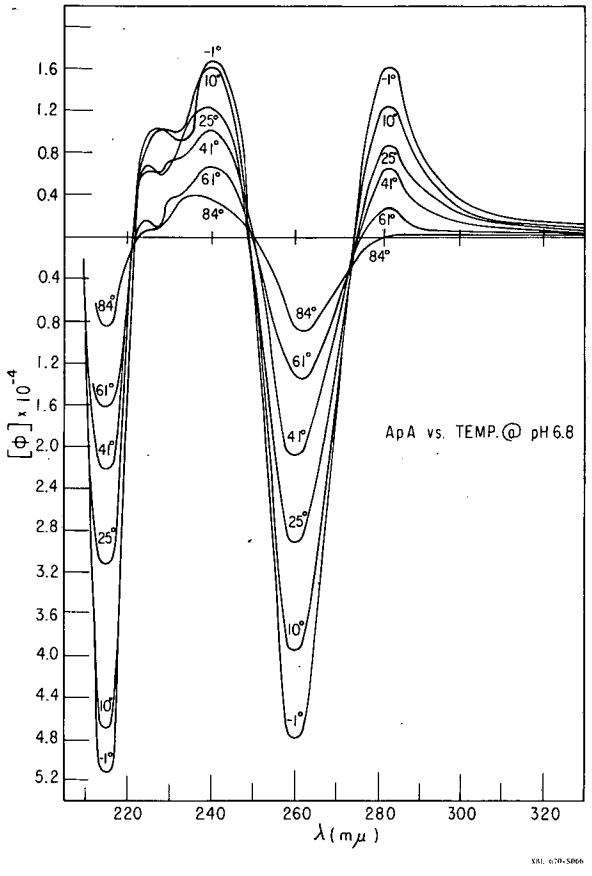

Fig. 7. Temperature dependence of the optical rotatory dispersion of adenyl (3'-5') adenosine.

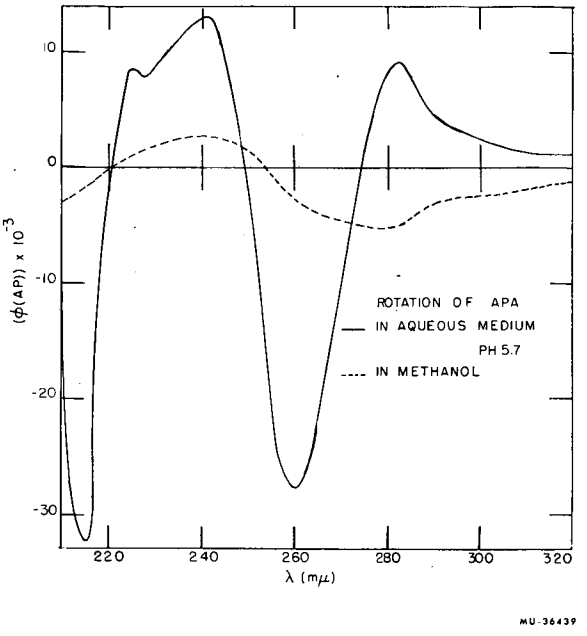

Fig. 8. Effect of alcohol on the optical rotatory dispersion of adenylyl (3'-5') adenosine.

Table I. Interactions important in determining dinucleoside phosphate conformations.

	Base 1	Sugar (3')	Phosphate	Sugar (5')	Base 2	Solvent
Base 1	--	(a)	(b)	(c)	(d)	(e)
Sugar (3')		--	(f)	(g)	(c)	(e)
Phosphate			--	(f)	(b)	(e)
Sugar (5')				--	(a)	(e)
Base 2	Same as upper				--	(e)
Solvent	right					(e)

a. See reference 22 for steric factors and reference 37 for H-bonding evidence.

b. These interactions are probably not very important; see reference 24 for calculations.

c. See reference 24 for calculations.

d. See reference 33 for data and reference 38 for calculations.

e. See reference 41 for a datum. Extensive theories are presented in references 39, 40.

f. See reference 37 for H-bonding evidence and reference 24 for calculations.

g. These interactions have not been studied; see reference 24 for calculations.

tation of the temperature dependence of optical studies on the dinucleoside phosphate leads to different results. The free energy of stacking at room temperature is about 0 ± 1 kcal/mole, with cytosine-containing dinucleoside phosphates interacting as strongly as those containing only purines.[35] Furthermore, there are significant differences between purine (3'-5') pyrimidine and pyrimidine (3'-5') purine interactions.[36, 35]

The interpretation of the optical studies may be incorrect,[35] and/or small differences in interactions can lead to significant effects on conformation. We do know that besides the important base-base interactions (studied by aggregation)[33] there are significant base-sugar interactions. This is illustrated by the differences in behavior between ribose-containing dinucleoside phosphates and those containing deoxyribose.[37]

One way to try to separate and assess the various factors is to calculate the potential energy for the interactions for molecules in a vacuum and then somehow add the effect of the solvent. Base-base interactions in vacuum have been calculated[38] to range from -5 to -10 kcal/mole. A calculation[24] of the lowest potential energy conformation for cytidyl (3'-5') cytidine, CpC, in vacuum gives a conformation in which a base prefers to stack on a ribose instead of the other base. Even if these potentials were accurate (which they are not), the solvent would change the calculated conformations.

Everyone talks about the solvent, but nobody does anything about it. The most popular theories[39, 40] ascribe hydrophobia to the bases. (Some critics ascribe hydrophobia to the theorists.) This means it is not so much that the bases come together because they like each other; it is more that they morbidly dislike water. However, the fact is that adenine, and probably the other bases, prefer water to a vacuum. A value of -13 kcal/mole has been obtained[41] for the standard free energy of transferring adenine from a vacuum to an aqueous solution at room temperature. It is clear that much work and thought are needed. However, combination of calculated values for interactions in vacuum and measured values for interactions

with solvent may eventually lead to the desired knowledge.

Trinucleotides

The main reason for studying dinucleoside phosphates in such detail is in the hope that they can teach us about nucleic acids. Cantor[42, 43] found that the optical properties and presumably the conformations of trinucleoside diphosphates were predictable from the dimers. Figure 9 illustrates this. Any optical property of a dimer can be thought of as the sum of the properties of the monomers plus an interaction term. If one assumes that only adjacent monomers interact significantly, then the property of a trimer (per monomer unit) can be written as:

$$^3P_{ABC} = 2P_{AB} + 2P_{BC} - P_B,$$

where P_{ABC}, P_{AB}, and P_B are the properties of the trimer, dimer, and monomer. The dotted lines in Fig. 9 were calculated in this way from the measured molar rotation of the dinucleoside phosphates and mononucleotides. Similar results occur for the absorption curves. We conclude that the bases in dinucleoside phosphates have relative orientations very similar to those in trinucleoside diphosphates. If this is still true for higher polymers, the time spent on dinucleoside phosphates will be profitable. The large amount of detail obtainable about the structure of each dinucleoside phosphate can be applied directly to RNA molecules.

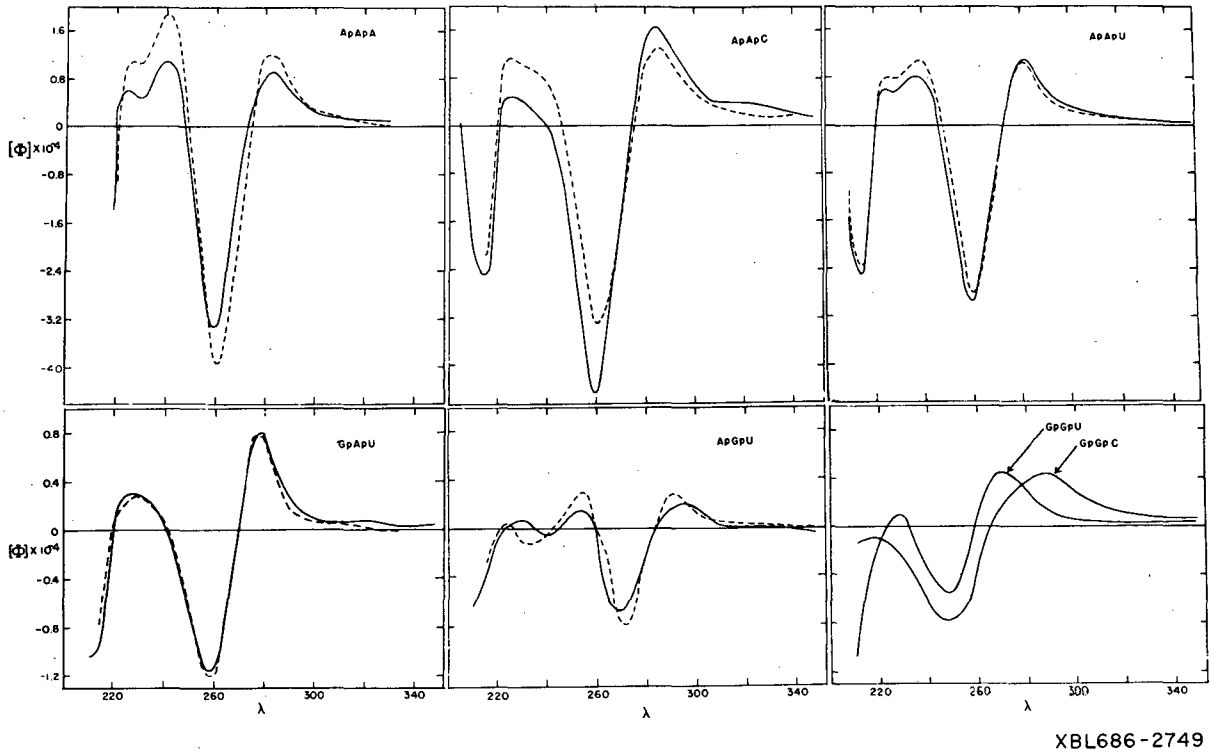

Fig. 9. Comparison of the measured optical rotatory dispersion of some trinucleoside diphosphates (solid line) and curves calculated from the dinucleoside phosphates (dotted lines). The good agreement implies that the bases in the trimer have relative orientations very similar to those in the dimers. (From Ref. 42.)

Polynucleotides

In 1959 Doty and coworkers[44] concluded that naturally-occurring RNA molecules consisted of about 50% random coil and 50% double-strand helix similar to DNA. This picture has since been sharpened, but not changed fundamentally. We have been trying to determine the conformation of the single-strand part, and the nature of the non-single-strand part. Furthermore, we want to know how the amount of each part changes with solvent.

If the single-strand region of an RNA molecule has optical properties predictable from the dinucleoside phosphates, we essentially know its structure. The optical rotation at pH 7 of homopolynucleotides of uridylic acid, cytidylic acid, and adenylic acid agree well with extrapolations from the dimers. Thus the neutral homopolymers do have similar conformations to the dinucleoside phosphates.[45] The rotation at low ionic strength and pH 7 for the RNA from tobacco mosaic virus (TMV) is compared in Fig. 10 with that calculated from the dinucleoside phosphates. The base composition of the RNA is known, and by assuming the most probable nearest neighbor distribution, we can sum the appropriately weighted dinucleoside phosphate curves. The agreement implies that in this solvent tobacco mosaic virus RNA is single stranded with the bases stacked as in the dinucleoside phosphates. Good! We now understand the single-strand segments of RNA molecules.

Raising the ionic strength of the solution produces a large change in rotation, as shown in Fig. 11. The blue shift of the curve and the change in magnitude is consistent with double-strand formation. Formation of poly G + poly C double-strand complexes and poly A + poly U double-strand complexes give similar changes.[46] We thus agree generally with the earlier conclusions. RNA molecules can curl around to form hairpin loops held together by adenine-uracil and guanine-cytosine base pairs.[44, 47] The strands in the double-strand regions are antiparallel and analogous to DNA; the double-strand regions are thus made up of Watson-Crick base pairs.

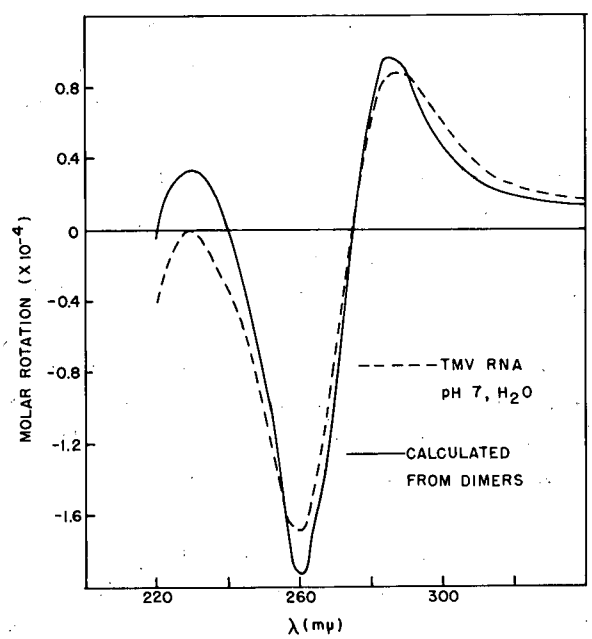

XBL 670-5051

Fig. 10. Comparison of the measured optical rotatory dispersion of tobacco mosaic virus RNA at pH 7 in water (dotted line) with a curve calculated from the dinucleoside phosphates. The good agreement implies that TMV RNA under these conditions is single stranded with a structure like the dinucleoside phosphates. [From Vortex 26, 318 (1965).]

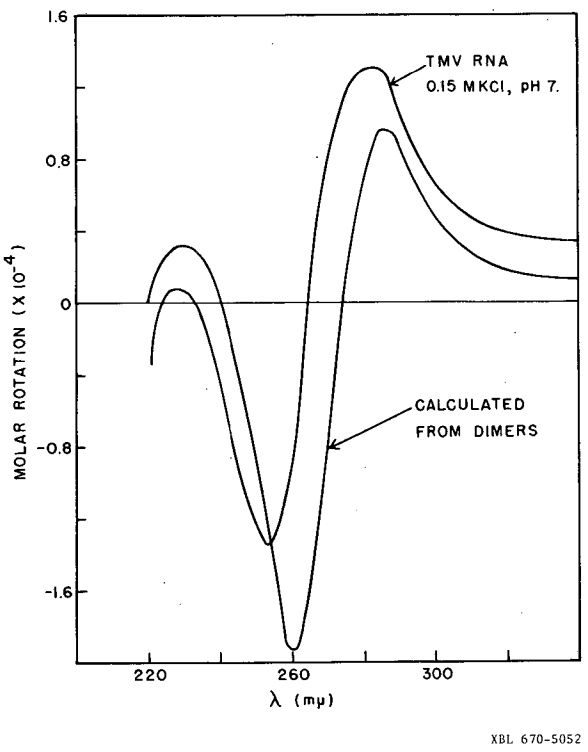

Fig. 11. Comparison of the measured optical rotatory dispersion of tobacco mosaic virus RNA at pH 7 in 0.15 M KCl with a curve calculated from the dinucleoside phosphates. The blue shift of the measured curve implies that TMV RNA under these conditions contains some double-stranded structure. [From Vortex 26, 318 (1965).]

To determine the relative amounts of single-strand and double-strand regions in TMV RNA, the optical rotatory dispersion data as a function of ionic strength and temperature have been analyzed quantitatively.[48] We did not assume that only single- and double-strand regions existed, instead we asked the following question: What are the minimum number of spectral components necessary to fit the data with a given accuracy? That is, how many different shapes of rotatory dispersion curves are present in the data? We found that two spectral components were needed to fit the data within experimental error. The forty curves measured for TMV RNA over the range of 10^{-4} M to 1 M salt concentration and 0°C to 90°C temperature could be represented by the sum of only two curves. These curves can be chosen so that the amount of each present in the measured data, at any temperature and ionic strength, represents the amount of single-strand and double-strand regions present in the molecule. The results found for TMV RNA are shown in Fig. 12. Low ionic strength and high temperature favor single-strand regions, while high ionic strength and low temperature can produce up to about 70% double-strand.

The single-strand curve was chosen to have the same shape as that calculated from the sum of the dinucleoside phosphates. The double-strand curve that resulted is very similar to that measured for the 100% double-stranded RNA of the replicative form of MS-2 virus.[48] Pure double-stranded RNA molecules give analyzable fiber x-ray diffraction patterns.[49] These double-stranded RNA molecules form a base-paired helix; but the two bases are not coplanar, and the base pair is not perpendicular to the helix axis as in the B form of DNA. The optical rotatory dispersion curve for DNA is also very different from that of double-stranded RNA.

If we looked no further, we might be convinced that we understood RNA structure: single-

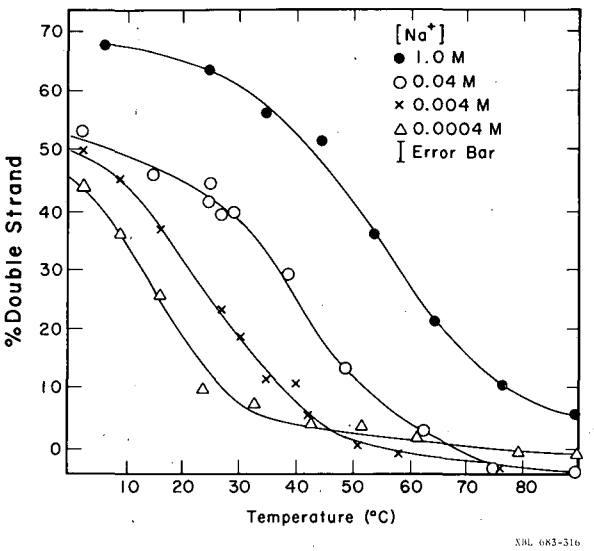

Fig. 12. Percent double-strand structure in tobacco mosaic virus RNA, estimated from optical rotation measurements. (From Ref. 48.)

strand regions are like the dinucleoside phosphates; double-strand regions are characterized by the x-ray structure of replicative forms of RNA. This means only Watson-Crick base pairs formed from antiparallel strands exist in the double-strand region. Of the 120 possible interactions among the 16 dinucleoside phosphates (Table II), only 10 correspond to Watson-Crick base pairs with antiparallel strands. If nearest-neighbor interactions are dominant, then knowledge of these 10 interactions would be sufficient to predict the stability and optical properties of any double-strand region. However, the actual situation is more complicated (as usual).

Base-Pairing Models

Study of the dinucleoside phosphates at high concentrations, which favor intermolecular interactions, shows that they do not primarily form base-paired complexes involving only two molecules. Instead they form higher aggregates[25, 50] involving base stacking, base intercalation,[30] and maybe base pairing. The self-interaction of ApA involves both stacking and intercalation;[30] the self-interaction of GpC[51] and GpG[52] to form high-molecular-weight aggregates probably involves all three types of base interaction. Mixtures of ApApA and UpUpU definitely lead to hydrogen-bonded base pairs, but form a triple-stranded complex.[53] The simple models are apparently more complicated than the double-strand regions they are supposed to represent. There are two possibilities: the models are poor or the supposed double-strand regions are complicated.

We are presently trying to resolve this problem in three ways. Polymers of known sequence which form double strands can be studied. Poly A + poly U and poly G + poly C have already been studied by Yang and coworkers.[46] The six polymers of an alternating sequence of two bases would give the remaining possible nearest-neighbor interactions. Studies of interaction of trinucleoside diphosphates[50] and further work on dinucleoside phosphates will show us how oligomers interact. For example, are parallel interactions of Watson-Crick base pairs more or less stable than antiparallel interactions? That is, how does the ApG + CpU interaction compare with GpA + CpU? If ApG and GpA are both stacked in a right-handed helix,

Table II. The 120 possible interactions among the dinucleoside phosphates. The symbol WC denotes the 10 interactions which could lead to Watson-Crick base pairs for antiparallel strands; the symbol ‖ denotes the 6 additional interactions which could lead to Watson-Crick base pairs for parallel strands.

	ApA	ApU	UpA	UpU	CpC	CpG	GpC	GpG	ApC	GpU	CpA	UpG	ApG	CpU	GpA	UpC
ApA	(a)			WC(b)												
ApU		WC	‖													
UpA			WC													
UpU																
CpC								WC								
CpG						WC	‖									
GpC							WC(c)									
GpG								(d)								
ApC									(e)	WC(e)		‖				
GpU										(e)	‖					
CpA		Same as upper right										WC				
UpG																
ApG														WC		‖
CpU															‖	
GpA																WC
UpC																

a. See reference 30.

b. See reference 53.

c. See reference 51

d. See reference 52.

e. See reference 50.

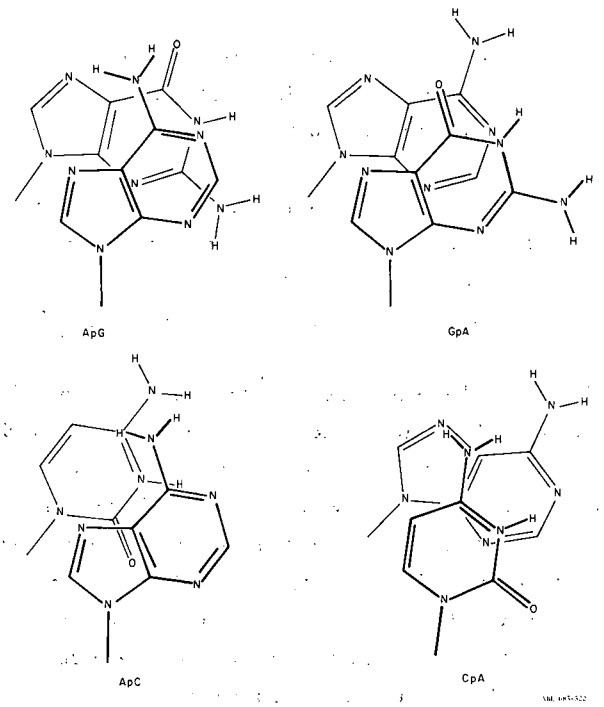

Fig. 13. Scale drawing of the bases in sequence isomers of dinucleoside phosphates assumed to have the geometry of a single strand of DNA. The pattern of groups available for hydrogen bonding are different.

Fig. 13 shows that the availability of groups for hydrogen bonding are quite different. A purine-pyrimidine dinucleoside phosphate is even more different, as illustrated by ApC and CpA. More interesting are the many non-Watson-Crick pairs. The extremely strong self-attraction of GpG[52] is particularly intriguing. Finally, of course, we are trying to determine what are the actual structures present in the non-single-strand regions of ribonucleic acids. Are there multi-strand regions and base pairs other than A-U or G-C? We think there are. Transfer RNA molecules and other small (~100 bases) RNA molecules, which cannot form long sequences of complementary base pairs, are likely to form structures like those found in concentrated solutions of oligomers.

WHAT NEXT?

Research is like mountain climbing in that it is impossible to pick the best route until one is climbing and seeing the obstacles or easy sections up close. We will continue to study the dinucleoside phosphates: at low concentrations as models for single-strand RNA regions and at high concentrations as models for non-single-strand regions. Bases other than the four coding bases will be studied. The many "odd" bases[2] found in transfer RNA molecules are first on the list. Further calculations of the optical rotatory dispersion and circular dichroism are in progress.[54] The results can be tested against polynucleotides of known structure, such as the B form of DNA, replicative forms of RNA, and double-stranded homopolymers. When the calculated curves become trustworthy, calculations can be done for any sequence and length of double-strand region. This should make interpretation of measured curves in terms of structure more detailed and more accurate. Beyond this, the route is unclear. We will keep plodding until we get to the top of the mountain, or somebody else gives us a ride up.

SUMMARY

There are two problems in the structure of a ribonucleic acid: the linear sequence of bases and the three-dimensional arrangement of the molecule. Solving these problems will be helpful in understanding the biological function of nucleic acids. This account emphasizes their role in protein synthesis.

The problem of determining the sequence of four bases in a ribonucleic acid molecule of 1000 units is posed. A method is proposed in which one needs only to determine the chain length of certain fragments of the molecule. The fragments are those which have been produced by partial hydrolysis with a base-specific enzyme and which contain one end of the original molecule.

Knowledge of the rules which characterize the three-dimensional structure of a ribonucleic acid molecule can be gained by studying small subunits of the molecule. Evidence is presented that the bases in a dinucleoside phosphate in water at pH 7 tend to stack. Adenine, guanine, and cytosine stack the most; and uracil stacks the least. The relative orientation of bases in single-strand regions of ribonucleic acids is very similar to that in the dinucleoside phosphates. The nature of the base-paired regions of ribonucleic acids is less clear. Long base-paired regions probably contain only Watson-Crick pairs between two antiparallel strands. Short base-paired regions may contain other than Watson-Crick pairs and more than two strands. Analogies for these structures are found in concentrated oligonucleotide solutions.

REFERENCES

1. Two books which discuss this idea and describe the evidence for it are: J. D. Watson, Molecular Biology of the Gene (W. A. Benjamin, Inc., New York, 1965) and V. M. Ingram, The Biosynthesis of Macromolecules (W. A. Benjamin, Inc., New York, 1965).
2. A summary plus a description of current work is given in: Cold Spring Harbor Symposia on Quantitative Biology, Vol. XXXI, The Genetic Code (Cold Spring Harbor Laboratory of Quantitative Biology, Cold Spring Harbor, N. Y., 1967).
3. G. G. Brownlee, F. Sanger, and B. G. Barrell, Nature 215, 753 (1967); B. G. Forget and S. M. Weissman, Science 158, 1695 (1967).
4. S. Mandeles and I. Tinoco, Jr., Biopolymers 1, 183 (1963).
5. J. N. Davidson, The Biochemistry of the Nucleic Acids (John Wiley and Sons, Inc., New York, 1965).
6. J. H. Anderson and C. E. Carter, Biochemistry 4, 1102 (1965).
7. N. W. Y. Ho and P. T. Gilham, Biochemistry 6, 3632 (1967).
8. R. Monier, M. L. Stephenson, and P. C. Zamecnik, Biochim. Biophys. Acta 43, 1 (1960).
9. H. von Portatius, P. Doty, and M. L. Stephenson, J. Am. Chem. Soc. 83, 3351 (1961).
10. R. S. Yolles, Biochim. Biophys. Acta 87, 583 (1964).
11. A. Steinschneider and H. Fraenkel-Conrat, Biochemistry 5, 2729 (1966).
12. S. Mandeles, J. Biol. Chem. 242, 3103 (1967).
13. M. Takanami, J. Mol. Biol. 23, 135 (1967) and references cited.
14. R. K. Ralph, R. J. Young, and H. G. Khorana, J. Am. Chem. Soc. 84, 1490 (1962).
15. W. E. Razzell and H. G. Khorana, J. Biol. Chem. 236, 1144 (1961).
16. R. V. Tomlinson and G. M. Tener, Biochemistry 2, 697 (1963).
17. P. J. Highton and M. Beer, J. Mol. Biol. 7, 70 (1963).

18. M. Dole, Northwestern University, personal communication.
19. J. D. Watson and F. H. C. Crick, Nature 171, 737 (1953).
20. P. J. Gomatos and I. Tamm, Proc. Natl. Acad. Sci. U. S. 50, 707, 878 (1963).
21. A. K. Kleinschmidt, A. Burton, and R. L. Sinsheimer, Science 142, 961 (1963).
22. A. E. V. Haschemeyer and A. Rich, J. Mol. Biol. 27, 369 (1967).
23. J. Donohue and K. N. Trueblood, J. Mol. Biol. 2, 363 (1960).
24. R. C. Davis, Ph. D. Thesis, U. of California, Berkeley, 1967.
25. I. Tinoco, Jr., R. C. Davis, and S. R. Jaskunas, in Molecular Associations in Biology, B. Pullman, Ed. (Academic Press, Inc., New York, 1968).
26. M. M. Warshaw and I. Tinoco, Jr., J. Mol. Biol. 20, 29 (1966).
27. (a) J. Brahms, A. M. Michelson, and K. E. Van Holde, J. Mol. Biol. 15, 467 (1966). (b) C. A. Bush and J. Brahms, J. Chem. Phys. 46, 79 (1967).
28. J. Brahms, J. C. Maurizot, and A. M. Michelson, J. Mol. Biol. 25, 465, 481 (1967).
29. S. I. Chan, B. W. Bangerter, and H. H. Peter, Proc. Natl. Acad. Sci. U. S. 55, 720 (1966).
30. S. I. Chan and J. H. Nelson, J. Am. Chem. Soc., in press (1968).
31. S. L. Davis, Ph. D. Thesis, U. of California, Berkeley (1965).
32. C. A. Bush and I. Tinoco, Jr., J. Mol. Biol. 23, 601 (1967).
33. P. O. P. T'so, I. S. Melvin, and A. C. Olson, J. Am. Chem. Soc. 85, 1289 (1963).
34. M. P. Schweizer, S. I. Chan, and P. O. P. T'so, J. Am. Chem. Soc. 87, 5241 (1965).
35. R. C. Davis and I. Tinoco, Jr., Biopolymers, in press (1968).
36. T. N. Solie, Ph. D. Thesis, U. of Oregon (1965).
37. A. Adler, L. Grossman, and G. D. Fasman, Proc. Natl. Acad. Sci. U. S. 57, 423 (1967); P. O. P. T'so, S. A. Rapoport, and F. J. Bollum, Biochemistry 5, 4153 (1966).
38. P. Claverie, B. Pullman, and J. Caillet, J. Theoret. Biol. 12, 419 (1966).
39. O. Sinanoglu and S. Abdulnur, Photochem. Photobiol. 3, 333 (1964).
40. W. Kauzman, Adv. Protein Chem. 14, 1 (1959).
41. L. B. Clark, G. G. Peschel, and I. Tinoco, Jr., J. Phys. Chem. 69, 3615 (1965). The standard enthalpy of vaporization is given, but the information necessary to obtain the free energy is present.
42. C. R. Cantor and I. Tinoco, Jr., J. Mol. Biol. 13, 65 (1965).
43. C. R. Cantor and I. Tinoco, Jr., Biopolymers 5, 821 (1967).
44. P. Doty, H. Boedtker, J. Fresco, R. Haselkorn, and M. Litt, Proc. Natl. Acad. Sci. U. S. 45, 482 (1959).
45. C. R. Cantor, S. R. Jaskunas, and I. Tinoco, Jr., J. Mol. Biol. 20, 39 (1966).
46. P. K. Sarkar and J. T. Yang, J. Biol. Chem. 240, 2088 (1965); Biochemistry 4, 1238 (1965).
47. J. R. Fresco, B. M. Alberts, and P. Doty, Nature 188, 98 (1960).
48. D. W. McMullen, S. R. Jaskunas, and I. Tinoco, Jr., Biopolymers 5, 585 (1967).
49. S. Arnott, W. Fuller, F. Hutchinson, R. Langridge, M. H. F. Wilkins, M. Spencer, and J. H. Venable, J. Mol. Biol. 27, 507, 525, 535, 549 (1967).
50. S. R. Jaskunas, C. R. Cantor, and I. Tinoco, Jr., Biopolymers submitted.
51. S. Podder, unpublished work in this laboratory.
52. M. N. Lipsett, J. Biol. Chem. 239, 1256 (1964).

53. H. T. Miles, J. Frazier, and F. M. Rottman, quoted in Ann. Rev. Biochem. 36, 407 (1967).
54. W. C. Johnston, unpublished work in this laboratory.

ON THE HYDRATION OF DNA. I. THE PREFERENTIAL HYDRATION AND STABILITY OF DNA IN CONCENTRATED TRIFLUOROACETATE SOLUTION†

Mary-Jane B. Tunis and John E. Hearst

The hydration of DNA is an important factor in the stability of its secondary structure. Methods for measuring the hydration of DNA in solution and the results of various techniques are compared and discussed critically.

The buoyant density of native and denatured T-7 bacteriophage DNA in potassium trifluoroacetate (KTFA) solution has been measured as a function of temperature between 5° and 50°C. The buoyant density of native DNA increased linearly with temperature, with a dependence of $2.3 \pm 0.5 \times 10^{-4}$ g·cc^{-1} °C^{-1}. DNA which has been heat-denatured and quenched at 0° in the salt solution shows a similar dependence of buoyant density on temperature at temperatures far below the T_m and also above. However, there is an inflection region in the buoyant density vs T curve over a wide range of temperatures below the T_m. Optical density vs temperature studies showed that this is due to the inhibition by KTFA of recovery of secondary structure on quenching. If the partial specific volume is assumed to be the same for native and denatured DNA, the loss of water of hydration on denaturation is calculated to be about 20% in KTFA at a water activity of 0.7 at 25°C.

By treating the denaturation of DNA as a phase transition, an equation has been derived relating the destabilizing effect of trifluoroacetate to the loss of hydration on denaturation. The hydration of native DNA is abnormally high in the presence of this anion, and the loss of hydration on denaturation is greater than in CsCl. In addition, trifluoroacetate appears to decrease the ΔH of denaturation.

---

†Abstract of a paper in Biophysics (in press), 1968.

ON POLYMER DYNAMICS IV. THE ZERO FREQUENCY INTRINSIC VISCOSITY OF POLYMER MOLECULES WITH HYDRODYNAMIC INTERACTION AND EXCLUDED VOLUME†

J. E. Hearst, E. Beals, and R. A. Harris

The theory and model of Harris and Hearst has been extended to approximately include the effect of hydrodynamic interaction and excluded volume. The results agree in both the coil and rigid rod limits with existing theories and experiment. The absence of a linear dependence of $[\eta]$ upon an appropriate power of the molecular weight introduces some doubt as to the validity of conventional methods of interpretation of viscosity data.

---

†Abstract of paper in J. Chem. Phys. (in press), 1968.

CHLOROPHYLL *a* INTERACTIONS WITH CHLOROPLAST LIPIDS *IN VITRO*[†]

Terry Trosper and Kenneth Sauer

Purified chloroplast glycolipids--galactosyldiglycerides and sulfoquinovodiglyceride--form relatively strong complexes with chlorophyll *a*, as measured by their ability to dissociate chlorophyll dimers in carbon tetrachloride solution. The chloroplast lipids form stable monolayers at a water-nitrogen interface, with maximum packed areas of 39, 44, and 73 $Å^2 \cdot molecule^{-1}$ for sulfolipid, monogalactolipid, and digalactolipid, respectively. Mixed monolayer of chlorophyll *a* with sulfolipid or monogalactolipid exhibit compression behavior characteristic of ideal two-dimensional solutions.

[†]Abstract of a paper submitted to Biochim. Biophys. Acta, 1968.

FUNCTIONAL PHOTOSYNTHETIC UNIT SIZES FOR EACH OF THE TWO LIGHT REACTIONS IN SPINACH CHLOROPLASTS†

Jeffrey Kelly and Kenneth Sauer

From studies in flashing light of electron transport reactions of spinach chloroplasts, we have been able to estimate the concentration, relative to chlorophyll, of the reaction centers or pools of intermediates closely associated with photosystems I and II. Relatively long flashes (6-100 msec) of saturating red light produce a maximum yield of cytochrome c reduction by reduced trimethyl-p-benzoquinone in the presence of 3-(3, 4-dichlorophenyl)-1, 1-dimethyl urea corresponding to 1 equivalent per 445 chlorophylls for photosystem I. Similar illumination patterns for the Hill reaction using 2, 6-dichlorophenolindophenol and/or ferricyanide lead to a maximum reduction of 1 equivalent per 55 chlorophylls for photosystem II. From other published results it appears that the larger photosystem-II unit results from a secondary pool of endogenous intermediate electron acceptors, and that very short (10^{-4} sec) flashes would produce evidence for a primary rate-limiting component in smaller concentration.

For long flashes, the rate-limiting step for the dark reaction regenerating system-I activity has a first-order rate constant of 13 sec^{-1} at room temperature. The rate constant for system II, also first-order, is about 30 sec^{-1}, but is reduced to half this value in the absence of phosphorylation cofactors and the phosphorylation uncoupler, methylamine. Both of these rate-limiting steps appear to result from components endogenous to the broken chloroplasts.

---

†Abstract of a paper published in Biochemistry 7, 882 (1968).

EXCITATION TRANSFER BY CHLOROPHYLL a IN MONOLAYERS AND THE INTERACTION WITH CHLOROPLAST GLYCOLIPIDS†

Terry Trosper, Roderick B. Park, and Kenneth Sauer

In mixed monolayers with purified chloroplast glycolipids and other colorless lipids, chlorophyll a fluorescence exhibits a decrease in quantum efficiency with increasing chlorophyll concentration. The fluorescence, which is strongly polarized in dilute films, becomes progressively depolarized as the area fraction of chlorophyll increases, and is completely depolarized in a pure chlorophyll a monolayer. The observed behavior is consistent with an inductive resonance mechanism of energy transfer among the chlorophyll molecules with a critical transfer distance of 20 to 90 Å, depending on the model chosen for the energy transfer mechanism.

The purified glycolipids--mono- and digalactosyl deglycerides and sulfoquinovodiglyceride--separately form stable, compressible monolayers of the liquid-expanded type on an aqueous subphase and in an atmosphere of nitrogen. At maximum compression the three glycolipids occupy areas of 55, 80, and 47 $Å^2 \cdot \text{molecule}^{-1}$, respectively, in the monolayer. Mixed monolayers of chlorophyll a with, separately, the monogalactolipid and the sulfolipid behave upon compression as two-dimensional solutions. The fluorescence polarization at high chlorophyll concentrations in mixed monolayers indicates that several of the lipid diluents facilitate local ordering of the pigment molecules.

---

†Abstract of a paper published in Photochem. Photobiol. 7, 451 (1968).

THE EPR SIGNAL IN RHODOSPIRILLUM RUBRUM

Donald R. Gentner and Melvin Calvin

INTRODUCTION

The EPR spectra of photosynthetic materials have been studied for more than 10 years. Despite early optimism, little progress has been made towards determining the identity of the molecule or molecules responsible for the EPR signal. Beinert, Kok, and Hoch[1] have isolated from red algae a pigment complex containing the special chlorophyll (P700) and a group of associated molecules. They found light-induced reversible EPR signals in this complex similar to those observed in intact systems. The work of Weaver and Bishop[2] and Androes, Singleton, and Calvin[3] also indicates that the light-induced EPR signal is closely associated with the photochemical reaction center. Sistrom and Clayton[4] investigated a mutant of the photosynthetic bacteria Rhodopseudomonas spheroides which had the normal complement of bacterial chlorophyll and carotenoid pigments but lacked the special chlorophyll (P870). This mutant showed neither the dark- nor light-induced EPR signals. Loach et al.[5] have, by titrating with redox reagents, produced a signal in the dark in bacteria which is similar to the light-induced signal, and find a midpoint potential of about 0.44 V. In another experiment, they found that the full light-inducible signal remained after 95% of the pigments had been chemically bleached with K_2IrCl_6, indicating that the majority of chlorophyll molecules are not directly responsible for the EPR signal.

MATERIALS AND METHODS

Instrumentation

EPR spectra were measured with an X-band spectrometer operating at approximately 9.5 GHz with superheterodyne detection. In order to improve the signal-to-noise ratio of the EPR spectra and the kinetic curves, the measurements were repeated many times and averaged on one of the digital memory devices currently on the market. The sample was illuminated by a Sylvania DFA projection lamp. Light passed through a water bath and lens, and into a light pipe. Light emerging from the light pipe is reflected onto the sample, which rests on the bottom of a rectangular microwave cavity with slits machined into the bottom to allow the light to pass. For the early experiments, a lucite light pipe was used; but this was replaced by a quartz light pipe when it was discovered that lucite has an absorption band near 900 nm, which is in the region of maximum absorption of R. rubrum.

The sample cavity was in a metal Dewar of conventional design. With the use of liquid nitrogen and/or liquid helium the sample could be maintained at temperatures between 300° and 1.5°K. Temperature was measured with a copper-constantan thermocouple, carbon resistors, and, below 4.2°K, by measuring the vapor pressure above the liquid helium. Good thermal contact was assured since the sample was in direct contact with the microwave cavity, which was made of gold-plated brass. The thermocouple and carbon resistor were also in direct contact with this cavity. At 4.2°K and below, the sample and microwave cavity were

directly immersed in the liquid helium bath. For this reason much of the low temperature work was done below the lambda point of helium (2.2°K) to eliminate bubbling inside the cavity.

Growth and Preparation of Samples

Rhodospirillum rubrum cultures used in these studies were originally obtained from R. Y. Stanier (Strain S 1). The bacteria were grown in 125 ml and 1 liter bottles on Modified Hutner's Medium.[6] The medium was innoculated with 0.1 to 0.2% by volume of old R. rubrum culture, and the cells harvested after three to five days, by which time they had attained their maximum density.

For whole cell preparations, the culture was centrifuges at 850 g for 15 minutes. A small amount of the resulting thick suspension of cells was pipeted onto a quartz slide and dried for about ten minutes under nitrogen gas; no effort was made to dry the sample thoroughly. The samples were normally almost opaque. Chromatophore fragments from R. rubrum were prepared by the method of Loach et al.,[5] and similarly dried on a quartz slide.

Quantitative Determination of Number of Unpaired Electrons

In order to determine the absolute number of unpaired electrons in an unknown, the EPR spectrometer must be calibrated with a sample containing a known number of spins. We used a sample containing about 0.1% chromium as an impurity in magnesium oxide. The spectrum of chromium in the cubic lattice of magnesium oxide consists of a single line at g value of 1.980. There are also four lines of low intensity due to the Cr^{53} isotope with 9.5% natural abundance. The main chromium line is shifted from the free electron position to higher field by about thirty gauss. The EPR signals observed in photosynthetic systems normally have a g value close to that of the free electron and can therefore be observed at the same time as the chromium with little overlap of the two signals. In practice, the chromium sample was normally present in the microwave cavity and served as a continuous measure of the apparatus sensitivity. The number of unpaired electrons in the chromium sample was approximately known from its preparation, but the value used was obtained by calibration of the chromium sample against a sample of phosphorus-doped silicon, obtained from E. A. Gere of Bell Telephone Laboratories, which Gere had originally calibrated against copper sulfate.[7]

Line Widths and g Values

Line widths and g values were measured by comparison with the chromium hyperfine lines of the chromium standard, which was present in the microwave cavity at the same time as the sample being measured. The g value of chromium in magnesium oxide was determined to be 1.9804 ± 0.0002 by comparison with phosphorus-doped silicon, using Gere's value of 1.99875 ± 0.0001 for the g value of the phosphorus-doped silicon. Low's value of 17.3 Oe for the splitting between the hyperfine lines of chromium was used.[8]

RESULTS

EPR Spectra of R. rubrum at Room Temperature

The EPR signals observed at room temperature in dried films of R. rubrum may be described on the basis of kinetic response to light. The signal observed after the sample has

been in the dark for several hours, we call the dark signal. Upon illumination the signal height increases, typically by a factor of ten, with a rise time of a few seconds. When the light is turned off again, the signal decays by half within a few seconds. At this point, if the sample is illuminated again, the signal height will return to its former value in the light in a few seconds. If, however, the sample remains in the dark, the signal height will slowly decay to the original dark value. This decay is exponential, with a time constant of 150 minutes. (The kinetics of the other photo-changes will be discussed in more detail later.) Thus we see that the room-temperature signals in dried films consist of three components: a fast light-induced signal with rapid rise and rapid decay kinetics, a slow light-induced signal with rapid rise but very slow decay kinetics, and a dark signal which is present without illumination.

This behavior in dried films is different from that observed in aqueous suspensions of the bacteria, where only the dark and the fast light-induced signals are observed. In addition, the room-temperature kinetics of the fast light-induced signal in aqueous suspensions are about four times as fast as the kinetics we have observed in dried films.

The dark signal is shown in Fig. 1. It has a line width of 12.5 ± 0.5 Oe, a g value of 2.0038 ± 0.0003, and an unsymmetrical line shape. If malate—the carbon source in the normal growth medium—is replaced by succinate, the dark signal has a similar shape and g value, but the width is narrowed significantly to 10.5 ± 0.5 Oe. The slow and fast light-induced signals have the same line width (9.7 ± 0.2 Oe) and g value (2.0025 ± 0.0003). Both signals have a Gaussian line shape. Replacement of malate by succinate in the growth medium has no effect on the shape, line width, or g value of the light-induced signals.

EPR Spectra of R. rubrum at Low Temperature

Table I summarizes a series of experiments in which a quantitative study was made of the number of unpaired electrons in the various signals as a function of illumination and temperature. These data were taken with a single sample. Similar results were obtained when the experiment was repeated with a different sample, but the relative proportions of the various signals can vary as much as ±50% between samples. In experiment I, the dark signal was observed at room temperature; and then the sample was cooled to liquid nitrogen (LN) temperature while still in the dark, whereupon the same dark signal was observed. Upon illumination at LN temperature, a small, reversible, light-induced signal was produced with rapid rise and decay kinetics. In experiment II, the sample was illuminated at room temperature; and after the light had been turned off for a few minutes, leaving the dark and the slow light signals, the

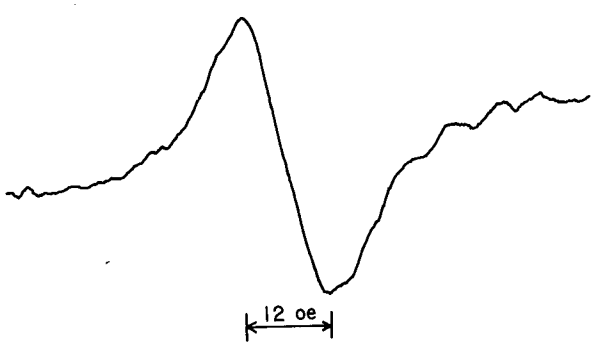

XBL676-1092

Fig. 1. Dark EPR signal in dried films of whole cell R. rubrum at room temperature. The magnetic field increases to the right.

Table I. Studies of number of unpaired electrons in EPR signals.

		Number of Unpaired Electrons ($\times 10^{-14}$)				
		# 300°K			81°K	
	Experiment	D	SL	FL	D	FL
I	Cooled in dark	1.3	--	--	1.3	0.97
II	Cooled after light	0.89	3.3	7.3	3.1	0.92
III	Cooled in light	2.5	1.0	7.3	12.5	0.6

sample was cooled to LN temperature, freezing in these signals. Again a small, reversible, light-induced signal was observed with similar kinetics and number of unpaired electrons as observed in experiment I. In experiment III, the sample was illuminated at room temperature and then cooled to LN temperature while the light was still on. In this case the entire light signal was frozen in, although a small, reversible, light-induced signal was again observed with similar kinetics and number of unpaired electrons as observed in experiments I and II. Unfortunately, the accuracy of these measurements is not sufficient to determine whether the reversible signal observed at LN temperatures represents a portion of the room-temperature fast light signal or is in addition to it. What we do conclude, however, is that signals observed at room temperature are essentially frozen in (or frozen out) at LN temperatures, except for a relatively small light-induced signal which is completely reversible.

The signals observed in R. rubrum at liquid helium temperature are identical in these respects to those observed at liquid nitrogen temperature. The reversible light-induced signal at low temperatures has the same g value, width, and line shape as the room temperature light-induced signals, within experimental error.

Kinetics

Figure 2 shows typical rise and decay kinetics for whole cell R. rubrum at room temperature. Figure 3 shows the kinetics of the same system at 2°K. The great majority of the rise and decay curves at various temperatures could be fitted quite well by the sum of two exponentials. For purposes of comparing various curves, it was found most useful to combine the two exponential time constants according to the ratio of their contributions to the initial signal. For example, if a given kinetic curve can be approximated by the following equation,

$$S = S_0 (.25\ e^{-t/0.1} + .75\ e^{-t/1.0})$$

we would calculate an "effective time constant" as,

$$.25(0.1) + .75(1.0) = .775.$$

The individual measured time constants and the ratio of their contributions to the observed kinetic curve had a rather large variation from sample to sample at a given temperature. The "effective time constant," when calculated in this manner, was less variable between samples and also had a smoother variation with temperature. In addition, there were a few cases

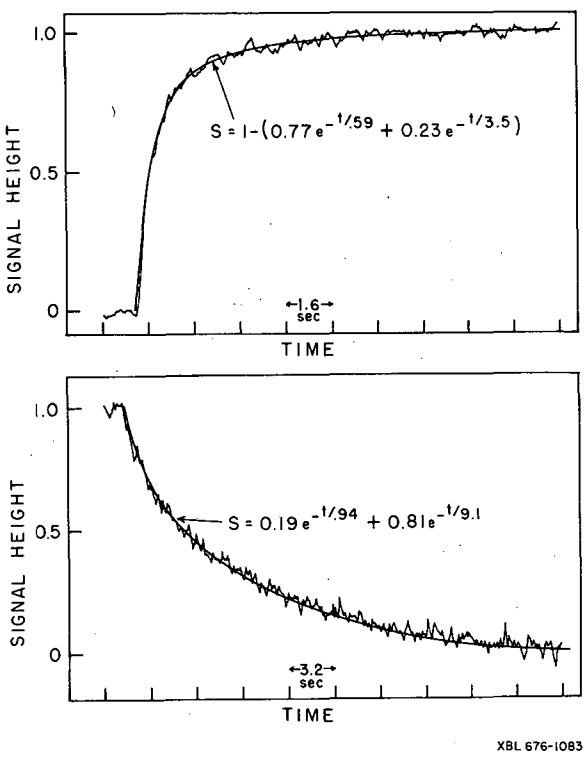

Fig. 2. Room temperature rise (top) and decay (bottom) curves of a dried film of whole cell R. rubrum.

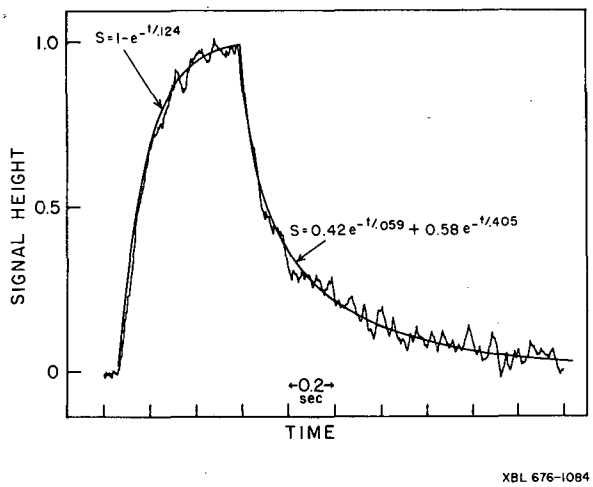

Fig. 3. Rise and decay curves for a dried film of whole cell R. rubrum at 2°K.

where the kinetic curve resolved into two exponentials with time constants differing by a factor of five or less. In such cases there is considerable leeway in the choice of exponentials to obtain a good fit; the various choices yield closely the same effective time constant, however, and much of their arbitrary nature is eliminated.

Figure 4 shows the "effective time constant" calculated for a series of decay curves as a function of temperature. The "effective time constants" for the rise curves have an identical temperature dependence but are lower by a factor of approximately 3.5.

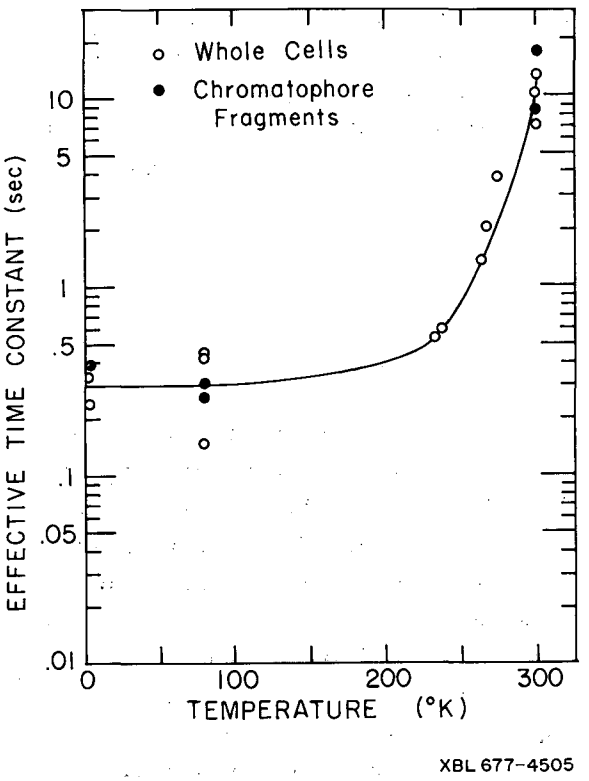

Fig. 4. The "effective decay times" of the light-induced EPR signal in dried films of R. rubrum.

Bacterial Chlorophyll Molecules per Unpaired Electron

At low light intensities, the height of the light-induced signal in R. rubrum is proportional to light intensity; but at high light intensities (about 10^{16} quanta/cm^2 sec in our case), light saturation is observed, and a maximum number of unpaired electrons is produced. It is of interest to inquire whether this maximum number of unpaired electrons corresponds to any other quantity in the sample, such as the number of bacterial chlorophyll molecules. Beinert and Kok[9] have reported such a comparison, and obtain a value of 63 bacterial chlorophylls per light-induced unpaired electron. Unfortunately their accuracy was uncertain (the authors state that their results may be in error by a factor of 2 or 3).

In our measurement, the number of chlorophyll molecules in the sample was determined from optical density measurements. The molar extinction coefficient of bacterial chlorophyll in acetone has recently been determined by Sauer, Lindsay Smith, and Schultz[10] to be 6.92×10^4 mole^{-1}cm^{-1} at 770 nm. Using this value, we determined the molar extinction coefficient of bacterial chlorophyll in 4:1 acetone water (6.63×10^4 mole^{-1}cm^{-1} at 770 nm). By measuring the optical density of chlorophyll in the in vivo system and then extracting all of the chlorophyll with 4:1 acetone-water and again measuring the optical density, we obtained a minimum value of 1.16×10^5 mole^{-1}cm^{-1} for the molar extinction coefficient of bacterial chlorophyll in R. rubrum at the 880 mm absorption maximum.† This value assumes that all of the in vivo chlorophyll is equally represented in the 880 mm band, but our final calculation is actually independent of this assumption.

Two independent measurements gave values of 29 and 32 bacterial chlorophyll molecules per unpaired electron. The fast light-induced EPR signal corresponds to about 55% of the total observed signal intensity; assuming this value and taking the average value of 30 bacterial chlorophyll molecules per total unpaired electron, we calculate that the number of bacterial chlorophyll molecules per fast light-induced unpaired electron is 55 ± 15. Most of the uncertainty in this value is due to possible systematic errors, especially those related to the calibration of the number of unpaired electrons.

DISCUSSION

Kinetics

The most striking aspect of these kinetic data is that the time constants decrease (that is, the reaction rates increase) as the temperature is decreased. We normally expect chemical reaction rates to decrease as the temperature is lowered. Androes, Singleton, and Calvin[3] measured the kinetics of the light-induced EPR signal in R. rubrum and found that the reaction rates increased as the temperature was lowered. The lowest temperature at which they worked was 115°K; the slow time response of their instrument did not allow them to obtain any detailed data. Some optical density changes have been found in photosynthetic bacteria at low temperatures. Workers in Chance's[11, 12] group have studied the irreversible light-induced oxidation of a cytochrome in Chromatium at low temperature, but in this case the rates decrease as the temperature is lowered. Arnold and Clayton[13] observed a reversible light-induced increase in optical density at 420 nm in Rhodopseudomonas spheroides at low temperature. They found that the decay of the optical density change, when compared with the room-temperature decay, is somewhat slower at 250°K and considerably faster at 77 and 1°K.

The sharp increase in rates which we observe between 300 and 200°K, and the fact that the rates do not begin to increase as the temperature is lowered to below 2°K, indicates that electron (or hole) migration must be involved in the production and decay of the EPR signal, even if it is not the sole rate-controlling step. Any mechanism involving the movement of molecules would have too high an activation energy to show this behavior. In one model which we have considered, the kinetics are determined by the rate of transfer of an electron from a donor molecule to an acceptor molecule. We assume that this transfer is intrinsically rapid, but the donor-acceptor system has a certain amount of thermal motion, and the electron transfer is possible only in one of its configurations. At high temperature, the rise and decay rates of the EPR signal are determined by the rate of movement of the molecules (relatively slow). At low temperature, however, the molecular system is frozen into its various possible configurations. Most of the systems are in configurations where they are unable to transfer an electron, and their light-induced signals will be either frozen in or frozen out. A small proportion of the systems will be in a position where electron transfer is possible; for these, we will observe the rapid intrinsic rate. This picture corresponds fairly well to the observed behavior.

Bacterial Chlorophyll Molecules per Unpaired Electron

The value of 55 bacterial chlorophylls per fast-light unpaired electron which we obtained is particularly interesting with regard to the picture of a "special chlorophyll" molecule in a

photochemical reaction site. In photosynthetic bacteria this special chlorophyll normally represents 2 to 5% of the total chlorophyll.[14] In R. rubrum the special chlorophyll is commonly referred to as P890; analogous pigments, P890 and P870, are found in the bacteria Chromatium and Rhodopseudomonas spheroides, respectively. The relative proportions of the special and ordinary chlorophylls are often measured spectroscopically, assuming that the peak extinction coefficients of the two pigments are equal. Using this method, the number of bacterial chlorophyll molecules per P890 has been determined variously as forty[15] and fifty.[16] Nishimura[17] has studied the production of ATP in R. rubrum by light flashes of varying intensities and found that there is one reactive center for every 43 bacterial chlorophylls. The close correspondence between the number of fast-light unpaired electrons and the number of P890 molecules supports the idea that these electrons are closely associated with the photochemical reaction center.

The Molecule Responsible for the Light-Induced EPR Signal

There have been several experiments on mutants lacking the special chlorophyll, and on pigment extracts containing the photochemical reaction center, which indicate that the light-induced signal is associated with the photochemical reaction center. The fact that we can observe reversible light-induced EPR signals at 2°K also implies a close association with the site where the light energy is trapped, at least for part of the signal in R. rubrum.

Figure 5 shows the commonly accepted redox scheme for the primary process in bacterial photosynthesis. Although only a few compounds are indicated in the figure, each dashed arrow represents an electron transport chain containing a number of different molecules. In the dark, all these compounds will be in some mixture of oxidized and reduced states. When the light is turned on, electrons are transferred in the direction of the arrows: bacterial chlorophyll and all compounds to the right of it become more oxidized; all compounds to the left of the solid arrow become more reduced. Loach[5, 18] has found that the action of light in producing the EPR signal in R. rubrum can be mimicked by mild oxidation. Thus the light-induced EPR signal is produced by oxidation, and the molecule responsible for it should be on the redox chain terminating in bacterial chlorophyll. We conclude that the unpaired electron responsible

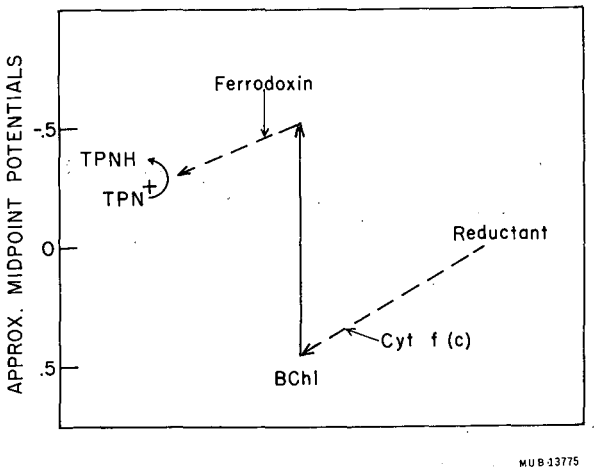

Fig. 5. The primary process of photosynthesis in bacteria.

for the light-induced EPR signal resides on the special chlorophyll in the reaction center or on an electron-donor molecule in close association with it.

SUMMARY

Dried films of whole cell R. rubrum have a small EPR signal in the dark. Illumination at room temperature results in two reversible light-induced signals, one with a decay time of a few seconds, the other with a decay time of a few hours. We have observed reversible light-induced EPR signals in R. rubrum down to temperatures below 2°K. The kinetics of the photochanges were measured at temperatures between 1.7°K and room temperature; and in most cases, the rise and decay curves could be fitted by two exponentials.

The rise and decay rates of the EPR signal increase rapidly as the temperature is lowered from room temperature to 200°K; below 200°K the rates are approximately constant. At room temperature, illumination with saturating light intensity produces one unpaired electron for every 55 bacterial chlorophyll molecules.

FOOTNOTES AND REFERENCES

†The 880 nm absorption band in vivo is considerably narrower than the 770 nm band in acetone-water. This accounts for much of the increase of the extinction coefficient in the in vivo system. Rough measurements indicate that the oscillator strength is 30% higher in the in vivo system compared with acetone-water. This is quite interesting in the light of Sauer, Lindsay Smith, and Schultz's[10] finding that the oscillator strength of the red band in bacterial chlorophyll increases by 14.5% in going from the monomer to the dimer.

1. H. Beinert, B. Kok, and G. Hoch, Biochem. Biophys. Res. Commun. 7, 209 (1962).
2. E. C. Weaver and N. I. Bishop, Science 40, 1095 (1963).
3. G. M. Androes, M. F. Singleton, and M. Calvin, Proc. Nat. Acad. Sci. U.S. 48, 1022 (1962).
4. W. R. Sistrom and R. K. Clayton, Biochim. Biophys. Acta 88, 61 (1964).
5. P. A. Loach, G. M. Androes, A. F. Maksim, and M. Calvin, Photochem. Photobiol. 2, 443 (1963).
6. G. Cohen-Bazire, W. R. Sistrom, and R. Y. Stanier, J. Cellular Comp. Physiol. 49, 25 (1957).
7. E. A. Gere, private communication.
8. W. Low, Phys. Rev. 105, 801 (1957).
9. H. Beinert and B. Kok, Biochim. Biophys. Acta 88, 278 (1964).
10. K. Sauer, J. R. Lindsay Smith, and A. J. Shultz, J. Am. Chem. Soc. 88, 2681 (1966).
11. B. Chance and M. Nishimura, Proc. Nat. Acad. Sci. U.S. 46, 19 (1960).
12. D. De Vault and B. Chance, Biophys. J. 6, 825 (1966).
13. W. Arnold and R. K. Clayton, Proc. Nat. Acad. Sci. U.S. 46, 769 (1960).
14. R. K. Clayton, Photochem. Photobiol. 1, 201 (1962).
15. J. C. Goedheer, Biochim. Biophys. Acta 38, 389 (1960).
16. W. J. Vrendenberg and L. N. M. Duysens, Nature 197, 355 (1963).
17. M. Nishimura, Biochim. Biophys. Acta 59, 183 (1962).
18. M. Calvin and G. M. Androes, Science 138, 267 (1962).

MEASUREMENT OF SPIN-LATTICE RELAXATION IN COMPLEX SPIN SYSTEMS

Melvin P. Klein and Donald E. Phelps

A complete exploitation of NMR in the study of molecular motion would require an analysis of the fluctuating local fields at every spin in the molecule. One would like, for example, to measure the longitudinal relaxation rate of each spin. When the spins are coupled together, one cannot identify each line in the NMR spectrum with a particular spin, but studies of the longitudinal relaxation behavior of each line can still yield the desired information.

Various experimental methods[1-7] have been used to measure longitudinal relaxation of individual lines, but they all suffer to some extent from either or both of two major defects: a) the initial state from which the spins relax is not well characterized; b) the spin system is perturbed by measurement of the recovery to equilibrium. In this report we describe a new method which avoids both these problems entirely.[8]

The initial state of the spins is established by a nonselective[9] 180° pulse of the type used in standard T_1 measurements. After a time τ, a nonselective 90° pulse is applied, and the entire free induction decay following this pulse is recorded. From the Fourier transform of this decay, according to a well known theorem,[10] one obtains directly the partly relaxed spectrum. The history of this spectrum as a function of τ gives the full relaxation behavior.

Figure 1 is a superposition of such Fourier transformed free induction decays from a mixture of 50 vol. % acetone/10^{-3} M $FeCl_3$, as a function of τ. The spectra have been displaced isometrically proportional to the logarithm of the pulse spacing to display the characteristic recovery functions. The induction decays were obtained with an extensively modified Varian HR 60 spectrometer operating at 60 MHz in conjunction with an NS 544 Averager. The 90° pulse duration was 50 μsec. As expected, the water protons relax more rapidly than the acetone protons.

The limiting factor on frequency resolution in this experiment is the static field inhomogeneity, exactly as for ordinary slow passage field sweep resonances. However, a problem arises if the longitudinal relaxation rates are comparable to the inhomogeneity broadening

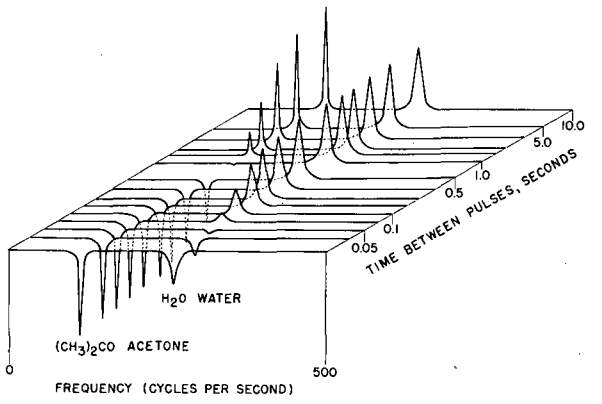

XBL 682-125

Fig. 1. Longitudinal relaxation surface for the system acetone-10^{-3} M $FeCl_3$. Each spectrum results from the Fourier transform of the free induction decay following the second pulse of a 180°-90° pulse sequence. The time interval between pulses is indicated on the right-hand edge of the spectrum. The spectra are displaced isometrically on a logarithmic scale.

$1/T_2^*$. In this case, errors in setting the initial pulse produce an initial transverse magnetization which persists long enough to interfere with the induction decay following the 90° pulse. In our experiments, the interfering transverse magnetization was destroyed by producing a temporary, large static field gradient between the 180° and 90° pulses.

Apart from its main purpose, this experiment could be useful in the analysis of equilibrium spectra containing overlapping lines. For example, an exact accidental superposition of two transitions cannot be recognized in the equilibrium spectrum but becomes evident in our experiment through the time development of intensity of the two transitions.

The principle outlined above may be applied to measure differential transverse relaxation times and differential diffusion coefficients. A Carr-Purcell[11] pulse sequence, as routinely employed for the measurement of transverse relaxation times, produces spin echoes, each of which may be Fourier transformed to reveal the partially relaxed spectra. The well-known method of determining diffusion coefficients by performing spin echo experiments in the presence of a pulsed field gradient[10] may be combined with the Fourier transform method to permit the simultaneous measurement of diffusion coefficients of chemically shifted species. Macromolecules may have relatively rigid regions coexisting with more flexible regions, and these may have different microscopic diffusion coefficients which could be determined by this method.

REFERENCES

1. N. Bloembergen, E. M. Purcell, and R. V. Pound, Phys. Rev. 73, 679 (1948).
2. L. E. Drain, Proc. Roy. Soc. (London), Ser. A, 62, 301 (1949).
3. H. C. Torrey, Phys. Rev. 76, 1059 (1949).
4. I. Solomon, Phys. Rev. Letters 2, 301 (1959).
5. J. Jonas, (private communication).
6. E. J. Wells, paper presented at 8th ENC, Pittsburgh, March 1967.
7. J. H. Noggle, J. Chem. Phys. 43, 3304 (1965).
8. The experiment was proposed by J. H. Noggle (private communication).
9. H. S. Gutowsky, R. L. Vold, and E. J. Wells, J. Chem. Phys. 43, 4107 (1965).
10. I. J. Lowe and R. E. Norberg, Phys. Rev. 107, 46 (1957). A. Abragam, Principles of Nuclear Magnetism (Oxford Univ. Press, New York, 1961), Chap. IV.
11. H. Y. Carr and E. M. Purcell, Phys. Rev. 94, 630 (1954).
12. E. O. Stejskal, J. Chem. Phys. 43, 3597 (1965).

AN IMPROVED METHOD FOR THE AUTORADIOGRAPHY OF TRITIUM ON CHROMATOGRAMS

Gerald A. Corker, Thomas R. Dehner, and Melvin Klein

INTRODUCTION

Many common isotopes important in biological systems, such as ^{14}C, ^{35}S, and ^{32}P, can be detected easily by using the combined techniques of thin-layer or paper chromatography and radioautography. If the chromatogram containing the radioactive element is placed in opposition to a film, the β-particles emitted by the isotope penetrate the emulsion leaving a darkened track on the developed film. This technique has proven very useful for the detection of elements emitting medium- or high-energy β-particles. Tritium, however, emits a very soft beta (max. energy .018 MeV) with a small range. Detection of compounds containing low levels of tritium by the above technique has not been too successful due to lack of penetration of the β-particles into the emulsion.

The following is a preliminary report on the development of a process for detecting low levels of tritium utilizing the combined techniques of thin-layer chromatography and scintillation counting.

METHOD

We are seeking to overcome the small penetration distance of tritium β-particles by converting the beta emission into photon emission, in situ, by incorporating a scintillator into the adsorbant of a thin-layer chromatogram. With the scintillator in close proximity to tritium, the β-particle causes an excitation of the scintillator resulting in photon emission. Generally, most of the photon emission could not be detected because of the light-scattering nature of the powder of the chromatogram. However, by rendering the powder transparent, more efficient light transmission occurs. Powdered polyethylene has been found suitable as the adsorbant material, for it forms an almost transparent film when heated at 120° for several minutes.

EXPERIMENTAL

A chemically inert scintillator (approx. 2% by weight)—either phenylbiphenyloxadizole-1, 2, 3 [PBD], 4, 4'-bis-(2-butyloctyloxy)-p-quaterphenyl [BOQP], 2, 5-diphenyloxazole (PPO), or a mixture containing manganese-activated zinc silicate and silver-activated zinc sulfide—was mixed uniformly with powdered polyethylene. The resulting mixture was used to prepare a chromatogram 25 mm thick using an acetone slurry (50 g powder to 200 ml acetone).

The uniformity of the scintillator distribution on the plates was checked by visual inspection of their fluorescent emission in a darkened box containing a uv light source to affect excitation. Each plate was then developed using an acetone/water (80/29) solvent system, and the uniformity checked again by the same method. No movement of the scintillator was detected. The powdered polyethylene was then fused into a transparent film by heating at 120° for several minutes, and the uniformity of fluorescence was checked again by visual inspection.

In order to test the effect of the scintillator on the characteristics of the chromatogram, three plates—one containing PBD, one containing the inorganic mixture, and one without a fluor—were prepared and spotted with phenylalanine hydrochloride. The plates were developed in 80/20 acetone-water and sprayed with ninhydrin in order to locate the amino acid. The amino acid displays approximately the same R_f value on all three plates. This system would not be good for chromatography of this material because the amino acid HCl ran very near the solvent front. However, the important conclusion is that the scintillators did not appear to influence the movement.

Two plates, one with PBD and one with the inorganic materials, were spotted with some tritiated phenylalanine hydrochloride. The test solution contained 1.07×10^6 dpm per lambda (λ). Four spots were applied to each of the plates [10^4, 10^5, 10^6, and 10^7 dpm], and the plates were developed until the amino acid had migrated up a third of the plate. Following fusion of the polyethylene, the chromatograms were placed in opposition to film for a specific period of time. Three different types of film were used: Kodak Royal X Pan, Kodak Medical X-ray "no screen," and Kodak Medical X-ray Royal Blue. The spots containing 10^7 and 10^6 dpm caused an intense darkening of all three films with both scintillators. The spot with 10^5 dpm also caused a detectable darkening of the Royal Blue and the no screen X-ray film; however, the X-pan film was spoiled by an unknown exposure in the area of this spot. The spot containing 10^4 dpm did not expose any of the films. By visual inspection of the darkened areas, the combination of the organic fluor and the Royal Blue X-ray film appear to be the most sensitive combination. Separate polyethylene plates containing either the organic scintillator BOQP or the inorganic scintillator mentioned above were prepared. Several different concentrations of each scintillator (2, 1, 5, 1.0, and 5%, and 8, 4, 2, and 1%, respectively) were used. Six spots (10^3, 5×10^3, 10^4, 5×10^4, 10^5, and 10^6 dpm) of the tritiated amino acid were applied to each plate. The powder was fused without development of the plates and the resulting chromatograms placed in opposition to the Royal X-Pan film. The film was exposed for 34 hrs and developed with Kodak D-19 developer. The spots containing activity as low as 5×10^3 dpm caused a detectable darkening of the film. The darkening of the film and the level of detectability of the activity appears to be independent of the scintillator concentration in the concentration ranges examined. These experiments need to be repeated to include the development of the chromatogram prior to the fusion. If development is not included, the tritiated compound is found in a ring in the area of application, thus concentrating the tritium.

CONCLUSION

These preliminary results suggest that this method is at least ten times as sensitive as current techniques utilizing autoradiography for the detection of tritium.[1]

In an attempt to increase this sensitivity, the possible use of photomultiplier detection of the photon emission is being investigated. A light-tight box fitted with mounts for a thin-layer plate and a photomultiplier has been constructed. After the photomultiplier output pulses are amplified and suitably shaped, they are collected in a pulse-height analyzer. Very preliminary results indicate a detection efficiency of 0.5 to 1.0 percent.

REFERENCES

1. T. Chamberlain, A. Hughes, A. W. Rogers, and C. H. Thomas, Nature 201, 774 (1964).

ORGANIC CHEMISTRY AND GEOCHEMISTRY

1, 2-DITHIANE-3-CARBOXYLIC ACID AND 1, 2-DITHIANE-4-CARBOXYLIC ACID. SYNTHESES, RESOLUTIONS, AND ABSOLUTE CONFIGURATIONS

Göran Claeson

INTRODUCTION

The first 6-membered cyclic disulfide (1, 2-dithiane) was prepared by Fredga, who in 1938 studied the chemistry and stereochemistry of 1, 2-dithiane-3, 6-dicarboxylic acid.[1-4] The interest in cyclic disulfides has increased enormously since the discovery of the fact that several natural products contain cyclic disulfides. The elucidation of the structure of lipoic acid, 1, 2-dithiolane-3-valeric acid, led to the synthesis of a large number of cyclic 5-membered disulfides and also to the synthesis of the 6-membered homologue 1, 2-dithiane-3-butyric acid.[5]

During recent years, the 1, 2-dithiane ring system has been extensively studied. Geometrically this ring system is analogous to cyclohexane. Foss has shown by X-ray crystallography that in the solid state 1, 2-dithiane-3, 6-dicarboxylic acid exists in the chair form.[6] NMR studies and dipole measurements have shown that in solution the chair form of 1, 2-dithiane is also the most favorable conformation, and that interconversions between chair forms can take place.[7-11]

For stereochemical and spectroscopic studies 1, 2-dithiane-3- and -4-carboxylic acids were needed; this report describes the preparations, resolutions, and determinations of absolute configurations of these acids.

Syntheses

1, 2-Dithiane-3-carboxylic acid was first prepared by Claeson, and mentioned in a short communication in 1960.[12] Four years later, several unsuccessful attempts to prepare the acid were described by Isenberg.[13] The synthesis described here starts from 2, 5-dibromovaleric acid, which is treated with potassium ethylxanthate (see Scheme 1). The reaction production is hydrolyzed with ammonia to the dimercapto acid, which is then oxidized to the cyclic disulfide in an excellent total yield. 1, 2-Dithiane-4-carboxylic acid has been synthesized by Claeson and Langsjoen;[14] the same method was used. However, the yield was raised by column chromatographing (silica gel) the crude acid instead of resorting to recrystallization. The optimum chromatographic conditions were first tried out with thin-layer chromatography (TLC).

Resolutions and Determinations of Configurations

The racemic 1, 2-dithiolane-3-carboxylic acid was resolved through recrystallizations of its salts with strychnine and ephedrine, and in the same way the enantiomers of 1, 2-dithiane-4-carboxylic acid were obtained via the quinine and cinchonidine salts. Optically active

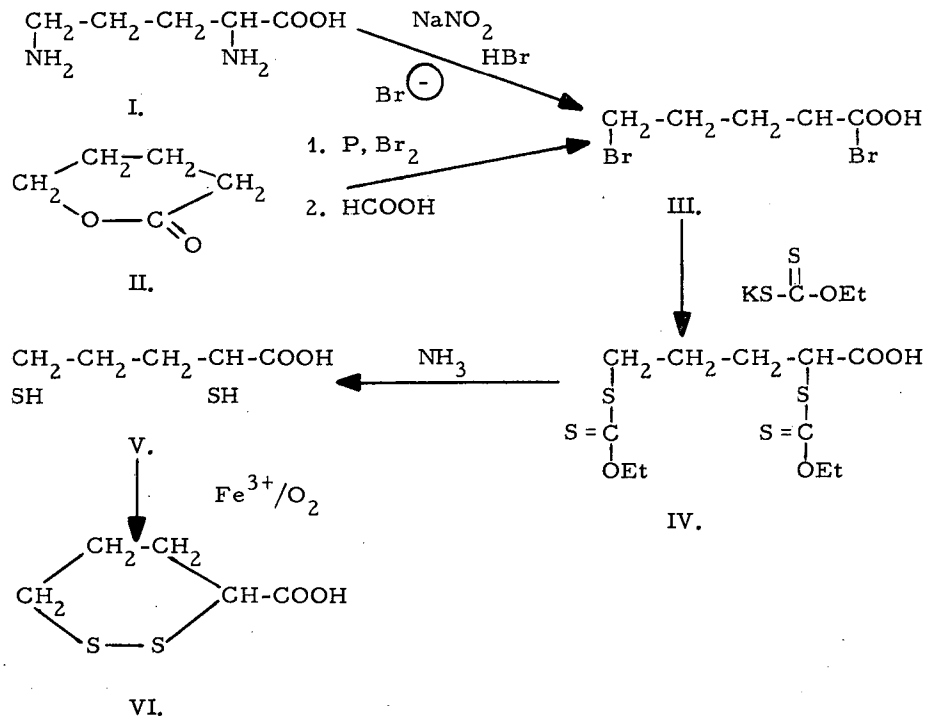

Scheme 1.

2, 5-dibromovaleric acid was prepared from the reaction of ornithine with nitrous acid in the presence of a large excess of bromide ion (see Ref. 15). This type of deamination is known to proceed with retention of configuration. Replacement of the bromine atoms of III with the xanthate groups was then performed under S_{N2} conditions. Hydrolysis of the xanthate groups and oxidation of the mercapto groups to the cyclic disulfide do not involve the optically active center. The reaction path from ornithine to 1, 2-dithiane-3-carboxylic acid thus involves only one inversion at the α-carbon of ornithine; and as the configuration of ornithine is known, the absolute configuration of 1, 2-dithiane-3-carboxylic acid is determined (Scheme 2). The dextrorotatory form has (R)- configuration according to the convention of Cahn, Ingold, and Prelog.[16] For further references and discussions of these reaction steps see Ref. 15.

The configuration of 1, 2-dithiane-4-carboxylic acid was determined by the Raney nickel desulfurization method,[17] introduced for stereochemical purposes by Fredga.[18] Thus, (+)-1, 2-dithiane-4-carboxylic acid was converted to (+)-2-methylbutyric acid, the configuration of which has been correlated with the system of glyceraldehyde by Stallberg-Stenhagen and Stenhagen.[19] L(-)-2-methylbutyric acid is represented by the Fischer projection formula VIIIa,[20] and (+)-1, 2-dithiane-4-carboxylic acid must have the corresponding formula VIIa, which can also be written as VIIb, and has the (S)- configuration.

The crude 2-methylbutyric acid obtained after the Raney Ni desulfurization was purified by gas-liquid chromatography and showed a specific rotation, $[\alpha]_D^{25}$, of +19.0° in ethanol, which is close to the highest data given in the literature (for references see Ref. 15). This indicates that 1, 2-dithiane-4-carboxylic acid has been completely resolved.

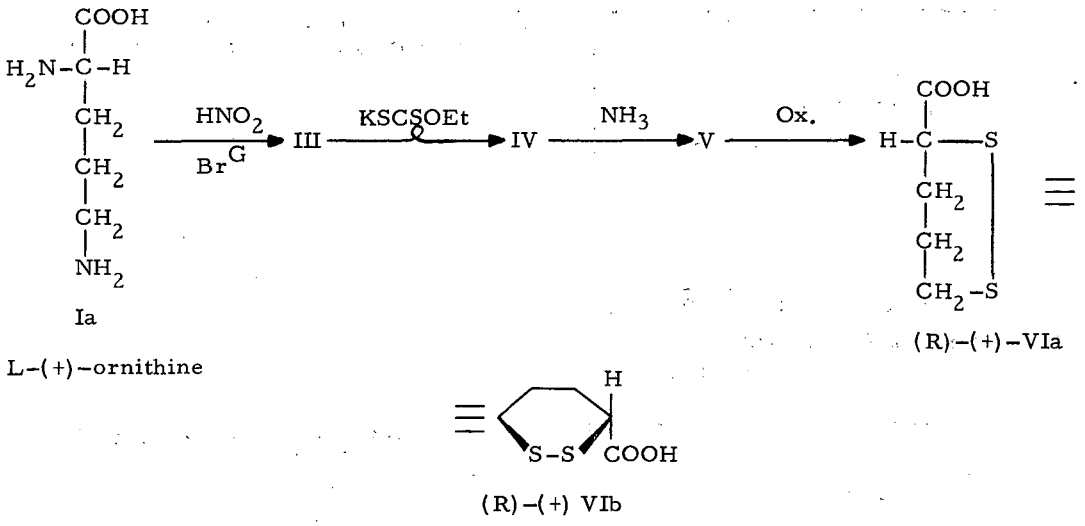

Scheme 2.

The symbol ⟶ indicates substitution with inversion of configuration.

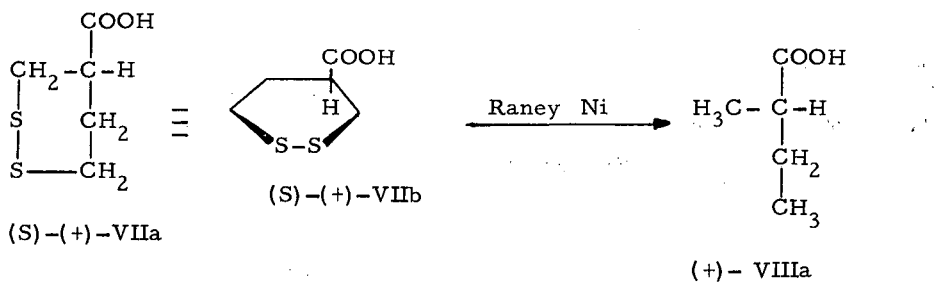

Scheme 3.

Melting Point Diagrams

Both of the 1, 2-dithianecarboxylic acids gave true racemates (Figs. 1 and 2). The (+)-form of 1, 2-dithiane-3-carboxylic acid gave a molecular compound (1:1) with the (-)-form of 1, 2-dithiane-4-carboxylic acid (Fig. 3), while the melting point diagram of the two (-)-forms shows a simple eutectic point (Fig. 4). In this case we cannot, however, consider the molecular compound a quasi-racemate for the sake of applying the Fredga quasi-racemate method.[21-23] The necessary requirement for the quasi-racemate method, namely, that the four groups attached to the asymmetrical carbon in one compound can be unambiguously correlated to corresponding groups in the other compound, is not met here. In addition, we have another complication. The disulfide group is in fact asymmetric in itself, with the two optical antipodes shown below:

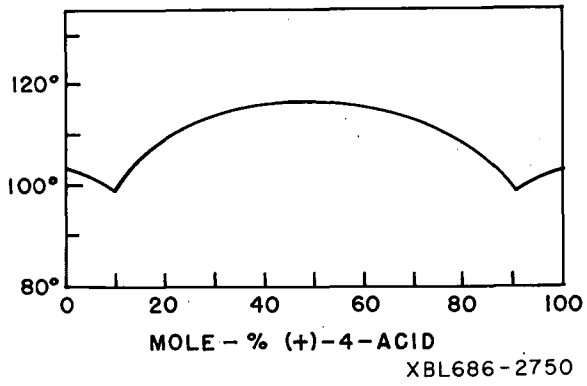

Fig. 1. (+)-1, 2-Dithiane-4-carboxylic acid, and (-)-1, 2-dithiane-4-carboxylic acid.

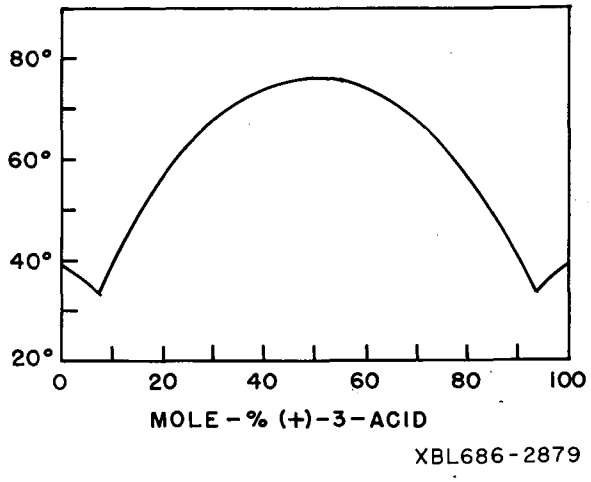

Fig. 2. (+)-1, 2-Dithiane-3-carboxylic acid, and (-)-1, 2-dithiane-3-carboxylic acid.

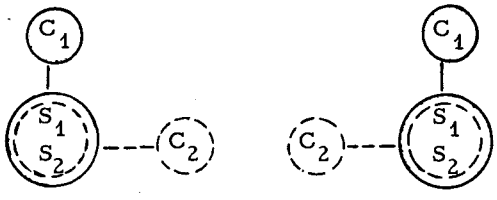

The barrier hindering the rotation about the bonds in 1, 2-dithianes has been studied in solutions.[8,9] But in the solid state, we may suppose that the acids discussed exist in chair forms with the carboxylic groups in the equatorial positions. That means that the optical antipodes of either of these acids in solid state also have opposite configurations at the disulfide bond. From the appearance of the phase diagrams (Figs. 3 and 4) and the known absolute configurations of the two acids, it seems likely that the disulfide asymmetry has a deciding influence upon the solid phase relationship.

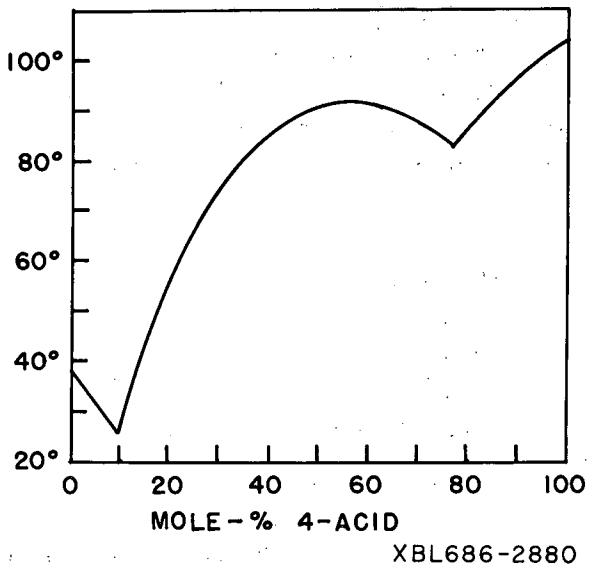

Fig. 3. (+)-1, 2-Dithiane-3-carboxylic acid, and (-)-1, 2-dithiane-4-carboxylic acid.

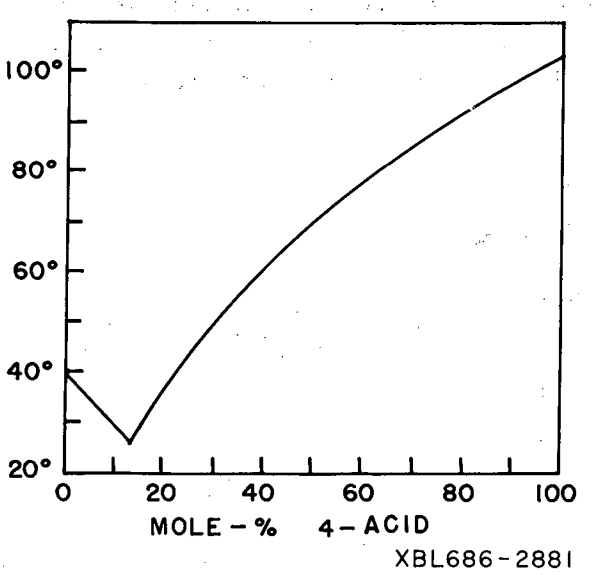

Fig. 4. (-)-1, 2-Dithiane-3-carboxylic acid, and (-)-1, 2-dithiane-4-carboxylic acid.

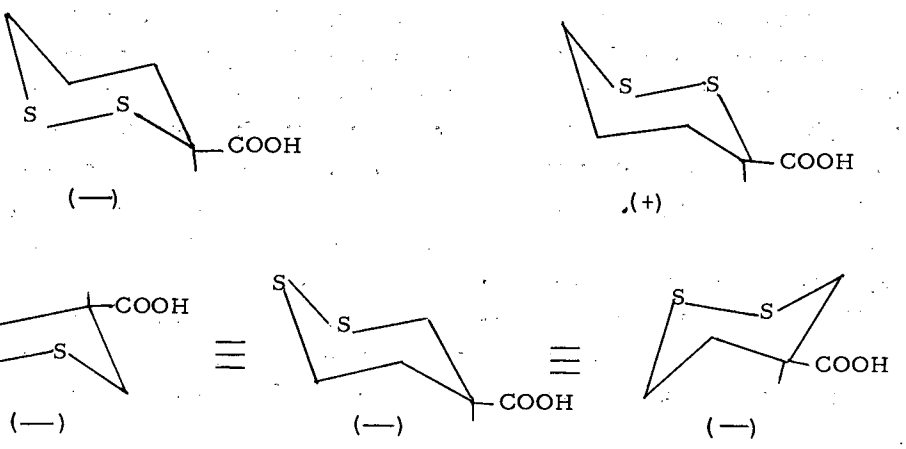

On the Absolute Configuration of 1, 2-Dithiane-3, 6-dicarboxylic Acid

Fredga has prepared the optically active 2, 5-dimercaptoadipic acids, and oxidized them to the corresponding optically active 1, 2-dithiane-3, 6-dicarboxylic acids.[1-4] As the oxidation does not involve the optically active centers, the absolute configuration of the disulfide would be known if the configuration of the mercaptoacids were known. The melting point diagrams between the (-)-form of X and the antipodes of IX

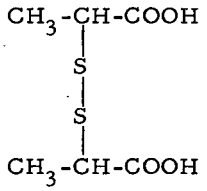

IX

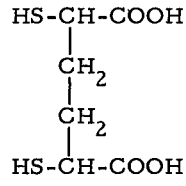

X

has been studied by Fredga.[4] The system (+)-IX and (-)-X shows a simple eutectic, but (-)-IX and (-)-X gives a molecular compound in the ratio 1:1. Fredga suggests that in the molecular compound -S-S- is probably isomorphously replaced by $-CH_2-CH_2-$ and the two $-CH_3$ by -SH. As the configuration of IX is known,[24] the suggestion above would give the configuration of X and XI as shown:

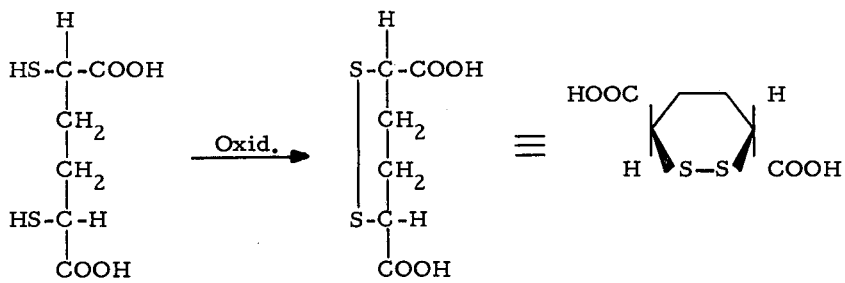

(+)-Xa (+)-XIa (+)-XIb

The optical rotatory dispersion (ORD) and circular dichroism (CD) spectra of 1, 2-dithiane-3, 6-dicarboxylic acid have been reported earlier.[25, 26] The ORD and CD curves of 1, 2-dithiane-3-carboxylic acid show the same Cotton effect as those curves of the dicarboxylic acid with the same sign of rotation.[27] The ORD and CD curves thus give a strong indication that the monocarboxylic acid with the same sign of rotation as the dicarboxylic acid also has the same configuration. As the absolute configuration of 1, 2-dithiane-3-carboxylic acid has been determined in this work (formula VIb in Scheme 2), the absolute configuration of 1, 2-dithiane-3, 6-dicarboxylic acid is given by formula XIb. This result is in agreement with the configuration already suggested by Fredga from his study of the phase diagrams.[4]

Fredga has also, by the quasi-racemate method, sterically correlated 1, 2-diselenane-3, 6-dicarboxylic acid to the sulfur analog, 1, 2-dithiane-3, 6-dicarboxylic acid.[2] Thus, the present investigation also suggests the steric correlation of the former acid to 1, 2-dithiane-3-carboxylic acid.

EXPERIMENTAL

2,5-Dibromovaleric Acid

1,5-Pentanediol, 208 g (2 moles), and 10 g of copper chromite catalyst were refluxed for 12 hr.[28] To the reaction mixture containing the crude 5-valerolactone was added 22 g of red phosphorus (dried at 110° overnight); while the mixture was stirred (and cooled to 0°), 120 ml of bromine was added dropwise. The temperature was then raised to 75-80°, and a further 80 ml of bromine was carefully added. After the mixture stood for 18 hr at this temperature, dry air was bubbled through the solution to remove hydrobromic acid and excess bromine. The acid bromide was decanted, and 106 g of formic acid (85%) was carefully added. The solution was left at room temperature overnight. Fractionation in vacuo gave 369 g (71%) of 2,5-dibromovaleric acid, b.p. 130-135°/1-2 mm, n_D^{20} = 1.5335. Literature values[29]: b.p. 150-152°/5 mm, n_D^{25} = 1.5347.

1,2-Dithiane-3-carboxylic Acid

To 11 g (0.041 mole) of 2,5-dibromovaleric acid was added 50 ml of water, and the acid was neutralized with potassium bicarbonate. Potassium ethylxanthate, 13.7 g (0.086 mole), was immediately added, and the mixture shaken until homogenous. After the mixture stood at room temperature for 24 hr, 75 ml of concentrated ammonia was added, and the solution left overnight in a stoppered flask. The ammonia was then removed at reduced pressure. The remaining neutral solution was made alkaline with an aqueous sodium hydroxide, and the xanthogen amide product was removed by extraction with ether. After the aqueous solution was acidified, the dimercaptoacid was extracted with ether. The ether solution was extracted with two 25-ml portions of 2 N sodium hydroxide, and the alkaline solution was diluted to 1500 ml and neutralized to pH 7.5. One ml of ferric chloride solution (1%) was added, and air bubbled through the dark blue solution until the color changed to yellow. The solution was acidified with hydrochloric acid and extracted with ether. The etherial solution was dried over anhydrous magnesium sulfate, and the ether removed at reduced pressure. The remaining pale yellow oil did not crystallize. When a small specimen was heated in a sublimation apparatus at 0.1 mm, white crystals were formed on the cold finger. The entire oily phase was seeded, and it thereupon crystallized immediately. The yield of 1,2-dithiane-3-carboxylic acid was 6.0 g (91%), m.p. 69-73°. Recrystallizations from benzenecyclohexane gave long colorless needles with m.p. 75-76°. The ultraviolet spectrum recorded in ethanol had λ_{max} 280 mμ (ϵ245) and λ_{infl} 245 mμ.

($C_5H_8O_2S_2$)	calc.	C: 36.56;	H: 4.91;	S: 39.05;	Eq. wt. 164.3
	found	C: 36.41;	H: 4.98;	S: 39.09;	Eq. wt. 164.3

1,2-Dithiane-4-carboxylic Acid

1,2-Dithiane-4-carboxylic acid was prepared by the method of Claeson and Langsjoen[14] via β-benzylthioethyl-benzylthiomethylmalonic acid. The crude 1,2-dithiane-4-carboxylic acid was most efficiently purified, not by fractional crystallization, but by column chromatography. The optimum conditions were tried out with thin-layer chromatography. A 35-cm long and 4.5-cm wide column of silica gel (for TLC) was employed, using as moving phase

chloroform:acetic acid (9:1) at a flow rate of 80 ml/hr. Samples (10 ml) were collected and analyzed with TLC using the ascending method and the same solvent mixture. The chromatograms were developed (after drying in air) by exposure to iodine vapor. The chromatographic purification gave 1, 2-dithiane-4-carboxylic acid directly in a pure form and in a better yield (80%) than had been reported earlier (59%) when the acid was purified by recrystallizations.[14]

(+)-1, 2-Dithiane-3-carboxylic Acid from Ornithine

In a 500-ml three-necked flask—fitted with two dropping funnels, a gas outlet tube, and a magnetic stirrer—were placed 10.1 g (0.06 mole) of L-(+)-ornithine hydrochloride and 124 g (1.2 moles) of sodium bromide dissolved in 300 ml of water. One of the dropping funnels was filled with 10.5 g (0.15 mole) sodium nitrite dissolved in 50 ml of water, and the other with 17.4 ml (0.15 mole) of 46% hydrobromic acid and 40 ml of water. The flask was cooled in an ice bath, and the solutions of sodium nitrite and hydrobromic acid were added dropwise, accompanied by vigorous stirring. The nitrogen was collected over water in a graduated vessel. After 2 hr, about half of the solution had been added. The reaction rate had then decreased considerably; therefore the cooling bath was removed. After a further 4 hr, all of the solution had been added, and the flask was left at room temperature for 2 hr; at this point nitrogen gas evolution had ceased, and a total of 3100 ml of gas had been collected. The reaction mixture was extracted with ether, and the ether solution was then extracted with a solution of 5 g of sodium bicarbonate in 100 ml of water. To this water solution was immediately added 22.4 g (0.14 mole) of potassium ethyl xanthate, and the mixture shaken until homogenous. After the mixture stood at room temperature for 24 hr, 120 ml of concentrated ammonia was added, and the solution left for 26 hr in a stoppered flask. The reaction mixture was then worked up and oxidized in the same way as described above. After evaporation of the ether solution, 2.2 g of a yellow oil remained; this was extracted with boiling petroleum ether (30-60°). The hot petroleum ether was allowed to cool slowly. White crystals (m.p. 71-75°) formed and were filtered. On further cooling, a second crop of crystals could be collected, and after 24 hr at -5° a third crop of white crystals had formed and was filtered. The m.p. of the third fraction was 26-30°, $[\alpha]_D^{25}$ = +147°, and the equiv. weight was 164.5. A gas-liquid chromatogram on SE 30 showed a purity of about 99.5%, and the retention time was the same as that of authentic 1, 2-dithiane-3-carboxylic acid. The isolated acid was identified as 1, 2-dithiane-3-carboxylic acid on the basis of its m.p. and mixed m.p. with an authentic sample with the same optical rotation, and by comparison of its UV and IR absorption spectra with those of the authentic sample.

Raney-Nickel Desulfurization of 1, 2-Dithiane-4-carboxylic Acid

To a solution containing 164 mg (1.00 mmole) of 1, 2-dithiane-4-carboxylic acid (m.p. 103-104°, $[\alpha]_D^{25}$ = -167°) and 2.4 g potassium hydroxide in 20 ml of water was added, in portions, 6g of Raney-nickel alloy; and the mixture was refluxed for 24 hr. The nickel was filtered off and washed with sodium hydroxide solution. The combined aqueous phases were concentrated in vacuo, acidified with sulfuric acid, and extracted with ether. The ether solution was dried over magnesium sulfate, and the ether distilled. The remaining acid (92 mg) was purified by gas-liquid chromatography using a 1/4-in. × 10-ft stainless steel column packed with 5% SE 30 on dimethylchlorosilane (DMCS)-treated Chromosorb G. At a column temperature of 140°,

with a helium flow rate of 40 ml/min, the reaction product had a retention time of 3.0 min, which is identical with that of authentic 2-methylbutyric acid. The chromatographed acid, 52 mg (51%), gave an infrared spectrum which was indistinguishable from that of authentic 2-methylbutyric acid. The acid showed levorotation with $[\alpha]_D^{25}$ = -19.0° (c = 1.1, 96% ethanol).

Preliminary Tests on Resolution

1, 2-Dithiane-3-carboxylic acid

Racemic acid (0.001 mole) and optically active base (0.001 mole) were dissolved in hot ethanol (96%). The solutions were left at room temperature. If no crystals formed, the solutions were put in a refrigerator until crystals or oils did form. The crystals were filtered, and the acid liberated and extracted with ether. The ether was removed, and the optical activity measured in 95% ethanol. The results are given in Table I.

Table I

Base	ml ethanol	mg salt	$[\alpha]_D^{25}$ of the acid
Cinchonine	4.0	oil	--
Cinchonidine	4.0	105	-19°
Morphine	3.5	oil	--
Brucine	2.0	41	±0°
Strychnine	10.0	161	-68°
Quinine	2.0	184	-31°
Quinidine	3.0	oil	--
Ephedrine	3.0	133	+22°

1, 2-Dithiane-4-carboxylic acid

The preliminary tests on resolution have been published earlier.[14]

Optical Resolutions

(-)-1, 2-Dithiane-3-carboxylic acid

Racemic acid, 30.1 g (0.183 mole), and 61.3 g (0.183 mole) of strychnine were dissolved in 3000 ml of hot 96% ethanol. The solution was left to crystallize at room temperature, and then in a refrigerator overnight. The salt was filtered off, dried, and weighed. About 0.2 g of the salt was made alkaline with sodium hydroxide solution, and the base extracted with chloroform. The acid was liberated from the aqueous alkaline solution with hydrochloric acid, and then extracted with ether. The ether was dried with magnesium sulfate, the acid isolated, and the optical activity measured in 96% ethanol. The main part of the precipitate was recrystallized from ethanol until the liberated acid showed constant optical activity (Table II). The acid seemed to racemize and decompose easily under alkaline conditions. The heating time necessary for dissolving the strychnine salt was therefore kept as short as possible.

Table II

Crystallization	1	2	3	4	5	6	7	8
ml 96% ethanol	3000	1700	1400	900	900	750	700	650
g salt obtained	54.0	38.0	33.1	26.0	25.0	21.0	19.3	18.7
$[\alpha]_D^{25}$ of acid	-78°	-121°	-139°	-152°	-160°	-166°	-168°	-168°

The acid from 3.90 g of the strychnine salt was isolated as described above, and 1.2 g of a pale yellow oil was obtained. The oil crystallized after a few minutes in refrigerator. Recrystallizations from petroleum ether (b.p. 30-60°) gave white crystals with m.p. 37.8-39.5°, $[\alpha]_D^{25}$ = -172°.

$(C_5H_8O_2S_2)$ calc. equiv. wt. 164.3
found equiv. wt. 164.0

(+)-1, 2-Dithiane-3-carboxylic acid

The mother liquor from the first crystallization of the strychnine salt was evaporated to dryness at room temperature, and the acid isolated as described above. Recrystallization from petroleum ether gave 7.8 g of acid with $[\alpha]_D^{25}$ = +100° (96% ethanol). This acid and 7.8 g of ephedrine were dissolved together in hot ethanol. Recrystallizations and measurements of the optical activity were performed as described for the strychnine salt. The results are shown in Table III.

Table III

Crystallization	1	2	3	4	5
ml 96% ethanol	100	80	70	60	50
g salt obtained	8.7	7.3	5.64	4.60	4.15
$[\alpha]_D^{25}$ of the acid	140°	150°	162°	168°	167°

The acid was isolated from 3.9 g of the ephedrine salt, and two recrystallizations from petroleum ether (b.p. 30-60°) gave 1.4 g of white crystals with m.p. 38-39.5°, $[\alpha]_D^{25}$ = +171°.

$(C_5H_8O_2S_2)$ calc. equiv. wt. 164.3
found equiv. wt. 164.9

(-)-1, 2-Dithiane-4-carboxylic acid

Racemic acid, 15.4 g (0.094 mole), and 30.5 g (0.094) of quinine were dissolved in 1000 ml of boiling 96% ethanol. After the solution stood 24 hours in a refrigerator, 30.0 g salt had separated; this was recrystallized four times. The change in optical activity of the liberated acid was measured as described for 1, 2-dithiane-3-carboxylic acid. The results are shown in Table IV.

Table IV

Crystallization	1	2	3	4	5
ml 96% ethanol	1000	1000	750	650	575
g salt obtained	30.0	17.1	15.0	12.4	10.3
$[\alpha]_D^{25}$ of the acid	-49°	-129°	-142°	-164°	-163°

To 10.1 g of the quinine salt from the last recrystallization was added a slight excess of 2 N sodium hydroxide solution. The quinine was extracted with chloroform, and to the remaining aqueous solution hydrochloric acid was added carefully. At first, a small amount of a brown, oily precipitate formed. This was filtered and discarded. The colorless aqueous solution was cooled in an ice bath and more hydrochloric acid added under stirring. The formed colorless crystals were filtered and dried. One crystallization from benzene-petroleum ether gave 2.1 g of acid with m. p. 103-104°, $[\alpha]_D^{25}$ = -167°. The acidic aqueous diltrate was extracted with ether and a further 0.4 g of acid was obtained. After two recrystallizations this gave the same melting point as the bulk of the acid.

$(C_5H_8O_2S_2)$ calc. equiv. wt. 164.3
found equiv. wt. 165.2

(+)-1, 2-Dithiane-4-carboxylic acid

From the mother liquors of the first two quinine salt crystallizations, the quinine was removed and the acid obtained in an alkaline, aqueous solution as described for the (-)-form. Acidification with hydrochloric acid gave 7.7 g of an acid with m. p. 102-113° and $[\alpha]_D^{25}$ = +65°. Extraction of the acidic aqueous solution gave a further 1.2 g of acid with m. p. 106-109° and $[\alpha]_D^{25}$ = +117°. To 7.6 g (0.046 mole) of the acid with $[\alpha]_D^{25}$ = +65° was added 13.6 g of cinchonidine. The mixture was dissolved in 125 ml of boiling ethanol. After the solution stood 48 hr in a refrigerator, the salt thus obtained was filtered. The acid was liberated from a small sample and its optical rotation measured; the main part of the salt was recrystallized five times. The optical activity of the liberated acid had then reached a constant value; and, therefore, the bulk of the salt was decomposed and the acid was recrystallized from benzene-petroleum ether. The m. p. was 102-103° and $[\alpha]_D^{25}$ = +166°.

$(C_5H_8O_2S_2)$ calc. equiv. wt. 164.3
found equiv. wt. 163.6

Melting Point Diagrams

The contact method[30, 31] was used for a preliminary study of the melting point diagrams. For accurate measurements, weighed amounts of the components were dissolved in a few drops of ether. After evaporation of the solvent, the residue was carefully powdered and dried in a desiccator. Some of the mixtures did not crystallize at room temperature, but could be brought to crystallization in a refrigerator. The melting points were determined in a Kofler hot stage microscope.

SUMMARY

1, 2-Dithiane-3-carboxylic acid and 1, 2-dithiane-4-carboxylic acid have been synthesized and resolved into optical antipodes via alkaloid salts. Their rotatory powers are of the same magnitude, $[\alpha]_D^{25}$ = 171° and 167° respectively. The absolute configuration of 1, 2-dithiane-3-carboxylic acid has been determined by synthesis from ornithine, and the absolute configuration of 1, 2-dithiane-4-carboxylic acid by Raney nickel desulfurization to 2-methylbutyric acid. The melting point diagrams between the optical antipodes have been discussed. The configuration of 1, 2-dithiane-3, 6-dicarboxylic acid has been related to that of 1, 2-dithiane-3-carboxylic acid by means of their ORD and CD curves.

REFERENCES

1. A. Fredga, Ber. 71, 289 (1938).
2. A. Fredga, Arkiv Kemi, Mineral. Geol. 12 A, No. 27 (1938).
3. A. Fredga, J. Prakt. Chem. [2] 150, 124 (1938).
4. A. Fredga, Arkiv Kemi, Mineral. Geol. 14 B, No. 15 (1941).
5. M. W. Bullock, J. A. Brockman, E. L. Patterson, J. V. Pierce, and E. L. R. Stockstad, J. Am. Chem. Soc. 74, 3455 (1952).
6. O. Foss and T. Reistad, Acta Chem. Scand. 11, 1427 (1957).
7. G. Claeson, G. Androes, and M. Calvin, J. Am. Chem. Soc. 82, 4428 (1960).
8. G. Claeson, G. Androes, and M. Calvin, J. Am. Chem. Soc. 83, 4357 (1961).
9. A. Lüttringhaus, S. Kabuss, W. Maier, and H. Friebolin, Z. Naturforsch. 16 b, 761 (1961).
10. N. Isenberg and H. F. Herbrandson, Tetrahedron 21, 1067 (1965).
11. H. T. Kalff and E. Havinga, Rec. Trav. Chim. 81, 282 (1962).
12. G. Claeson, Acta Chem. Scand. 13, 1709 (1959).
13. N. Isenberg, Ph.D. Thesis, Rensselaer Polytechnic Institute, New York, 1963.
14. G. Claeson and A. Langsjoen, Acta Chem. Scand. 13, 840 (1959).
15. G. Claeson and H. -G. Jonsson, Arkiv Kemi 26, 247 (1966).
16. R. S. Cahn, C. K. Ingold, and V. Prelog, Experientia 12, 81 (1956).
17. G. R. Pettit and E. E. van Tamelin, Org. Reactions 12, 356 (1962).
18. A. Fredga, Arkiv Kemi 6, 277 (1953).
19. S. Ställberg-Stenhagen and E. Stenhagen, Arkiv Kemi, Mineral Geol. 24 B, No. 9 (1947).
20. J. P. Greenstein and M. Winitz, Chemistry of the Amino Acids (Wiley, New York, 1961), v. 1, p. 157.
21. A. Fredga, in The Svedberg 1884 30/8 1944, A. Tiselius and K. O. Pedersen, Eds. (Almqvist and Wilsells Publishers, Uppsala and Stockholm, 1944), p. 261.
22. A. Fredga, Arkiv Kemi, Mineral Geol. 14 B, No. 27 (1941).
23. A. Fredga, Tetrahedron 8, 126 (1960).
24. A. Fredga, Arkiv Kemi, Mineral Geol. 12 B, No. 22 (1936).
25. C. Djerassi, A. Fredga, and B. Sjoberg, Acta Chem. Scand. 15, 417 (1961).
26. C. Djerassi, H. Wolf, and E. Bunnerberg, J. Am. Chem. Soc. 84, 4552 (1962).
27. G. Claeson and E. A. Dratz, unpublished observations.
28. L. E. Schniepp and H. H. Geller, J. Am. Chem. Soc. 69, 1545 (1947)

29. R. Merchant, J. N. Wickert, and C. S. Marvel, J. Am. Chem. Soc. 49, 1828 (1927).
30. L. Kofler and A. Kofler, Mikro-Methoden (Universitatsverlag Wagner, Innsbruck, 1948), p. 115.
31. M. Matell, Stereochemical Studies on Plant Growth Substances. Thesis, Uppsala (1953), p. 16.

CHARGE TRANSFER COMPLEXES WITH HEXAFLUOROBENZENE AND PENTAFLUOROBENZONITRILE AS ACCEPTOR COMPONENTS

Gerald A. Corker and Melvin Calvin

Charge transfer associations are a well-established phenomena and a rather extensively investigated one also.[1] Since the acceptor component of such complexes normally does not exist as a liquid under standard conditions,[2] we wish to report on two organic liquids which function as acceptor components with suitable complementary molecules.

As indicated in Fig. 1 (by the presence of an extended shoulder in the spectra of the mixture), pentafluorobenzonitrile (PFBN) complexes with N, N, N', N'-tetramethyl-p-phenylenediamine (TMPD), with N, N-dimethylaniline (DMA), and with phenothiazine in cyclohexane. In addition, crystalline complexes of TMPN-PFBN and DMA-PFBN are obtained when the pure materials are mixed.

These two organic bases also form solid complexes with hexafluorobenzene (HFB) when the materials are mixed in the pure state in a ratio of 1:1. However, new absorption bands are not detected in the spectra (in cyclohexane solutions) of mixtures of TMPD or DMA with HFB. When HFB is used as a solvent for TMPD or DMA, the solutions are visibly yellow. However, with time a reaction occurs, as evidenced by the formation of a black precipitate.

The solid complex formed between TMPD-PFBN, which is orange, was analyzed by a combination extraction and spectroscopic method and by vapor phase chromatography, and was found to contain a ratio of the two components of 1:1, which agrees with an elemental analysis of this complex.

Analysis of DMA-PFBN or DMA-HFB complexes were complicated by the presence of excesses of the liquid components on the crystalline complexes. When attempts are made to dry the crystals, the crystals dissociate as the excesses evaporate, until the crystals and the two components totally disappear. The TMPD-HFB complex was not analyzed. The complex between phenothiazine and PFBN was not isolated as a crystalline material.

The association constants for the TMPD-PFBN and DMA-PFBN complexes were determined according to the method of Hildebrand and Benesi.[3] The data obtained for these complexes, plotted according to the Hildebrand-Benesi equation, are shown in Fig. 2. The association constants and extinction coefficients are given in Table I.

Although the NMR spectrum of the TMPD-PFBN complex suggested that free radicals were present in this complex (evidenced by line broadening compared to TMPD in CCl_4), no radical species could be detected by EPR in any of the complexes reported here—either in solution or in the solid complexes. Nor did illumination with ultraviolet or visible light produce a detectable level of paramagnetic species.

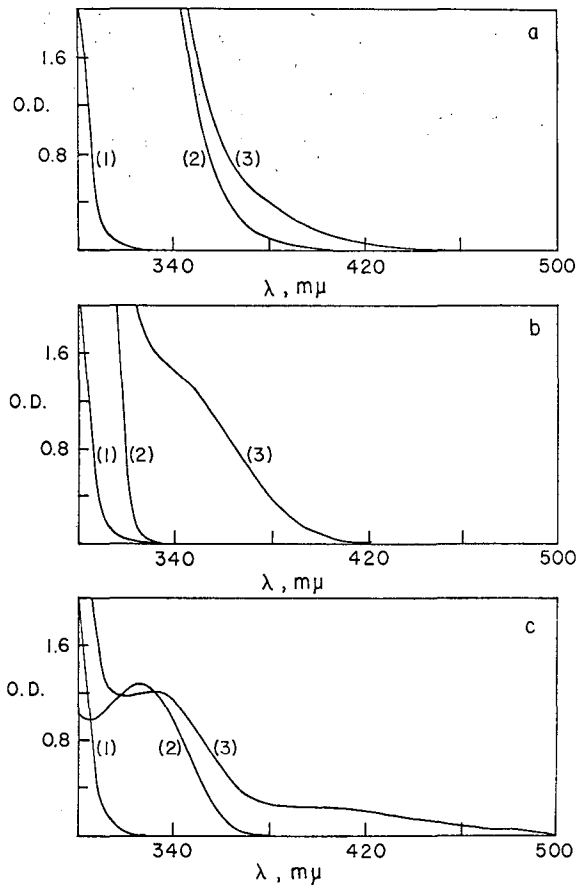

Fig. 1. Optical spectra in cyclohexane in one cm cells. (a) 1. 0.74 M PFBN, 2. 1.3×10^{-3} M phenothiazine, 3. mixture of 1.3×10^{-3} M phenothiazine and 0.11 M PFBN. (b) 1. 0.74 M PFBN, 2. 4.5×10^{-3} M DMA, 3. mixture of 4.5×10^{-3} M DMA and 0.66 M PFBN. (c) 1. 0.74 M PFBN, 2. 5.0×10^{-4} M TMPD, 3. mixture of 5.0×10^{-4} M TMPD and 0.74 M PFBN.

Table I. Association constants and extinction coefficients for TMPD-PFBN and DMA-PFBN complexes.

Concentrations				K	
PFBN	TMPD	DMA	(mμ)	(moles/1)	(1/mole cm)
0.08 to 0.73 M	5.0×10^{-4} M	0	380	4.0	800
0.08 to 0.73	5.0×10^{-4}	0	400	4.1	700
0.08 to 0.73	5.0×10^{-4}	0	420	4.3	600
0.07 to 0.66 M	0	4.5×10^{-3} M	340	2.7	500
0.07 to 0.66	0	4.5×10^{-3}	350	3.1	400
0.07 to 0.66	0	4.5×10^{-3}	360	3.1	310

The cell path length was 1 cm in all these experiments.

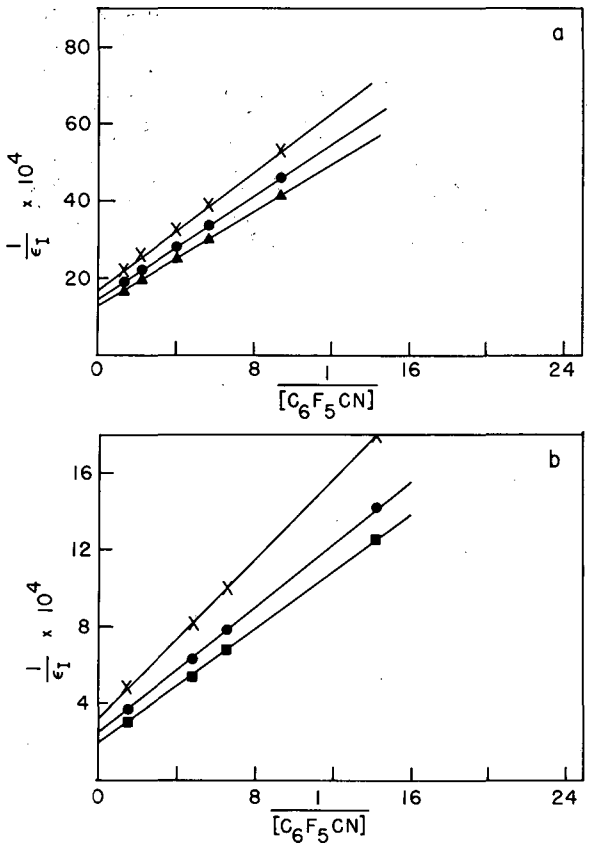

Fig. 2. Hildebrand-Benesi plots of charge transfer absorption. (a) TMPD-PFBN complex at 380 mμ (closed triangles), 400 mμ (closed circles), and 420 mμ (crosses). (b) DMA-PFBN complex at 340 mμ (closed squares), 350 mμ (closed circles), and 360 mμ (crosses).

REFERENCES

1. F. J. Bullock, Comprehensive Biochemistry, M. Florkin and E. H. Stotz, Eds. (Elsevier Publishing Company, Amsterdam-London-New York, 1967).
2. G. Briegleb, Electron-Donator-Acceptor Komplexe, (Springer, Berlin, 1961).
3. H. Benesi and J. H. Hildebrand, J. Am. Chem. Soc. 70, 2832 (1948); 71, 2703 (1949).

ORGANIC GEOCHEMICAL STUDIES. I. MOLECULAR CRITERIA FOR HYDROCARBON GENESIS[†]

Eugene D. McCarthy and Melvin Calvin

In the examinations of ancient sediments for traces of organic compounds that may be residues of living systems, it is important to be able unequivocally to distinguish between compounds produced abiogenically and those that are products of life. In this paper we discuss such criteria as molecular specificities, optical activity, and carbon-isotope ratios. Molecules that consist of isoprene units are particularly important in geochemistry, and abiogenic construction of such molecules now seems possible.

[†]Abstract of a paper published in Nature 216, 642 (1967). Supported in part by the National Aeronautics and Space Administration.

ORGANIC GEOCHEMICAL STUDIES. II. A PRELIMINARY REPORT ON THE DISTRIBUTION OF ALIPHATIC HYDROCARBONS IN ALGAE, BACTERIA, AND A RECENT LAKE SEDIMENT†

Jerry Han, Eugene D. McCarthy, William Van Hoeven, Melvin Calvin, and W. H. Bradley

This work was carried out as a contribution to the question of whether algal oozes could give rise to oil shales. Although there is a predominance of C_{17} normal alkane in modern algae and bacteria, there is little of it in the lake sediment (algal ooze) that we examined. It is possible that this ooze might be a particularly suitable substrate for certain nonphotosynthetic bacteria that might convert the C_{17} alkane into higher molecular-weight hydrocarbons.

---

†Abstract of a paper published in Proc. Natl. Acad. Sci. U.S. 59, 29 (1968). Supported in part by the National Aeronautics and Space Administration.

PHOTOCHEMISTRY AND RADIATION CHEMISTRY

SOME THERMODYNAMICS OF PHOTOCHEMICAL SYSTEMS[†]

Robert T. Ross

A limit on the thermodynamic potential difference between the ground and excited states of any photochemical system is established by evaluating the potential difference at which the rates of photon absorption and emission are equal; the relationship between absorption and emission is given by a Planck-law relation, provided that there is thermal equilibrium between the sublevels of each electronic band. The actual potential developed may be evaluated if the quantum yield of luminescence is known. The maximum amount of power storage obtainable is evaluated by lowering the potential difference until the product of the potential difference and the fraction of the quanta retained is maximized. The history and applications of the Planck-law relation between absorption and emission spectra are discussed briefly, and applications of the potential difference calculation are mentioned.

[†]Abstract of paper published in J. Chem. Phys. 46, 4590 (1967).

THE PHOTOLYSIS OF 2, 3, 3-TRIPHENYLOXAZIRIDINE-- DIRECT EVIDENCE FOR PHENYLNITRENE

Janet Splitter

In a previous study,[1] several 2-phenyl, 3-aryloxaziridines were found to undergo photofragmentation to the aldehyde and presumably phenylnitrene.[2] Although aniline and azobenzene were the chief end products from the N-phenyl part of the molecule and also are the same products resulting from other phenylnitrene precursors,[3] a characteristic trapping reaction in diethylamine to form 2-diethylamino-3H-azepine[4] was not successful.[5] Evidence was presented indicating that photofragmentation of these oxaziridines occurs via the triplet state to give triplet phenylnitrene, whereas azepine formation most likely occurs via the singlet state of phenylnitrene.

When 2, 3, 3-triphenyloxaziridine (I) was found to be a stable oxaziridine,[6] a detailed study of its photolysis was possible. When irradiated in diethylamine, (I) gave only traces of azepine, although the major photoreaction was fragmentation[7] to benzophenone and phenylnitrene.

Phenylnitrene was demonstrated in the photolysis of (I) at 77°K in acetophenone and in methylene chloride-Fluorolube solution.[8] Its EPR absorption spectrum at 6701 gauss was identical in all characteristics to the ground state triplet phenylnitrene EPR absorption spectrum produced from the photolysis of phenylazide in Fluorolube.[3c, 9] There was no indication of diphenylmethylene in the photolysis solution.[10] In the g = 2 region, there was a pronounced signal in both the phenylazide and (I) photolysis solutions. These were similar, with the main difference being in the weak signals associated with each.

In Table I are given the results of the photolysis of α, α, N-triphenylnitrone and (I) under various conditions. In Fig. 1 is a summary of the results.

It had been found previously[6] that an almost quantitative yield of the oxaziridine could be produced from the nitrone (.001 M) by 4.5 min irradiation under oxygen with a Pyrex filter in various solvents. The oxaziridine has very little absorption above 280 mμ; and prolonged irradiation with Pyrex filter, as in Experiments 1 and 2, had minimal effect on the yield of oxaziridine. When the irradiations were carried out under nitrogen, there was some decrease of oxaziridine in diethylamine (Exp. 3), but a large decrease in acetone (Exp. 4), and a corresponding increase in benzophenone. In contrast, in benzene (Exp. 5) under nitrogen there was still a high yield of oxaziridine. In Experiment 6, p-dimethylaminobenzaldehyde was added after the irradiation of the nitrone to oxaziridine. Upon further irradiation under nitrogen, there was a definite increase in the amount of benzophenone with a corresponding decrease of unchanged oxaziridine compared to Experiment 3. These results indicate sensitization by acetone and by p-dimethylaminobenzaldehyde of the photofragmentation to benzophenone and phenylnitrene.

The nitrone was irradiated to oxaziridine in Experiments 7 and 8, and then the oxaziridine was irradiated under nitrogen in quartz. In both cases there was a fairly high yield of benzophenone and appreciable amounts of imine. The imine yield was somewhat greater in diethylamine than in acetone. Experiment 9 is similar to Experiment 7, except that the oxaziridine

Table I. Products from the photolysis of α, α, N-triphenylnitrone and 2, 3, 3-triphenyloxaziridine.[a]

$$\phi_2C{=}\overset{O}{\overset{\nearrow}{N}}\text{-}\phi \xrightarrow{h\nu} \phi_2C{=}N\phi + \phi_2\overset{O}{\overset{/\backslash}{C}}\text{-}N\phi \xrightarrow{h\nu} \phi_2C{=}O + \phi NH_2 + \phi N{=}N\phi + \phi_2C{=}N\phi + \phi\overset{O}{\overset{\|}{C}}\text{-}N\phi_2$$

Experiment	Solvent	Photolysis conditions[b]	Unchanged oxaziridine	% yield[c] ϕ_2CO	ϕNH_2	$\phi N{=}N\phi$	$\phi_2C{=}N\phi$[d]	$\phi\overset{O}{\overset{\|}{C}}\text{-}N\phi_2$
1	$(C_2H_5)_2NH$	P, O, 10	88	-	-	-	-	-
2	CH_3COCH_3	P, O, 10	80	6	-	-	-	5
3	$(C_2H_5)_2NH$	P, N, 10	67	12	3	-	8	-
4	CH_3COCH	P, N, 10	21	55	-	2	5	8
5	C_6H_6	P, N, 10	81	11	-	-	-	1
6	$(C_2H_5)_2NH$	(P, O, 4-1/2 (P, N, 8[e]	32	36	46	-	3	-
7	$(C_2H_5)_2NH$	(P, O, 4-1/2 (Q, N, 4	18	47	7	2	22	-
8	CH_3COCH_3	(Q, N, 4	13	52	-	2	14	8
9	$(C_2H_5)_2NH$	(P, O, 4-1/2 (Q, O, 4	33	50	6	2	6	-
10	$(C_2H_5)_2NH$	Q, N, 4	12	29	2	-	54	-
11	CH_3COCH_3	Q, N, 4	32	31	-	-	17	8
12	C_6H_6	Q, N, 4	29	41	-	4	19	5
13	$(C_2H_5)_2NH$	Q, O, 4	34	45	3	-	10	-
14	CH_3COCH_3	Q, O, 4	40	34	-	-	12	7

(a) Irradiations (100 ml) were carried out in a water-cooled jacket around a 450 watt Hanovia type L mercury vapor lamp. Concentrations were 1×10^{-3} M in starting nitrone.

(b) P = Pyrex filter; Q = quartz; O = O_2; N = N_2; time of irradiation in min including about 2 min warm-up time of the lamp and including 4 min irradiation of the nitrone to the oxaziridine.

(c) Unchanged oxaziridine was determined by active O determination. After concentration to 5 ml, products were separated on an Aerograph A-90-P preparative gas chromatograph with a 10 ft × 1/4 in. column of 4.8% SE30 on Aeropak. Product analysis was by GLC retention time on an F&M Research chromatograph 5750 with a 6 ft × 1/8 in. column on 10% SE30 on Chrom W, ultraviolet absorption spectroscopy on a Cary 14 spectrophotometer, and mass spectroscopy on a Consolidated Electrodynamics Type 21-103C mass spectrograph. At an injection temperature of 300° in the gas chromatograph the oxaziridine yielded 60% anilide, 28% benzophenone, and 10% imine. The yields of the products determined by GLC were corrected for the products resulting from the thermal reaction of the unchanged oxaziridine.

(d) Imine formation is not due to benzophenone reacting with aniline under these conditions.

(e) p-Dimethylaminobenzaldehyde (DMB) was added after the irradiation to oxaziridine so that the resulting solution was 0.001 M in aldehyde. The aldehyde absorbed practically all the light above 280 mμ.

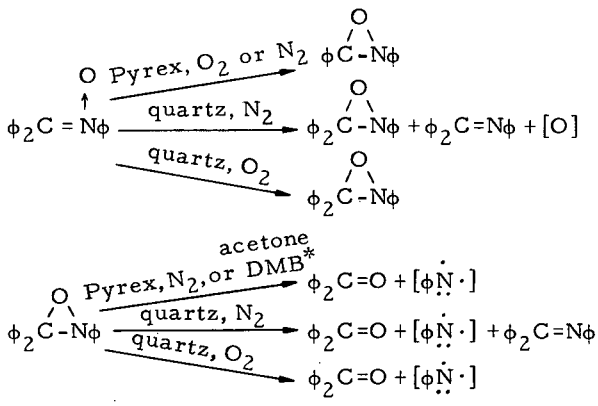

*DMB = p-dimethylaminobenzaldehyde

XBL 686-2882

Fig. 1. Irradiation of α, α, N-triphenylnitrone and 2, 3, 3-triphenyloxaziridine.

was irradiated under oxygen instead of nitrogen. There was a considerable decrease in the amount of imine when (I) was irradiated under oxygen, but little difference in the amount of benzophenone. Imine formation appeared to be sensitive to quenching by oxygen whereas benzophenone formation was not. When the irradiation in quartz was done without previously irradiating the nitrone to oxaziridine, the yield of imine was considerably increased in diethylamine (Exp. 10). The product distribution corresponded to a 40% yield of imine and 60% yield of oxaziridine from the nitrone with subsequent irradiation of the oxaziridine. In acetone (Exp. 11), the product distribution corresponded to about 10% imine being formed from the nitrone. In benzene (Exp. 12), the result was roughly similar to that in acetone. Irradiation in quartz under oxygen instead of nitrogen caused a large decrease in the amount of imine in diethylamine (Exp. 13). This indicated quenching of imine from both the nitrone and the oxaziridine. In acetone there was some decrease in imine (Exp. 14) and some increase in unchanged oxaziridine.

Although phenylnitrene was demonstrated in the photolyses at 77°K, the yields of products resulting from this intermediate in the room temperature photolyses were small, excepting Experiment 6. The yield of aniline in the diethylamine experiments was low, probably due partly to further photochemical reaction with benzophenone.[11] In Experiment 6, the yield of aniline was in the range found in the previous study.[1] With the yield of benzophenone lower than the yield of aniline, it is probable that the benzophenone reacted with the p-dimethylaminobenzaldehyde in preference to the aniline. The yields of azobenzene were also small.

DISCUSSION

From the results it is apparent that the nitrone with a suitable solvent deoxygenates photochemically, as well as rearranging to the oxaziridine. Literature reports on the photochemical deoxygenation of nitrones[12] in solution do not distinguish between deoxygenation of nitrone and deoxygenation of the oxaziridine. In this study with the oxaziridine being relatively stable, it is possible to do so.

Evidence[13] has been presented showing that the formation of 2, 3-diphenyloxaziridine from α, N-diphenylnitrone proceeds from the lowest excited singlet state of the nitrone without con-

siderable activation energy. The primary step of the reaction is not the twist of the two phenyl rings around the double bond but the movement of the oxygen atom to the α-carbon atom.[13] There is no concentration dependence of the quantum yields, indicating a reaction so fast that it was finished before deactivation of the excited nitrone molecule by collision with the ground state molecules occurred. Oxygen does not quench the reaction. The α, N-diarylnitrones show fluorescence rather than phosphorescence[14] in EPA glasses, indicating that intersystem crossing from the lowest singlet state is inefficient. When α, α, N-triphenylnitrone is irradiated with Pyrex filter there is almost complete conversion to oxaziridine. However, with quartz in diethylamine about 40% of the nitrone is deoxygenated; this photoreaction is quenched by oxygen, indicating a reaction from the triplet state. A similar wavelength dependence has been observed in the vapor phase photolysis of 2-picoline N-oxide.[12d] In Pyrex, there is rearrangement to 2-pyridine-methanol, while in quartz at 2537 Å there is fission of the N-O bond to yield 2-picoline. However, both these reactions are quenched by oxygen. The rearrangement is attributed to the $n\text{-}\pi^*$ transition and the deoxygenation to the $\pi\text{-}\pi^*$ transition. Although pyridine N-oxide and 3-picoline N-oxide undergo deoxygenation with Pyrex, the activation energy required is about 12 kcal mol^{-1}, whereas the activation energy for the rearrangement of 2-picoline N-oxide is about 3.4 kcal mol^{-1}. Pyridine N-oxide shows pale violet phosphorescence. In solution, pyridine N-oxide in Pyrex at room temperature shows only about 14% deoxygenation.[12b]

When α, α, N-triphenylnitrone is irradiated in quartz, higher singlet levels must be populated than when irradiated in Pyrex. These higher excited states may undergo intersystem crossing to the triplet before internal conversion to the lowest singlet state. Since the difference in amount of nitrone deoxygenation in diethylamine and acetone is so much greater than that of oxaziridine deoxygenation, it appears that diethylamine may have some effect on the intersystem crossing from the higher singlet level. There is evidence[15] that amines lead to higher conversions to the p-aminobenzophenone reactive $n\text{-}\pi^*$ triplet state. Amines are known to be good oxygen acceptors. A possible alternative is that amines may effect deoxygenation of the nitrone triplet state more efficiently than acetone.

Some heterocyclic N-oxides[12d, 16] are known to deoxygenate thermally at 160° and higher temperatures. The α, N-diarylnitrones deoxygenate readily in the gas chromatograph. However, α, α, N-triphenylnitrone has a high melting point and is not volatilized appreciably in the gas chromatograph at 300-320°. Mass spectrometry of heterocyclic N-oxides shows large $(P\text{-}16)^+$ peaks.[16a]

Although photosensitization of imine formation from nitrone was not shown, there has recently been reported the photosensitized deoxygenation of azoxybenzene.[17] The direct photolysis which is not quenched by oxygen yields the rearranged product, o-hydroxyazobenzene.

The oxaziridine photolysis also involves deoxygenation, which occurs to a greater extent in diethylamine than in acetone. However, the major fragmentation reaction is cleavage to benzophenone and phenylnitrene. The latter reaction occurs in both the direct and the photosensitized photolysis, indicating reaction from the triplet state.

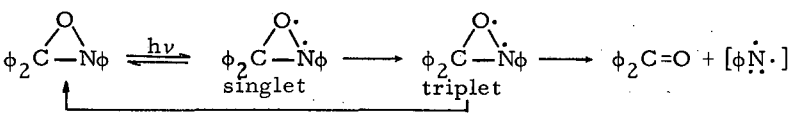

In the previous study[1] the photofragmentation of 3-p-dimethylaminophenyl-2-phenyloxaziridine was found to be quenched by oxygen, an effective triplet quencher. However, in this study the cleavage to benzophenone and phenylnitrene with unfiltered irradiation is not quenched by oxygen. Probably the triplet oxaziridine fragments faster than it reacts with oxygen.

It is of interest to note that oxaziridine (I) undergoes some fragmentation thermally in addition to the major thermal reaction, which is rearrangement to the anilide. In the gas chromatograph, 10% imine, 28% benzophenone, and 60% anilide are obtained from oxaziridine (I).

Imine formation in the oxaziridine photolysis is quenched by oxygen but appears not to be photosensitized. Although these results suggest that imine formation from the oxaziridine also originates from a triplet state, this triplet state must be at a higher level than the one that gives benzophenone and phenylnitrene. This triplet state could result from a different excited singlet state of the oxaziridine.

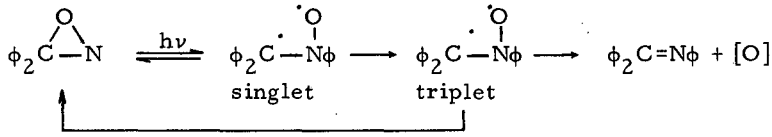

With the nitrone deoxygenating to an appreciable extent when irradiated in quartz in diethylamine, this pathway is a reasonable one. In fact, the triplet state in this scheme could be very similar to the nitrone triplet that leads to deoxygenation.

Rearrangement to the anilide occurs to a small extent in acetone and benzene. Although the rearrangement appears not to be quenched by oxygen, the yields are so small that it is difficult to draw conclusions from the data.

Although only traces of azepine are found on irradiation of oxaziridine (I) in diethylamine, benzophenone in equimolar amount (absorbing 60-70% of the light) either in Pyrex or quartz does not inhibit azepine formation in the irradiation of phenylazide in diethylamine. Since the photofragmentation of the oxaziridine presumably occurs via the triplet state to give triplet phenylnitrene, azepine formation appears not to be via the triplet state. Other evidence, such as nonquenching by oxygen, indicates azepine formation is via the singlet state.

FOOTNOTES AND REFERENCES

1. J. S. Splitter and M. Calvin, LCBQ reports, Dec. 1966, May 1967, Aug. 1967; in addition to photofragmentation there was rearrangement to the anilide as well as a small amount of imine formation.
2. Recently, E. Meyer and G. W. Griffin, Angew. Chem. 79, 648 (1967), have reported the photofragmentation of a spirooxaziridine in diethylamine, giving as the only products a 10% yield of 2-diethylamino-3H-azepine and a 9% yield of aniline. They postulated phenylnitrene as the intermediate.
3. a) K. A. Abramowitch and B. A. Davis, Chem. Rev. 64, 149 (1964); b) J. H. Hall, J. W. Hill, and H. Tsae, Tetrahedron Letters 1965, 2211; c) G. Smolinsky, E. Wasserman, and W. A. Yager, J. Am. Chem. Soc. 84, 3220 (1962).
4. W. v. E. Doering and K. A. Odum, Tetrahedron 22, 81 (1966).
5. Yields of aniline as high as 50% were obtained.

6. H. Ono and M. Calvin, to be published.
7. M. L. Scheinbaum, J. Org. Chem. 29, 2200 (1964), obtained the anilide from the irradiation of α, α, N-triphenylnitrone. In view of our work, it appears likely that the oxaziridine thermally isomerized during their irradiation.
8. Solutions were prepared by dissolving 18 mg (I) in 0.05 ml each of acetophenone and methylene chloride. Then 0.05 ml fluorolube was added to each solution in the EPR quartz tubes. The fluorolube formed a partial solution with the methylene chloride solution but not with the acetophenone solution. These solutions, which did not form glasses at 77°K after degassing, were irradiated for 30 min with the Hanovia Type L 450 watt mercury vapor lamp. The EPR spectrum was determined maintaining the irradiated (I) at 82°K.
9. We are indebted to Mr. James Chang for determining the EPR absorption spectra.
10. A. M. Trozzolo, W. A. Yager, G. W. Griffin, H. Kristinnsson, I. Sarkar, J. Am. Chem. Soc. 89, 3357 (1967), reported the EPR absorption spectrum of diphenylmethylene in the photolysis of triphenyl and tetraphenyl-oxiranes at 77°K.
11. a) S. A. Cohen and R. J. Baumgarten, J. Am. Chem. Soc. 89, 3471 (1967). b) Irradiation of a 0.001 M solution of benzophenone and aniline in acetone for 4 min, in quartz, under nitrogen showed loss of most of the aniline and less than half of the benzophenone. Benzophenone was much more stable to irradiation than were the aldehydes in the previous study.[1]
12. a) M. Ishikawa, S. Yamada, H. Hotta, and C. Kaneko, Chem. Pharm. Bull. 14, 1102 (1966); J. Streith, H. K. Darrah, and M. Weil, Tetrahedron Letters 1966, 5555; O. Buchardt, J. Becher, and C. Lohse, Acta Chem. Scand. 20, 2467 (1966). b) Algis Alkaitis and M. Calvin, to be published; the imine yield in these reports is relatively low, 14% maximum. c) However, G. B. Brown, G. Levin, and S. Murphy, Biochemistry 3, 880 (1964), report a 40% yield of adenine from the irradiation of adenine-N-oxide. d) N. Hata and I. Tanaka, J. Chem. Phys. 36, 2072 (1962); N. Hata, Bull. Chem. Soc., Japan, 34, 1440, 1444 (1961); deoxygenation of 2-picoline N-oxide was observed with 2537 Å irradiation, whereas deoxygenation of both pyridine N-oxide and 3-picoline N-oxide was observed with 2537 Å irradiation, all in gaseous state.
13. K. Shinzawa and I. Tanaka, J. Phys. Chem. 68, 1205 (1964).
14. R. P. Foss, unpublished data.
15. S. G. Cohen and J. I. Cohen, J. Am. Chem. Soc. 89, 164 (1967).
16. a) T. A. Bryce and J. R. Maxwell, Chem. Commun. 1965, 206; b) A. Chatterjee, P. Majumder, and A. Ray, Tetrahedron Letters 1965, 159.
17. R. Tanikaga, K. Maruyama, R. Goto, and A. Kaji, Tetrahedron Letters 1966, 5925.

ADDITIONAL EXPERIMENTS USING THE ION ACCELERATOR TO IRRADIATE BENZENE WITH HOT $^{14}C^{+}$ IONS AND ^{14}C ATOMS

Helmut Pohlit, Tz-hong Lin, Wallace Erwin, and Richard M. Lemmon

Our previous annual report (UCRL-17520, May 1967, pp. 15-17) described the use of our 10-kV ion accelerator for the irradiation of solid benzene with $^{14}C^{+}$ ions. In the present report we describe further work on the identification of products, and we present data on the relative amounts of the various products formed as we vary the conditions of the irradiations.

In Fig. 1 is shown a typical GLC tracing obtained on an aliquot portion of the target benzene after it is allowed to come to room temperature and then is injected into the column. The identity of each labeled compound is quite secure. For example, although no carrier biphenyl was present in the chromatogram shown in Fig. 1, the peak so labeled was trapped, carrier biphenyl was added, the mixture was subjected to hydrogenation conditions, and the resultant material rechromatographed. The retention time of the radioactivity was unchanged, and it coincided perfectly with the carrier biphenyl, which was also unaffected by the hydrogenation conditions.

U-2

The radioactive peak labeled U-2 in Fig. 1 is still unknown. Previously we observed that U-2, trapped from the GLC, and hydrogenated, gave ^{14}C peaks with retention times corresponding to toluene and methyl cyclohexane. This finding has now been confirmed; the two carriers were added, and exact coincidences of mass and radioactive tracings were obtained.

When U-2 is trapped from the GLC and reinjected, about 90% of the ^{14}C activity shows up unchanged as U-2. However, 10% of the activity is in a new peak with a shorter retention time. This seems to indicate that U-2 is partly changed in the hot detector of the GLC, and further studies on the thermal lability of U-2 are planned.

We bubbled HBr gas into a benzene solution of U-2 for about 5 min. Subsequent GLC examination showed that no change occurred in the U-2 peak. This surprising result will be checked, and further tests using HBr will be done.

We suspected at one time that U-2 was cyclooctatetraene; however, the latter has a retention time of 6.8 min as compared to 8.8 min for U-2. Further, neither cyclooctatetraene, methyl cycloheptatriene, nor styrene coincide with any of the small radioactive peaks between CHT and U-2 in Fig. 1.

RADIOPURITY OF THE MAJOR PRODUCTS

To make sure that no radioactive compounds were being masked in the large benzene peak, this peak was trapped from the GLC into n-pentane; one aliquot was rechromatographed and its specific activity determined. Another aliquot was hydrogenated in n-pentane over PtO_2 for 1 hr at 23°C and 20 psi H_2 pressure. The sample was purified again on GLC, trapped, and the specific activity determined. A third aliquot was treated with bromine, rechromatographed, and the specific activity checked again. The data in Table I show that within the limits of

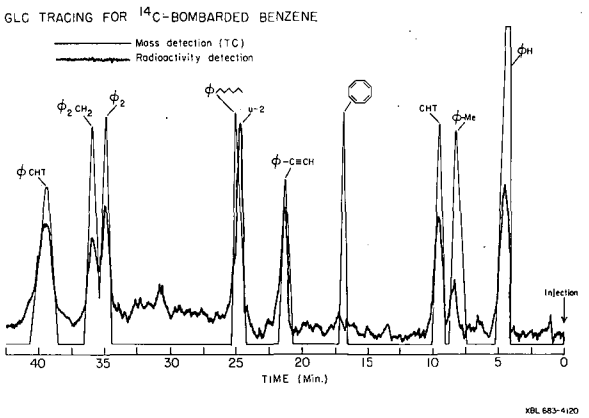

Fig. 1. GLC tracings for 30 μl of bombarded benzene, and added carriers, on carbowax 20M. Smooth curve: mass (TC). Jagged curve: radioactivity. CHT = cycloheptatriene.

Table I. Radiopurity of benzene.

Sample	#	Weight (mg)	Specific activity × 10^{-3} mg/dpm
Inject aliquots of n-pentane solution, trap benzene-^{14}C	1	4.627	1.945
	2	4.120	2.01
	3	3.077	1.93
Hydrogenation		2.126	1.925
Bromination repeated[a]	1	4.304	1.93
	2	1.430	1.96

a. Here the trapped benzene was reinjected and re-trapped in order to eliminate some background contamination which appeared in the first run.

experimental error (about ± 3%) the ^{14}C activity in the benzene peak area is indeed due to ^{14}C-benzene.

A similar type of check was made on the "CHT" (cycloheptatriene) peak area. The specific activity of ^{14}C-CHT, as trapped from the GLC, was compared with that of its Diels-Alder adduct with dimethyl-acetylene dicarboxylate (see Table II).

RELATIVE ^{14}C ACTIVITY IN THE MAJOR PRODUCTS

We have little information, at the present time, on how the various ^{14}C-containing compounds are formed during an irradiation. To see if some of the parameters under our control would qualitatively or quantitatively affect the products formed from the irradiation of solid benzene with hot $^{14}C^+$ ions, a series of experiments were made in which we determined where in the various parts of the gas chromatographic analyses we recovered the ^{14}C activity. The total ^{14}C activity contained in our samples after transfer out of the accelerator target box is, within the accuracy of our measurements, equal to the time-integrated ^{14}C-ion beam intensity at the target. We trapped and counted, not only the major peaks from the GLC, but also whatever emerges between the peaks. In addition, we trapped the activity emerging from the column for 1 hr after the last major peak had emerged. Finally, we recovered the activity which ordinarily would not leave the beginning of the column. We filled the normally empty injector tube with column support (20% carbowax 20 M on chromosorb W); and after the emergence of

Table II. Radiopurity of CHT.

Sample	#	Weight (mg)	Specific activity $\times 10^{-8}$ mole/dpm
Inject aliquots of n-pentane solution of ^{14}C-CHT and trap CHT	1	1.763	1.61
	2	2.822	1.61
	3	2.943	1.60
^{12}C-CHT trapped as above, ^{14}C samples	1	2.451	7.5 cpm (= background)
	2	ca. 3	7.3 cpm (= background)
Diels-Alder adduct isomer II	1	0.975	1.53
	2	2.035	1.525

Table III. ^{14}C activity distribution for a GLC injection.

Area trapped from GLC	% of total activity injected
Pre-benzene	0.4
Benzene	3.8
Benzone to toluene	0.8
Toluene	1.8
CHT	4.3
CHT to phenylacetylene	3.2
Phenylacetylene	2.2
Phenylacetylene to U-2	0.6
U-2	2.7
U-2 to biphenyl	8.0
Biphenyl	1.5
Diphenylmethane	2.5
Phenyl-CHT	6.4
1 hr at 250°C	7.0
Remaining in injector filling	37.4
Total	82.6

the last peak (phenyl-CHT) from the GLC, this tube was removed and the contents emptied into a counting vial and counted. Table III is representative of many similar measurements.

We also determined the ^{14}C activity distribution for $^{14}C^+$ ions with 15-kV, 5-kV, and 1.5-kV energies. In another case, 5-kV ^{14}C atoms (neutrals) were used; and, finally, a 5-kV $^{14}C^+$ beam, which is usually about 2 mm in diameter, was spread to cover about a 2 cm diameter area. The ^{14}C activity found in the major products for each of the above irradiations is given in Table IV. As can be seen, no qualitative change was noted, and only minor quantitative changes were found.

Table IV. Percent of ^{14}C activity found based on total ^{14}C collected from target benzene.

Energy and Species	Benz.	Tol.	CHT	ϕ-C≡CH	U-2	ϕ-ϕ	ϕ-CH_2-ϕ	ϕ-CHT
15 kV	3.8	1.8	4.3	2.2	2.7	1.5	2.5	6.4
$^{14}C^+$ ion	3.4	1.2	3.8	1.8	2.0	1.1	2.1	5.2
5 kV	4.4	1.0	3.2	2.0	3.6	2.1	2.4	6.3
$^{14}C^+$ ion	4.2	1.4	3.2	2.1	3.2	1.5	2.2	5.8
1.5 kV	5.7	1.3	2.8	2.1	3.7	2.1	2.1	5.3
$^{14}C^+$ ion	5.8	1.2	2.8	2.3	4.1	2.0	2.7	5.3
5 kV spread $^{14}C^+$ ion beam	4.6	1.5	3.5	2.1	3.5	2.1	2.0	6.1
5 kV	4.6	1.5	3.4	1.8	2.8	2.0	2.1	5.3
^{14}C atoms	3.8	1.0	2.8	2.0	3.3	7.8(?)	1.6	7.0

HYDROGEN ATOM IRRADIATION OF CRYSTALLINE CHOLINE CHLORIDE

Richard M. Lemmon and Amar Nath

We are applying the technique of hydrogen-atom irradiation in an attempt to learn more about the radiolysis of crystalline choline chloride. It has been reported[1, 2] that the ESR spectra resulting from H atom irradiations of organic compounds are simpler than those resulting from more conventional γ-ray or electron irradiations. The reason for this is that the dominant mechanism appears to be a simple hydrogen abstraction, giving a single radical; hydrogen gas is the only other product:

$$RH + H\cdot \rightarrow R\cdot + H_2 \ .$$

Previous work in this laboratory[3] on the ESR spectrum of γ- and electron-irradiated choline chloride indicated that more than one radical was produced, and that the main radical that appeared on irradiation was (a) chain radiolysis initiating, not propagating, and (b) was not the result of H atom abstraction. The postulated formula for that radical was, approximately, $\cdot CH_2CH_2OH$, with the unpaired electron coupled about equally to the four hydrogens of the two methylene groups.

It seemed, therefore, of potential value in understanding choline chloride's radiolysis mechanism to irradiate the crystals with H atoms and to determine whether the resultant, presumably H-abstracted, radical bore any resemblance, in its ESR spectrum, to our previously observed[3] radical. A further second object of this work is to determine whether the H-irradiation radical initiates the same highly efficient radiolysis as does the ionizing radiation.

EXPERIMENTAL AND RESULTS

The choline chloride was recrystallized from EtOH-Et_2O. Its elemental analysis was satisfactory (both C and H within 0.3% of calculated values). In order to maximize crystal surface areas, we used small crystals (less than 0.2 mm in the largest dimension).

The H-atom irradiations were performed on the equipment shown in Fig. 1.

The hydrogen used was "research grade," obtained from Air Products Co., Mountain View, California. Our microwave generator was the Raytheon 125-watt "Microtherm." The microwave cavity was an all-brass cylindrical device, approximately 5 × 2.5 in., constructed here. In the glove box (dry atmosphere) the choline chloride crystals (or malonic acid—see below) were placed on the glass frit, and then protected by the stopper from atmospheric moisture. This assembly was then attached, as shown in Fig. 1, to the quartz tube passing through the cavity. After the assembly was evacuated, H_2 was passed into the system, and its pressure maintained at approximately 1 mm by continuously operating the mechanical pump, and by suitably adjusting the needle valve. The 125-watt microwave generator was operated at full power; a Tesla coil was operated near the quartz tube, both to start the microwave discharge and to keep it operating steadily. In the irradiations described here, the system was kept operating for about 1 hr; the total time seems unimportant, however, as the yield of H

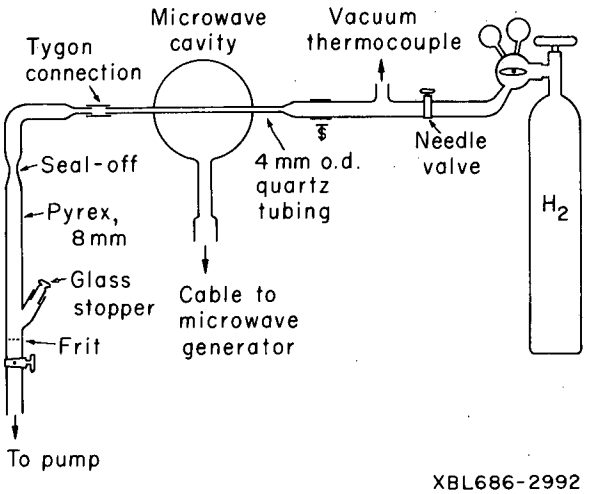

XBL686-2992

Fig. 1. Experimental apparatus.

atoms must be very pressure dependent, and there were wide pressure fluctuations (within the limits of 10 - 0.1 mm) during our irradiations.

Since there is a report[1] in the literature of an excellent 2-line ESR spectrum [from $HC(CO_2H)_2$] obtained on the H· irradiation of malonic acid, we first irradiated this compound. The resultant spectrum (obtained at room temperature, on a Varian E-3 EPR spectrometer), and shown in Fig. 2, is very similar to that of the earlier report.[1] Consequently, we were sure that our system was producing H atoms. We then irradiated a sample of choline chloride for 1 hr, and obtained the ESR spectrum shown in Fig. 3. In addition, we γ-irradiated a sample of choline chloride in order to compare the resultant ESR spectrum (Fig. 4) with that obtained previously[3] and with the spectrum of Fig. 3.

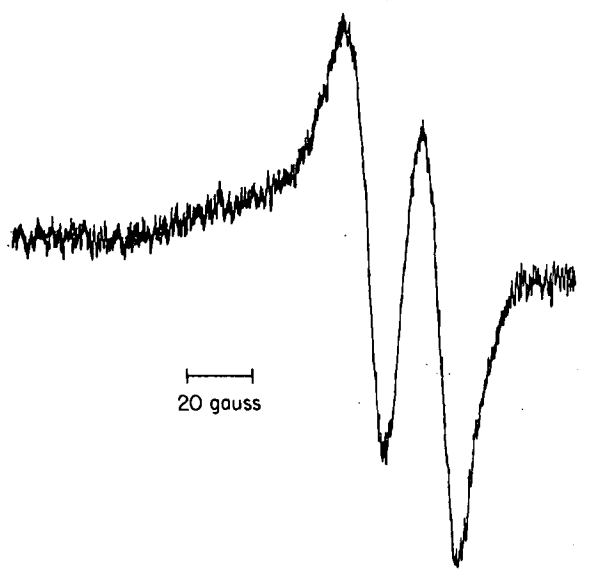

XBL686-2993

Fig. 2. ESR spectrum obtained on the H· irradiation of malonic acid.

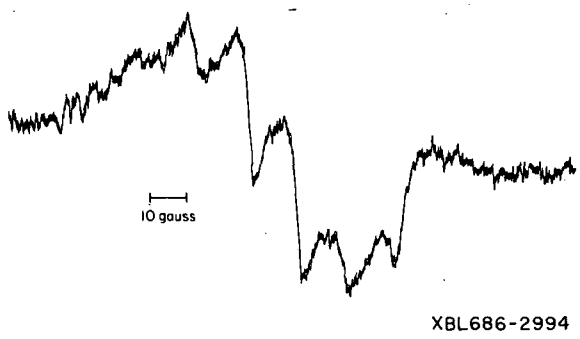

Fig. 3. ESR spectrum obtained on 1-hr H· irradiation of crystalline choline chloride.

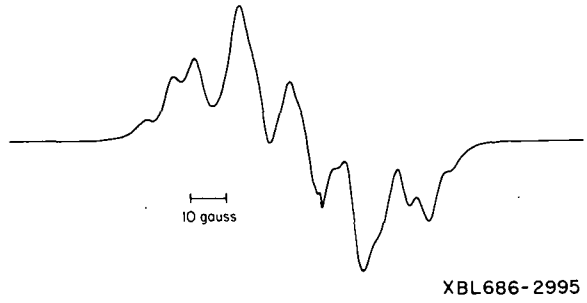

Fig. 4. ESR spectrum obtained on γ-irradiation of crystalline choline chloride.

DISCUSSION

The H atom-generated spectrum of Fig. 3 has both similarities and differences in comparison with the γ-ray-generated spectrum of choline chloride (Fig. 4). The γ-ray-generated spectrum we obtained is very similar to that reported earlier[3] for choline chloride irradiated with 4.5-MeV electrons. Both are approximately 5-peak spectra, but neither is close to an expected peak intensity ratio in the binomial distribution of 1-4-6-4-1. Although the H atom-generated spectrum (Fig. 3) is somewhat simpler than that of Fig. 4, it is difficult to understand how such a spectrum could arise following a hydrogen atom abstraction. One possibility might be an initial H abstraction from a $N\text{-}CH_3$ group, followed by a scission to the ethyl-ol radical that, we assume, gives rise to the five-peak spectrum:

$$\begin{matrix} H_2\dot{C} \\ H_3C\text{–}N^+\text{–}CH_2CH_2OH \\ H_3C \end{matrix} \longrightarrow \begin{matrix} H_2C \\ H_3C\text{–}N^+ \\ H_3C \end{matrix} + \cdot CH_2CH_2OH \,.$$

These preliminary results require confirmation. We also need to determine if our H atom-generated radical initiates the efficient chain decomposition mechanism that we have always observed on radiolysis with ionizing radiation.

REFERENCES

1. T. Cole and H. C. Heller, J. Chem. Phys. 42, 1668 (1965).
2. J. N. Herak and W. Gordy, Proc. Natl. Acad. Sci. U. S. 54, 1287 (1965).
3. R. O. Lindblom, R. M. Lemmon, and M. Calvin, J. Am. Chem. Soc. 83, 2484 (1961).

PUBLICATIONS AND PAPERS PRESENTED, 1967

ANIMAL, PLANT, AND BACTERIAL BIOCHEMISTRY

Reports Published

1. K. Schlesinger, E. L. Bennett, and M. Hebert, Effects of Genotype and Prior Consumption of Alcohol on the Rate of Metabolism of Ethanol-1-^{14}C, Quart. J. Studies Alc. 28, 231 (1967).

2. E. L. Bennett, Marie Hebert, and Ann Hughes, Tracer Studies of the Uptake of Organic Compounds by Planarians, in Chemistry of Learning, W. C. Corning and S. C. Ratner, Eds. (Plenum Press, New York, 1967), pp. 166-183.

3. E. L. Bennett, Interanimal Transfer of Trained Responses, in Proc. 5th Int. Cong. of "Collegium Internationale Neuropsychopharmalogicum," Washington, D. C., 1966. Excerpta Medica International Congress Series #129 (Excerpta Medica Foundation, 1967), pp. 231-235.

4. Mark R. Rosenzweig, Edward L. Bennett, and Marian C. Diamond, Effects of Differential Environments on Brain Anatomy and Brain Chemistry, in Psychopathology of Mental Development, J. Zubin and G. Jervis, Eds. (Grune and Stratton, 1967), pp. 45-56.

5. L. L. Simpson, F. Verster, and J. T. Tapp, Electrophysiological Manifestations of Experimental Botulinal Intoxication: Depression of Cortical EEG, Exp. Neurol. 19, 199-211 (1967).

6. E. L. Bennett and M. R. Rosenzweig, Strain Generality and Temporal Development of Cerebral Effects of Environmental Enrichment, Federation Proc. 26, 841 (1967). (Abstract)

7. E. L. Bennett, M. R. Rosenzweig, H. Morimoto, and M. Hebert, Stability of Strain Differences in Brain Acetylcholinesterase and Acetylcholine in Rats, 7th Int. Cong. of Biochem., 1011 (1967). (Abstract)

8. M. R. Rosenzweig, E. L. Bennett, and H. Morimoto, Rat Brain Acetylcholinesterase and Cholinesterase Activities as Functions of Age and of Differential Experience, 7th Int. Cong. of Biochem., 1014 (1967). (Abstract)

9. M. R. Rosenzweig, E. L. Bennett, and M. C. Diamond, Transitory Components of Cerebral Changes Induced by Experience, Proc. 75th Annual Convention of the American Psychol. Assoc., 105 (1967). (Abstract)

10. J. A. Bassham and R. G. Jensen, Photosynthesis of Carbon Compounds, in Harvesting the Sun - Photosynthesis in Plant Life, A. San Pietro, F. A. Greer, and T. J. Army, Eds. (Academic Press, New York, 1967), pp. 79-110.

11. H. W.-S. Chan and J. A. Bassham, Metabolism of ^{14}C-Labeled Glycolic Acid by Isolated Spinach Chloroplasts, Biochim. Biophys. Acta 141, 426-429 (1967).

12. R. A. Dilley, R. B. Park, and D. Branton, Ultrastructural Studies of Light-Induced Chloroplast Shrinkage, Photochem. Photobiol. 6, 407-412 (1967).

13. D. Branton and R. B. Park, Subunits in Chloroplast Lamallae, J. Ultrastructure Research 19, 283-303 (1967).

14. R. B. Park and S. Drury, The Effects of Daylength on Quantasome Structure and Chloroplast Photochemistry in Spinacia oleracea L. var. Early Hybrid #7, in Le Chloroplaste, C. Sironval, Ed. (Masson and Cie, Paris, 1967), pp. 328-334.

15. R. B. Park, Control of Membrane Differentiation and Quantum Conversion Efficiency in Chloroplasts, in Organizational Biosynthesis, H. J. Vogel, J. O. Lampen, and V. Bryson, Eds. (Academic Press, New York, 1967), pp. 373-385.

16. W. A. Jensen and R. B. Park, Cell Ultrastructure (Wadsworth Publishing Company, Inc., Belmont, California, 1967).

17. T. R. Dehner, H. W.-S. Chan, M. B. Caple, and M. Calvin, Tritium Incorporation Studies in Photosynthetic Bacteria, Proc. Nat. Acad. Sci. U. S. 58, 1556-1559 (1967).

18. A. A. Liebman, B. P. Mundy, and H. Rapoport, The Biosynthesis of Nicotine in Nicotiana glutinosa from Carbon-14 Dioxide. Labeling Pattern in the Pyrrolidine Ring, J. Am. Chem. Soc. 89, 664 (1967).

19. G. Blaschke, H. I. Parker, and H. Rapoport, Codeinone as the Intermediate in the Biosynthetic Conversion of Thebaine to Codeine, J. Am. Chem. Soc. 89, 1540 (1967).

20. H. Rapoport, C. H. Lovell, H. R. Reist, and M. E. Warren, Jr., The Synthesis of Thebaine and Northebaine from Codeinone Dimethyl Ketal, J. Am. Chem. Soc. 89, 1942 (1967).

21. R. O. Martin, M. E. Warren, and H. Rapoport, The Biosynthesis of Opium Alkaloids. Reticuline as the Benzyl-tetrahydroisoquinoline Precursor of Thebaine in Biosynthesis with Carbon-14 Dioxide, Biochemistry 6, 2355 (1967).

22. J. Palmer and V. Moses, Involvement of the Lac Regulatory Genes in Catabolite Repression in Escherichia coli, Biochem. J. 103, 358 (1967).

23. C. Prevost and V. Moses, Pool Sizes of Metabolic Intermediates and Their Relation to Glucose Repression in β-Galactosidase Synthesis in Escherichia coli, Biochem. J. 103, 349 (1967).

24. V. Moses, The Regulatory Process in the Derepression of Enzyme Synthesis: Alkaline Phosphatase of Bacillus subtilis, Biochem. J. 103, 650 (1967).

25. M. L. Eagleson and V. Moses, Metabolite-Promoted Heat Lability of β-Galactosidase and Its Relation to Catabolite Repression, Nature 214, 272 (1967).

Papers Presented

1. E. L. Bennett, Transitory Effects of Experience on Brain Weight and Behavior, 134th Annual Meeting AAAS, New York, December 1967.

2. E. L. Bennett (with D. Krech and P. Ragan), Effects of Brain Homogenate on Reinstatement of Early Memory, 134th Annual Meeting AAAS, New York, December 1967.

3. J. A. Bassham, Dynamic Metabolic Regulation of the Photosynthetic Carbon Reduction Cycle, Symposium on Comparative Biochemistry and Biophysics of Photosynthesis, Hakone, Japan, August 15, 1967.

4. J. A. Bassham, Photosynthetic Energy Transfer to Carbon Metabolism, Seventh International Congress of Biochemistry, Tokyo, Japan, August 26, 1967.

5. J. A. Bassham, Energy Utilization and Storage by the Photosynthetic Carbon Reduction Cycle, Ames Research Center, Moffett Field, Calif., April 21, 1967.

6. J. A. Bassham, Energetics of Photosynthesis, Ames Research Center, Moffett Field, Calif., April 20, 1967.

7. R. B. Park, The Ultrastructure of Fracture Faces and Deep Etch Faces of Spinach Thylakoids, Symposium on Comparative Biochemistry and Biophysics of Photosynthesis, Hakone, Japan, August 12, 1967.

BIOPHYSICAL CHEMISTRY AND BIOPHYSICS

Reports Published

1. M. P. Klein, Correlation of the EPR and Mossbauer Spectra of Ferrichrome A, in Magnetic Resonance in Biological Systems, (Pergamon, London, 1967), p. 395.

2. M. P. Klein and D. E. Phelps, Radio Frequency Hybrid Tees for Nuclear Magnetic Resonance, Rev. Sci. Instr. 38, 1545 (1967).

3. C. S. Fadley, S. B. M. Hagstrom, J. Hollander, M. P. Klein, and D. A. Shirley, Chemical Bonding Information from Photoelectron Spectroscopy, Science 157, 1571 (1967).

4. E. A. Dratz, A. J. Schultz, and K. Sauer, Chlorophyll-Chlorophyll Interactions, Brookhaven Symposia in Biology No. 19, 303-18 (1967).

5. R. T. Ross and M. Calvin, Thermodynamics of Light Emission and Free-Energy Storage in Photosynthesis, Biophys. J. 7, 595 (1967).

6. J. E. Hearst and R. A. Harris, On Polymer Dynamics: III. Elastic Light Scattering, J. Chem. Phys. 46, 398 (1967).

7. H. B. Gray, Jr., V. A. Bloomfield, and J. E. Hearst, Sedimentation Coefficients of Linear and Cyclic Wormlike Coils with Excluded Volume Effects, J. Chem. Phys. 46, 1493 (1967).

8. C. A. Bush and I. Tinoco, Jr., Calculation of the Optical Rotatory Dispersion of Dinucleoside Phosphates, J. Mol. Biol. 23, 601 (1967).

9. D. W. McMullen, S. R. Jaskunas, and I. Tinoco, Jr., The Application of Matrix Rank Analysis to the Optical Rotatory Dispersion of TMV RNA, Biopolymers 5, 589 (1967).

10. Charles R. Cantor and I. Tinoco, Jr., Calculated Optical Properties of 64 Trinucleoside Diphosphates, Biopolymers 5, 821 (1967).

Papers Presented

1. I. Tinoco, Jr., Optical Properties of Polynucleotides, Biochemistry and Biophysics Department, Iowa State University, Ames, Iowa, March 8, 1967.

2. I. Tinoco, Jr., The Optical Properties of Polynucleotides, 17th Annual Meeting of the Société de Chimie Physique, Paris, May 2-5, 1967.

3. I. Tinoco, Jr., Base-Base Interactions in Nucleic Acids, 40th Anniversary of the Institut de Biologie Physico-Chimique, Paris, May 8-11, 1967.

4. I. Tinoco, Jr., Structures of Biopolymers, Chemistry Department, University of Colorado, Boulder, Colorado, July 25-August 14, 1967.

5. I. Tinoco, Jr., Structures and Optical Properties of Nucleic Acids, Chemistry Department, Massachusetts Institute of Technology, Cambridge, Mass., Arthur D. Little Visiting Professor, October 30-November 3, 1967.

6. I. Tinoco, Jr., Biopolymers, Recent Advances in Physical Chemistry, Letters and Science Extension, University of California, Berkeley, Calif., December 5-12, 1967.

7. M. P. Klein, Determination of Valence States in Metalloproteins by Photoelectron Spectroscopy, Symposium on Physical Properties of Iron-Proteins, Stanford University, Stanford, Calif., April 17-19, 1967.

8. M. P. Klein, Application of Photoelectron Spectroscopy to the Determination of Charges on Atoms in Solids, Solid State Physics Seminar, University of California, Berkeley, Calif., April 26, 1967.

9. M. P. Klein, Application of the Mossbauer Effect to the Study of Iron Proteins, Biophysics Seminar, University of California, Berkeley, Calif., May 3, 1967.

10. M. P. Klein, Photoelectron Spectroscopy, Varian Associates Technical Seminar, Palo Alto, Calif., May 16, 1967.

11. M. P. Klein, Application of Photoelectron Spectroscopy to the Study of Proteins, Seminar in Physical Biology, Pomona College, Pomona, Calif., October 26, 1967.

12. K. Sauer, Optical Studies of Pigment Structure in Photosynthetic Bacteria, Department of Bacteriology, University of California, Davis, Calif., April 20, 1967.

13. K. Sauer, Chlorophyll Participation in the Light Reactions of Photosynthesis, Program on Biological Energy Conversion, University of California Extension, at Ames Research Center, Moffett Field, Calif., April 21, 1967.

14. K. Sauer, Exciton Interaction among Chlorophyll Molecules in Solution and in vivo, Conference on Quantum Biochemistry, University of California Extension, at Ames Research Center, Moffett Field, Calif., August 4, 1967.

ORGANIC CHEMISTRY AND GEOCHEMISTRY

Reports Published

1. Geoffrey Eglinton and Melvin Calvin, Chemical Fossils, Sci. Am. 216, No. 1, 32 (1967).

2. Melvin Calvin, Chemical Evolution, in Evolutionary Biology, Vol. 1, T. Dobzhansky, W. Hecht, and W. Steere, Eds. (Appleton-Century-Crofts, New York, 1967), pp. 1-25.

3. Melvin Calvin, Chemical Evolution, in Progress in Theoretical Biology, Vol. 1, F. F. Snell, Ed. (Academic Press, New York, 1967), pp. 1-34.

4. E. D. McCarthy and M. Calvin, The Isolation and Identification of the C_{17} Saturated Isoprenoid Hydrocarbon 2, 6, 10-Trimethyltetradecane from a Devonian Shale: The Role of Squalane as a Possible Precursor, Tetrahedron 23, 2609 (1967).

5. E. D. McCarthy, W. Van Hoeven, and Melvin Calvin, The Synthesis of Standards in the Characterization of a C_{21} Isoprenoid Alkane Isolated from Precambrian Sediments, Tetrahedron Letters, 4437 (1967).

6. E. D. McCarthy and Melvin Calvin, Organic Geochemical Studies: I. Molecular Criteria for Hydrocarbon Genesis, Nature 216, 642 (1967).

7. Melvin Calvin, Chemical Evolution of Life on Earth, in The Earth in Space, Hugh Odishaw, Ed. (Basic Books, Inc., New York, 1967), pp. 285-296.

8. Melvin Calvin, Chemical Evolution of Life and Sensibility, in The Neurosciences: A Study Program, G. Quarton, F. O. Schmitt, and T. Melnechuk, Eds. (Rockefeller University Press, New York, 1967), pp. 780-800.

9. David Boylan and Melvin Calvin, Volatile Silicon Complexes of Etioporphyrin I., J. Am. Chem. Soc. 89, 5472 (1967).

10. P. E. Brown, Mechanism of Action of Aminothiol Radioprotectors, Nature 213, 363 (1967).

PHOTOCHEMISTRY AND RADIATION CHEMISTRY

Reports Published

1. M. Ackerman and R. M. Lemmon, Product Inventory in the Radiolysis of Crystalline Choline Chloride, J. Phys. Chem. 71, 3350 (1967).

2. R. T. Ross, Some Thermodynamics of Photochemical Systems, J. Chem. Phys. 46, 4590 (1967).

Papers Presented

1. R. M. Lemmon, Radiation Chemistry of Choline Chloride, Ames Research Center, Moffett Field, Calif., July 27, 1967.

2. R. M. Lemmon, Product Inventory in the Radiolysis of Crystalline Choline Chloride, American Chemical Society Meeting, Chicago, September 12, 1967.

3. R. M. Lemmon, Reactions of Accelerated Carbon Ions with Benzene, 4th International Hot Atom Chemistry Symposium, Kyoto, Japan, October 13, 1967.

THESES

Work for the following Ph. D. theses was completed during 1967:

1. Eugene Desmond McCarthy, A Treatise in Organic Geochemistry, August, 1967, UCRL-17758.

2. Donald R. Gentner, Electron Paramagnetic Resonance Studies of Photosynthetic Systems, Sept. 1967, UCRL-17779.

3. Steven Gary Platt, Studies on the Dicyanamide Mediated Synthesis of Dipeptides (M. S. thesis), Dec. 1967, UCRL-17936.

4. Linda Kanner Phillips, Behavior of Some Transition Metal Porphyrins, Dec. 1967, UCRL-17853.

5. Gerald Aloysius Corker, The Use of a Nitroxide Radical as a Test Reagent of the Primary Processes of Photosynthesis, Sept. 1967, UCRL-17852.

6. Robert Charles Davis, Temperature Dependent Properties of Dinucleoside Phosphates, Nov. 1967, UCRL-17966.

PERSONNEL LIST

Senior Staff

Melvin Calvin, Director
James A. Bassham
Edward L. Bennett
Paul M. Hayes
John E. Hearst
Melvin P. Klein
Richard M. Lemmon
Vivian Moses
Roderic B. Park
Henry Rapoport
Kenneth H. Sauer
Ignacio Tinoco, Jr.

Research Staff

Byrdie D. Ayers
Patricia J. Chu
Lelia M. Coyne
Wallace R. Erwin
Marie S. Hebert
Joyce S. Hsu
Ann M. Hughes
Martha R. Kirk
Chantal Lafont
Lucy Martom
Hiromi Morimoto
Ann Orme
Donald E. Phelps
Dell H. Roadman
Stephanie L. Rosenbaum
Pamela Sharp

Postdoctoral Fellows

Albert Bobst
David B. Boylan
Kevin D. Cadogan
Marianne B. Caple
Henry W. -S. Chan
Goran Claeson
Henry H. Dearman
(visiting faculty)
Thomas R. Dehner
Edward A. Dratz
Urs Eppenberger
Anne-Lise Etienne
Catherine Fenselau
Eugene F. Friedman
Maurice M. Frojmovic
David Gill
Michael H. Harpold
Barrie S. Hesp
Claude Houssier
Richard G. Jensen
Benjamin Kirson
(visiting faculty)
Gotthard Krause
Didier Lafont
Claude Lussan
(visiting faculty)
Sister M. Clare Markham
(visiting faculty)
James R. Maxwell
Eugene D. McCarthy
Ian Morris
(visiting faculty)
Bradford P. Mundy
Amar Nath
Robert T. Ross
Hugo Sephton
Janet Splitter
Helmuth Springer-Lederer
John H. M. Thornley
(visiting faculty)
Charles Weiss, Jr.

Laboratory Assistants

Mark B. Dickison
Robert L. Chan
Elaine K. Earl
Peter M. Falk
Mark M. Lau
Hung J. Lee
Ethel M. LeFall
Arthur F. Levit
Marcy M. Matthai
William S. McAllister
Peter H. Ragan
Lily Wong

Graduate Students

Algis Alkaitis
Loring K. Bjornson
Roberto Bogomolni
Mary E. Brewer
Gerald A. Corker
David E. Downie
Abdalla M. El-Badry
Gerald Entine
Mark S. Fischer
Donald R. Gentner
Jerry Han
Stanley Jaskunas
Frederick A. Johnson
Jeffrey J. Kelly
Leo N. Kramer
Tz-hong Lin
Robert M. Macnab
Robert Mann
Hugh R. Matthews
Robert J. Miller
Kam-sik Ng
Howard Ono
Jon C. Palmer
Harriet Parker
Linda K. Phillips
Helmut Pohlit
George C. Ruben
Alfred J. Schultz
Lance L. Simpson
Alexander S. Sun
Nelson N. Teng
Harry G. Ungar
William Van Hoeven
Paul G. Wegfahrt, Jr.

Undergraduate Students (Research)

G. Stuart Baillie
Robert Bazell

Shops

Electronics

Robert Creedy
John A. Despotakis

Carpenter

Richard O'Brien

Glass

William Hart

Office

Evelyn Litton
Johanna Onffroy
Marilyn Taylor
Gerryann Wulbern